ANTENNA EFFICIENCY FROM MODEL MEASUREMENTS

WILLIAM E. FANNIN

1953

ANTENNA EFFICIENCY FROM MODEL MEASUREMENTS

-

William E. Fannin

ANTENNA EFFICIENCY FROM MODEL MEASUREMENTS

by

William E. Fannin
Lieutenant, United States Navy

Submitted in partial fulfillment
of the requirements
for the degree of
MASTER OF SCIENCE
in
ENGINEERING ELECTRONICS

United States Naval Postgraduate School
Monterey, California
1953

F22

This work is accepted as fulfilling

the thesis requirements for the degree of

MASTER OF SCIENCE

in

ENGINEERING ELECTRONICS

from the

United States Naval Postgraduate School

PREFACE

The literature research and experimental work were accomplished during a ten week association with the Electrical Division of the Douglas Aircraft Company, Inc., El Segundo, California. The experimental work was completed in the antenna laboratory with excellent assistance from the company personnel. It is hoped that this work will prove to be of value to the Douglas Aircraft Company in their effort to make accurate predictions of the communication range. The writer wishes to express his appreciation to Messrs. V. L. Tucker, M. R. Willis, Ernest Witten, and George Hines who were very generous in sharing their ideas and knowledge.

TABLE OF CONTENTS

SUMMARY

This paper is concerned with the efficiency of aircraft antennas. It is composed of two natural parts. The first part is a report of the results of an exhaustive search of the literature for possible methods and techniques to evaluate the antenna efficiency with the aid of scaled models. The second part is a report of the procedure, data, results, and the conclusions of the selected method of evaluation. The results obtained have not been checked by any other method and may need many in-flight tests for proper evaluation. Refinement of techniques and circuitry undoubtedly will improve the accuracy and reliability of the presented method.

LIST OF ILLUSTRATIONS

Photographs

Table

TABLE OF SYMBOLS AND ABBREVIATIONS

A_e	The effective aperture of any antenna.
A_{em}	The maximum effective aperture of any antenna.
A_1	The effective aperture of antenna 1.
A_{1m}	The maximum effective aperture of antenna 1.
A_2	The effective aperture of antenna 2.
A_{2m}	The maximum effective aperture of antenna 2.
$C(x)$	$\int_0^x \cos(\frac{\pi}{2}t^2)dt$, an expression in Schelkunoff's equations.
D	The directivity.
E	The voltage intensity in any direction.
E_s	The spatial r.m.s. voltage, defined as proportional to the square root of the average power.
E_θ	The electric field in the θ direction.
$E\phi$	The electric field in the ϕ direction.
E_t	The electric field at a test position.
G_o	The gain with respect to an isotropic radiator.
P	The power per unit solid angle in any direction.
P_{av}	The average power.
$P_{E\theta}$	The average power for the $E\theta$ polarization.
$P_{E\phi}$	The average power for the $E\phi$ polarization.
P_{in}	The input power.
P_{out}	The output power.
P_o	The power density of the incident wave.
R_a	The antenna resistance.

R_b	The bolometer resistance.
R_e	The slant length of the horn with the flare in the electric plane.
R_m	The slant length of the horn with the flare in the magnetic plane.
R_o	The loss resistance.
R_r	The radiation resistance.
R	The range separation of the transmitting and receiving antennas.
S(x)	$\int_0^x \sin(\frac{\pi}{2}t^2)dt$, an expression in Schelkunoff's equations.
V	The voltage in the receiver section.
VSWR	The voltage standing wave ratio.
W_1	The power in the termination of antenna 1.
W_2	The power in the termination of antenna 2.
$W_{1\theta}$	That portion of W_1 due to the $E\theta$ polarization.
$W_{1\phi}$	That portion of W_1 due to the $E\phi$ polarization.
$W_{2\theta}$	That portion of W_2 due to the $E\theta$ polarization.
$W_{2\phi}$	That portion of W_2 due to the $E\phi$ polarization.
W	The power in the terminating impedance.
X_1	The reactance of the PRD tuner that completes the r.f. circuit.
X_2	The reactance of the PRD tuner, shunt stub.
X_3	The reactance of the PRD tuner, series stub.
X	The value of the recorder scale in voltage.
Y	The value of the integrator counter.
Z_a	The antenna impedance.
Z_{in1}	The input impedance at point 1.

Z_{in2}	The input impedance at point 2.
a	The dimension of the horn antenna in the H plane.
b	The dimension of the horn antenna in the E plane.
d_r	The width or the physical aperture of the receiving antenna.
d_t	The width or the physical aperture of the transmitting antenna.
g	The gain in the z direction; (a notation of Schelkunoff).
g_e	The gain with the horn flare in the E plane.
g_m	The gain with the horn flare in the H plane.
k	A constant involving the distance between antennas.
l	The length from the probe to the waveguide short.
l_1	The physical length of antenna 1.
l_2	The physical length of antenna 2.
l_{e1}	The effective length of antenna 1.
l_{e2}	The effective length of antenna 2.
l_{opt}	The optimum length between the probe and the waveguide short.
mcs.	The frequency in megacycles.
r.f.	Radio frequency.
u	A variable in Schelkunoff's gain equations.
v	A variable in Schelkunoff's gain equations.
w	A variable in Schelkunoff's gain equations.
α	The effectiveness ratio.
Γ	The reflection coefficient.
γ	That factor in the effectiveness ratio due to mismatch.
η	The antenna efficiency

η_m	The ratio of the power received to the power transmitted when there are no standing waves.
θ	The latitude coordinate.
λ	The wave length in air.
λ_g	The wave length in the waveguide.
π	A mathematical constant.
ϕ	The longitude coordinate.

CHAPTER I

INTRODUCTION

The aircraft industry has the problem of predicting the range of air-borne communication equipment prior to delivery of the completed aircraft. This information is needed in the design stage in order that good location of components may be made. Excellent transmitting and receiving components are available from many industrial sources. High speed aircraft require clean airfoils to reduce drag losses. External antennas can not be tolerated. This has caused aircraft antennas to be flush mounted, or even mounted below the ground plane. The flush mounted antenna lies in the ground plane with an r.f. window of some suitable material for a cover, the entire installation being formed to fit the aerodynamic requirements. These techniques have caused many problems. Recent flight tests have shown that the predicted range often is in error by a ratio of two to one and in some cases as high as four to one.* It must be realized that the aircraft structure, and the location of a particular antenna on a specific aircraft, can cause an unsatisfactory radiation pattern. Since the aircraft contour and the antenna location are decided by the aircraft manufacturer, he has final control of the directional characteristics of radiation.

To gain needed information prior to manufacture, use has been made of the model range. In the strictest sense both the model and the

*Development Reports, Douglas Aircraft Co., Inc., Santa Monica Division Nos. 1092 and 1093.

electromagnetic field need to be properly scaled. The model range, as a tool, has been pioneered by such organizations as the Airborne Instruments Laboratory, Mineola, N. Y., the Antenna Laboratory of Ohio State University, and the Naval Air Test Center, Patuxent River, Md. There is evidence of close correlation between flight and model measurements.*

Possible causes of the reduction in predicted range could be the relative polarization between the transmitting and receiving antennas, the relative polarization between the propagated wave and the receiving antenna, the neglect of the surface coefficient of reflection, or the antenna efficiency. From the model range the directivity and relative radiation patterns can be obtained. One important piece of information is missing. How much power is being radiated for a specific amount of input power? This paper, limited in scope, is concerned with the evaluation of methods to determine the antenna efficiency by using models and then to adapt the selected method to the model range.

*Project TED No PTR EL 577 ET315-047 16 June 1952 ELECTRONICS TEST DIVISION USNATC PAX RIV MD.

CHAPTER II

METHODS OF SOLUTION

The problem under consideration is to evaluate the methods of determining the antenna efficiency with the use of scaled models. From the methods investigated one has been selected and efficiency measurements made. The degree of accuracy with which the scaled model reproduces the actual conditions is very important and should not be neglected. However modeling per se is not the immediate problem, therefore it is assumed that modeling reproduction requirements are fulfilled.

Four methods of solution are presented below. One of these has better chance of success than the others. This one, the comparison method, is presented more completely than the other three. These three are given in brief form along with foreseen advantages and disadvantages.

1. Direct Measurement with a Known Radiation Pattern.

By measuring the average output power in the radiated field and the input power at the input terminals the efficiency of the model antenna can be found. The average output power can be measured with the aid of the model range. A complete set of conical patterns of the model as a receiver are taken.* The entire spherical distribution of radiation is recorded. By a summation of the integrated values** the three dimen-

*For a more detailed description of the techniques used with the model range see the Appendix A, J. D. Kraus (13), or S. Silver (21).

**This procedure is presented in greater detail by P. S. Carter (1) and M. W. Scheldorf (18).

sional radiation pattern can be reduced to a sphere which contains the same volume. If the radiation patterns are recorded in power then this sphere can represent the average power radiated in all directions, an isotropic source. There is a direct relationship between the sphere and each part of the radiation pattern.

Assume that the three dimensional radiation pattern for transmitting and receiving are the same. If the field intensity is measured at a known position of the radiation pattern then the value of the equivalent sphere can be found. This can be changed into the average power by utilizing the following relationship. When one watt of power is radiated uniformly in all directions the field intensity at one mile will be 3.4033 millivolts per meter.*

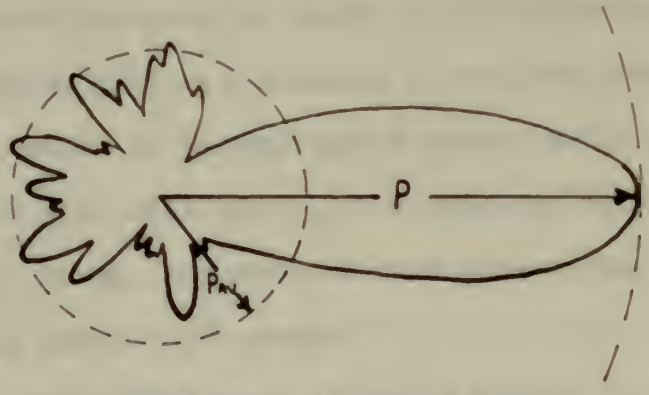

Figure 1.

Relation of the Radiation Pattern to the Equivalent Sphere

As an example let Figure 1 be the receiving and transmitting pattern. For convenience the point of the maximum radiation is set to

*P. S. Carter (1)

the polar plot value of 10 units. Then, upon integration, let the spherical radius be 3 units.

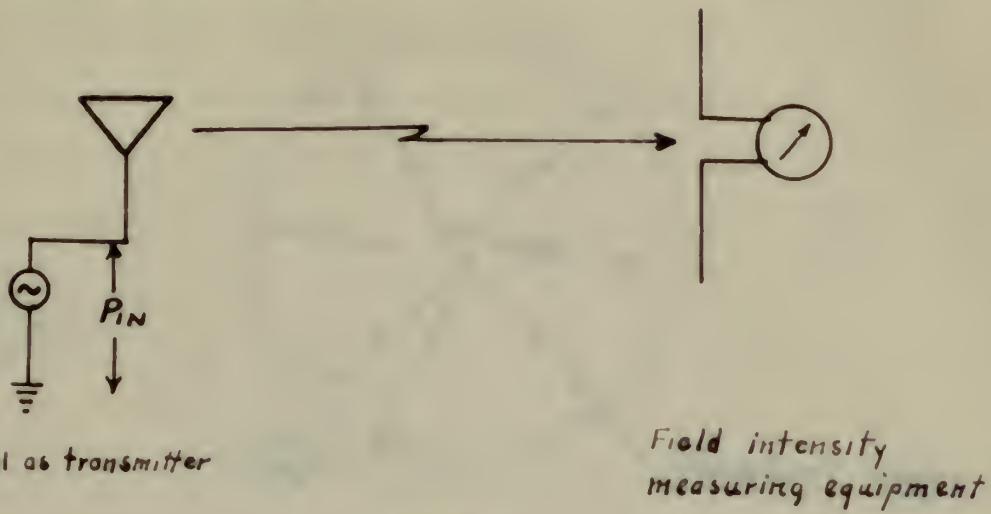

Figure 2.

Direct Measurement of Field Intensity

Let Figure 2 show a measurement at the maximum point of the lobe in Figure 1. Let the reading at this point be 22.688 millivolts/meter/mile, that is the field intensity if at a distance of one mile from the transmitter. This value, reduced to the equivalent sphere, would be 6.8066 mv/m/mile, $(22.688 \times \frac{3}{10})$. This value is the intensity for an isotropic source of two (2) watts. The ratio of this value to the measured input power is the antenna efficiency.

The advantages of this method are: it can be adapted to the model range and the procedure to obtain measurements is not difficult. The disadvantages are: the matching of the antennas, the reproduction of identical transmitting and receiving patterns, and the non-availability of field intensity measuring equipment at the scaled frequencies.

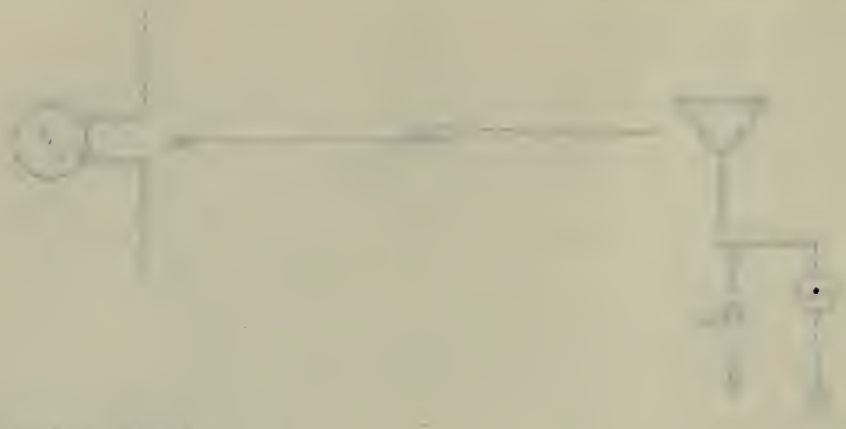

Scaled frequencies vary from about 1000 to 10000 mcs.

2. The Calorimetric Method.

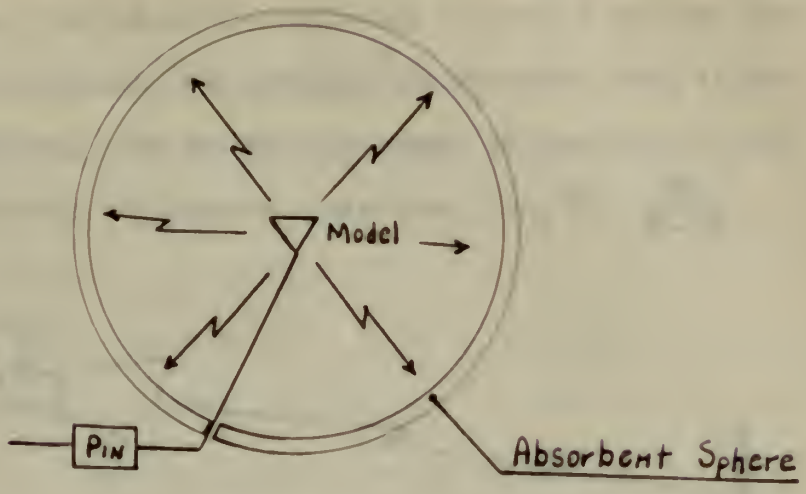

Figure 3.

Calorimetric Method

If the model were placed inside a large sphere, the interior constructed of absorbent and non-reflecting material, the rise in temperature due to the radiated power could be measured. The input power could be measured outside of the sphere. The efficiency would be the ratio of the power absorbed in the sphere to the power supplied to the model. This proposed method, although containing many practical difficulties, has the unique advantage of being frequency insensitive. The disadvantages are: procurement of the absorbent material, heat measurements, and feed line problems inside the sphere.

3. The Reflection Method.

The reflection method, or reradiation method, permits the radiation resistance of a model antenna, relative to a comparison antenna,

to be determined.* If the radiation resistance of the comparison antenna is known then the radiation resistance of the model can be found. The antenna resistance, the sum of the radiation resistance and the loss resistance, can be obtained from suitable measurements, such as the slotted line technique. The antenna efficiency is the ratio of the radiation resistance to the antenna resistance, i.e. $\eta = \frac{R_r}{R_r + R_o}$

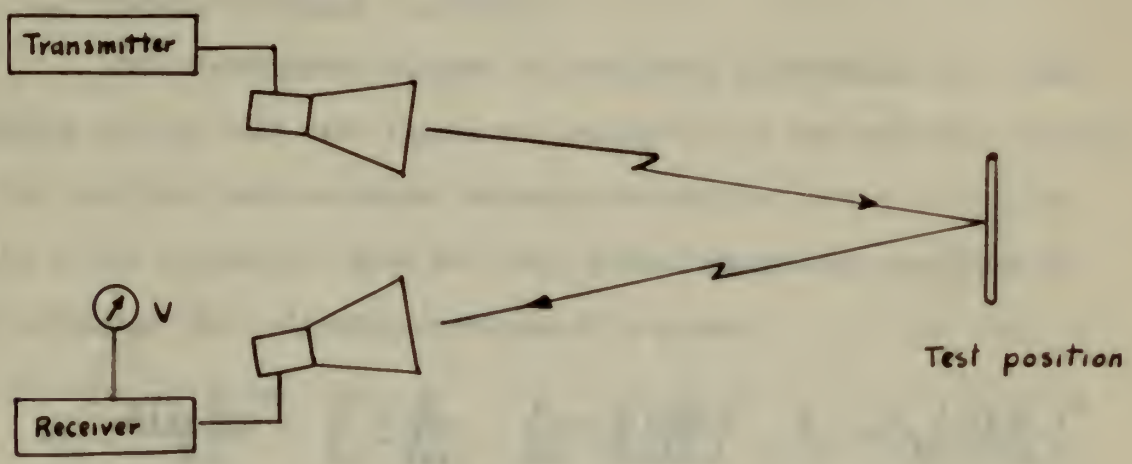

Figure 4.

Reflection Method

W_1 = the power that antenna 1 reradiated, the model antenna.

W_2 = the power that antenna 2 reradiated, the comparison antenna.

E_t = the field of the transmitting horn at the test position.

ℓe_1 = the effective length of the model antenna.

ℓe_2 = the effective length of the comparison antenna.

ℓ_1 = the physical length of antenna 1, the model antenna.

ℓ_2 = the physical length of antenna 2, the comparison antenna.

Rr_1 = the radiation resistance of antenna 1.

*E. Istvanffy (9) and J. D. Kraus (13) pp 459-461.

R_{r2} = the radiation resistance of antenna 2.

k = a constant involving the distance between the antennas.

η = the antenna efficiency.

R_o = the loss resistance of the model.

V = the detected voltage from the energy reradiated by an antenna at the test position.

$R_a = R_r + R_o$ = antenna resistance.

This development assumes the following conditions: (1) the antennas are one half wave length and resonant, (2) the radiation patterns of the model and the comparison antennas are similar, and (3) that the ratio of the effective length and the physical length are equal for the two antennas. The following development is given.

$$W_1 = \frac{k(E_t l_{e1})^2}{R_{r1}} \qquad \frac{l_1}{l_2} = \frac{l_{e1}}{l_{e2}} \qquad \frac{R_{r2}}{R_{r1}} = \frac{W_1}{W_2}\left(\frac{l_{e2}}{l_{e1}}\right)^2 \qquad R_{r1} = R_{r2}\left(\frac{V_2 l_1}{V_1 l_2}\right)^2$$

$$W_2 = \frac{k(E_t l_{e2})^2}{R_{r2}} \qquad \frac{W_1}{W_2} = \left(\frac{V_1}{V_2}\right)^2 \qquad \frac{R_{r2}}{R_{r1}} = \left(\frac{V_1 l_2}{V_2 l_1}\right)^2$$

With the radiation resistance known the efficiency of the model is

$$\eta = \frac{R_{r1}}{R_{r1} + R_o} = \frac{R_{r1}}{R_{a1}}$$

In Figure 4 the model and the comparison antennas are placed at the test position at different times. The radiation resistance and antenna efficiency can be obtained as shown above.

There are several disadvantages, which are: (1) the physical limitations require that the antennas be one half wave length and resonant; (2) a high possibility of reflections from the ground and nearby

objects which will disturb the electromagnetic field; and (3) the requirement that the radiation patterns be similar. An advantage of this method is that measurements may be made of a parasitic antenna.

4. The Comparison Method.

This method has been selected as more practical than the other methods. The power measurements are of relative powers thereby avoiding the difficulty of measuring absolute power. This method can be adapted readily to the model range. Efficiency measurements are based on this method.

a. Definition of essential terms.*

(1) The directivity is the ratio of the power per unit solid angle radiated in a chosen direction to the average power radiated in all directions. $D = P/ Pav$, where D is the directivity, P is the power intensity in a chosen direction, and Pav is the average power.

(2) The effective aperture is the ratio of the power W in the terminating impedance to the power density of the incident wave. $A_e = W/ P_o$, where A_e is the effective aperture, W is the power in the terminating impedance, and P_o is the power density of the incident wave.

(3) The effectiveness ratio is the ratio of the

*The definitions and the equations on this page are from J. D. Kraus (13) with the exception of the directivity which is from P. S. Carter (1). Other references are S. A. Scholkunoff and H. Friis (19), H. Friis (8) and R. S. Wehner (24).

effective aperture to the maximum effective aperture. $\alpha = A_e / A_{em}$, where α is the effectiveness ratio, and A_{em} is the maximum effective aperture.

(4) Gain (G_o) is the ratio of the maximum radiation intensity from subject antenna to the radiation intensity from an isotropic source with same power input.

b. Summary of relationships.

The following equations will be used to derive an expression of the efficiency.

(1) $D = P/P_{av}$

(2) $G_o = \alpha D$

(3) $D = 4\pi A_{em}/\lambda^2$

(4) $A_e = W/P_o$

(5) $\alpha = A_e/A_{em}$

The effectiveness ratio may assume values between zero and 1 ($0 \leq \alpha \leq 1$). This ratio may be considered as being composed of two factors, η the efficiency factor, and γ the mismatch factor so that $\alpha = \eta\gamma$. A perfectly matched, 100 per cent efficient antenna has an effectiveness ratio of unity. When matched for maximum power transfer ($\gamma = 1$) the effectiveness ratio equals the efficiency factor, $\alpha = \eta$. Under this condition the efficiency is the ratio of the effective aperture to the maximum effective aperture, $\eta = A_e / A_{em}$. The difference of the aperture values is due to the loss resistance. The same relationship of apertures can be obtained from Schelkunoff and Friis*. They give the following

*Schelkunoff and Friis (19) pp 180-182.

relations. The efficiency is the ratio of the radiation resistance to the antenna resistance, $\eta = R_r/(R_r + R_o)$. The effective aperture of a dissipative short dipole is $A_e = \frac{3\lambda^2}{8\pi} \frac{Rr}{Rr + R_o}$, and that of a non-dissipative short dipole is $A_{em} = \frac{3\lambda^2}{8\pi}$. The effective aperture for the non-dissipative dipole is the maximum effective aperture. If the efficiency of the receiving antenna is defined as the ratio of the power actually delivered to the load to that which could be delivered in the absence of heat loss, then the efficiency of the short dipole used as a receiver is the same as its' efficiency when used as a transmitter and

$$\eta = \frac{R_r}{R_r + R_o} = \frac{\frac{R_r}{R_r + R_o} \frac{3\lambda^2}{8\pi}}{\frac{3\lambda^2}{8\pi}} = \frac{Ae}{Aem}$$

The absolute gain, G_o, is equal to the directivity, D, when the antenna is perfectly matched and the efficiency is 100 per cent. $G_o = \alpha D$, where α is equal to unity. This is the assumed condition for the comparison horn when the impedance is matched.

The directivity is determined by the shape of the field pattern by graphical integration and is independent of the antenna loss or mismatch. A complete set of conical patterns taken on the model range will permit the directivity to be obtained. With the directivity known the maximum effective aperture can be calculated from the relationship, $D = 4\pi A_{em}/\lambda^2$.

c. Derivation of the efficiency expression.

Let Figure 5 represent the model (or comparison) antenna being illuminated by the transmitter. For convenience let the subscript

1 indicate the model and the subscript 2 indicate the comparison antenna.

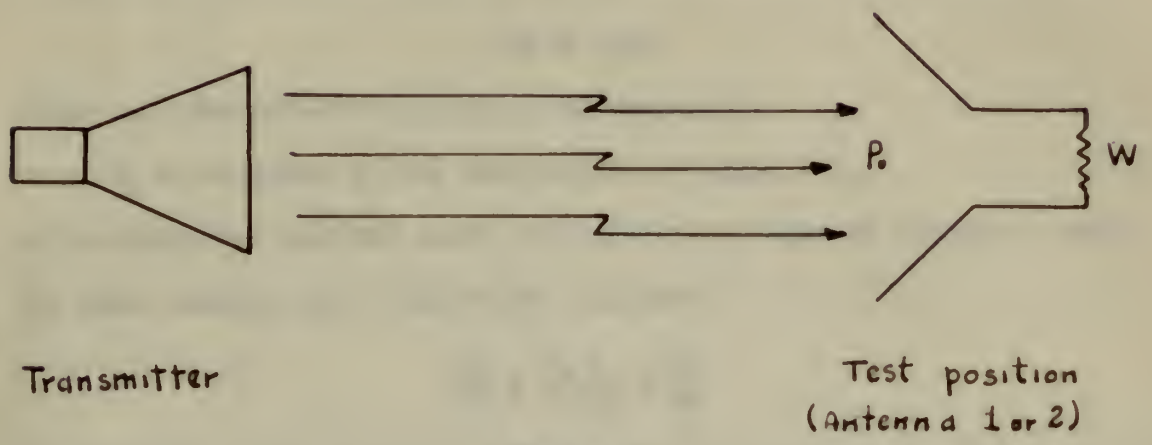

Figure 5.

Comparison Method

Assume that:

(1) at the test position the electromagnetic field is linearly polarized, of constant strength, of uniform intensity, and of constant phase across the aperture of the receiving antennas.

(2) the necessary matching can be accomplished for each antenna.

(3) the efficiency of the comparison antenna is 100 per cent.

The received power W is measured for antenna 1 and then for antenna 2. The antennas are not under illumination at the same time. The power received by antenna 1 is

$$W_1 = P_o A_1$$

where A_1 = the effective aperture of antenna 1.

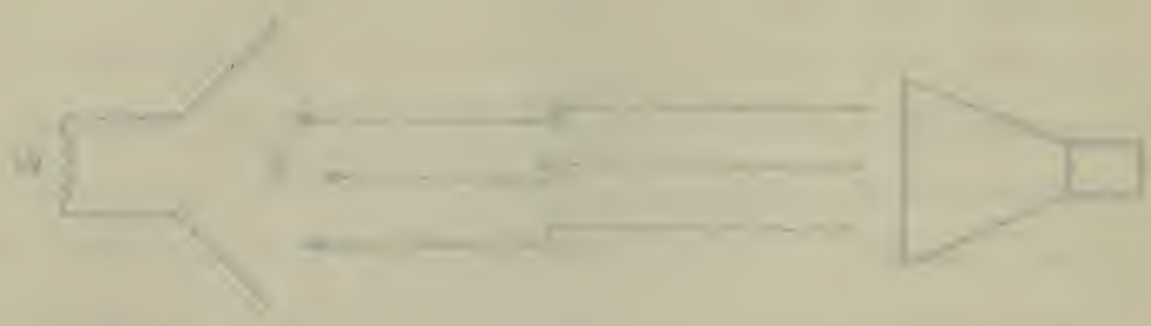

W_1 = the power in the termination of antenna 1.

P_o = the power density of the incident wave.

When antenna 2 replaces antenna 1 the power received by antenna 2 is

$$W_2 = P_o A_2$$

where A_2 = the effective aperture of antenna 2.

W_2 = the power in the termination of antenna 2.

By dividing the received power of antenna 1 by that of antenna 2, when the power density P_o is maintained constant

$$\frac{W_1}{W_2} = \frac{P_o\ A_1}{P_o\ A_2} = \frac{A_1}{A_2}$$

The mismatch factor for both antennas, and the efficiency factor for the comparison antenna, are equal to unity. Therefore $A_2 = A_{2_m}$ and $A_1 = \eta A_{1_m}$, where A_{1_m} and A_{2_m} are the maximum effective apertures of antennas 1 and 2. Thus,

$$\frac{W_1}{W_2} = \frac{\eta A_{1_m}}{A_{2_m}}$$

$$\eta = \frac{W_1\ A_{2_m}}{W_2\ A_{1_m}}$$

The value A_{2_m} can be calculated or taken from the curves given in the text of Scholkunoff and Friis.* This value could be obtained in the same manner as it was obtained for the model. The aperture values must consider the vertical and horizontal polarizations. Therefore it is necessary when the relative power measurements are made that the polarizations be considered. Thus $W_1 = W_{1_\theta} + W_{1_\phi}$ and $W_2 = W_{2_\theta} + W_{2_\phi}$. The power density of the incident wave P_o must remain constant for the period

*Scholkunoff and Friis (19) pp. 523 - 529

of the measurement. There are at least three ways that this may be accomplished. A monitor antenna may be placed in the field to observe the power intensity. A feedback loop in the bolometer amplifier may be used to keep the amplifier gain inversely proportional to the power intensity at the transmitter. Or the power intensity in the transmitter circuit may be monitored by using a directional coupler, a tuned detector and an amplifier. With a variable attenuator between the generator and the directional coupler the transmitted power may be made the same for each measurement.

The advantages of this method are: (1) no absolute power measurement is required and (2) it can be adapted to the techniques used on the model range.

The disadvantages are: (1) model range requirements must be observed and (2) conjugate matches at the antenna terminals must be made for each relative power measurement taken. The latter disadvantage is the most difficult part of this method.

CHAPTER III

SPECIAL REQUIREMENTS

1. Model range. The model range cannot reproduce the exact conditions found in normal operation, therefore "direct path" propagation is simulated. Reflections due to the ground and nearby objects between the transmitter and the receiver can prevent this "direct path" transmission. The illuminating antenna used for these experiments was a pyramidical horn with a beam width of about 15 degrees. Previous tests showed the field strength to vary less than 5 per cent over the receiving aperture. J. D. Kraus (13) and S. Silver (20) give the following model range requirements:

a. R, the distance between the receiving and transmitting antennas should be determined by:

(1) the uniform field requirement that $R \geq 2d_r^2/\lambda$, where d_r is the physical aperture of the receiving antenna.

(2) the uniform phase requirements that $R \geq 2d_t d_r/\lambda$, where d_t is the physical aperture of the transmitting antenna.

(3) the available radio frequency power.

(4) the receiver sensitivity.

b. The height (h) of the receiving antenna above ground should exceed d_r^2/d_t.

c. A matched detector system should be used.

d. A square law detector should be used.

e. The directivity of the test antenna should not be too broad.

f. The gain of the comparison antenna should be within 10 db of the unknown antenna.

2. Bolometer detector and tuner.

The PRD tuner was used to match the bolometer resistance to the antenna impedance. For the comparison antenna the tuner was matched to the coaxial transition. For the model antenna the tuner was placed as near as possible to the input terminals of the model. Photographs A and C show the tuner mounted for the model and the comparison horn. Figures 7, 8, 9a, 9b, 10, 11 and 12 show a sectional view of the tuner and the equivalent circuits when connected to the model and to the waveguide. Figures 7 and 8 show the sectional view and the equivalent circuit of the tuner, including the tuning stubs. Figures 9a and 9b show the r.f. and the detected signal circuits. Figure 10 is the equivalent circuit of the waveguide to coaxial transition to PRD tuner; the comparison circuit. Figures 11 and 12 show the equivalent circuit for the model antenna. Figure 12 represents the circuit for the tuner embedded in the model airplane. The bolometer resistance had an ohmic resistance of about 200 ohms and was calibrated for square law detection when the power level was one milliwatt or less.

It will be shown that the double stub tuner, including the bolometer resistance, can perform the necessary matching.

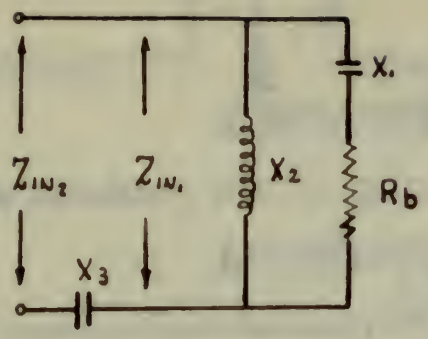

Figure 6a.

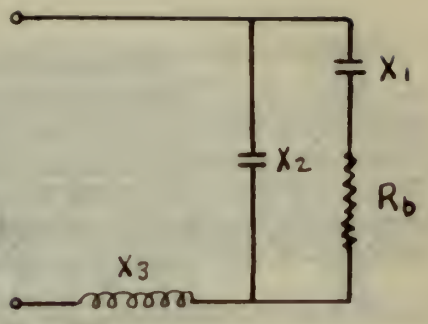

Figure 6b.

Equivalent Circuits of the PRD Tuner

The PRD tuner can be represented by either of the equivalent circuits in Figures 6a and 6b, depending upon the electrical length of the tuning stubs. At the frequencies of operation X_1, the r.f. bypass capacitance, may be considered a short circuit. Therefore

$$Z_{IN_1} = \frac{j R_b X_2}{R_b + jX_2} = \frac{R_b X_2^2}{R_b^2 + X_2^2} + j \frac{R_b^2 X_2}{R_b^2 + X_2^2}$$

By adding X_3 in series the reactance term can be cancelled. Then

$$Z_{IN_2} = R_{IN_2} = R_{IN_1} = \frac{R_b X_2^2}{R_b^2 + X_2^2} \qquad \text{where } -jX_3 = -j \frac{R_b^2 X_2}{R_b^2 + X_2^2}$$

For small values of X_2; $X_2 << R_b$

$$R_{IN_2} \simeq \frac{X_2^2}{R_b}$$

For large values of X_2; $X_2 >> R_b$

$$R_{IN_2} \simeq R_b$$

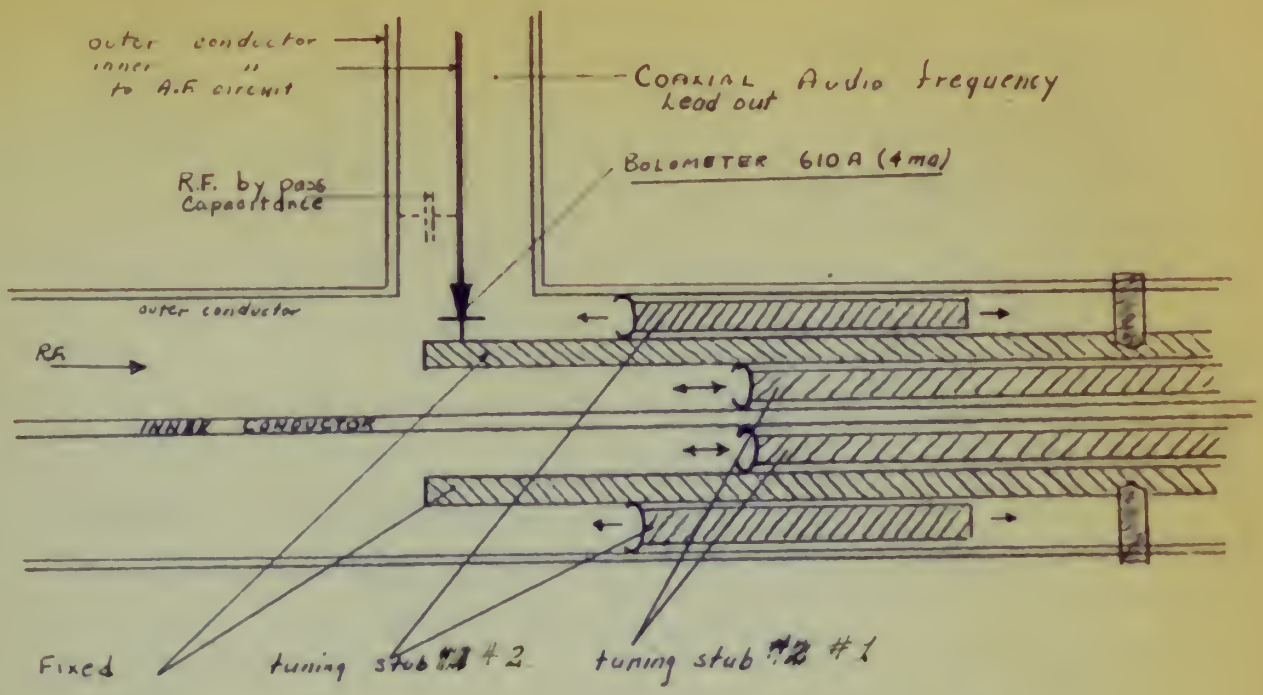

P.R.D. 612-A Bolometer Mount & Tuner

Fig. 7.

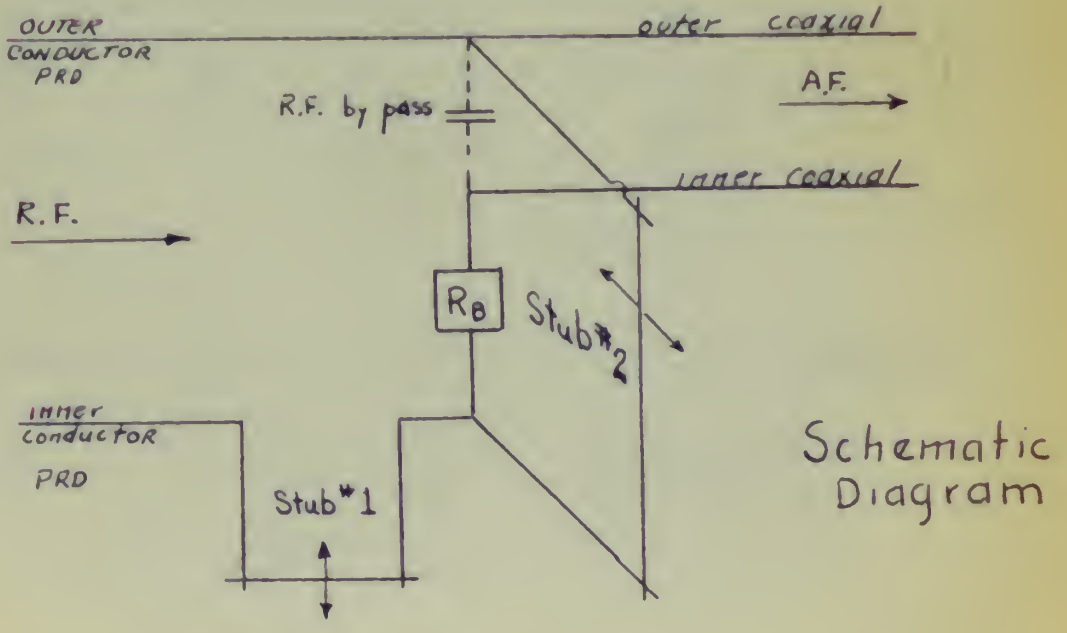

Schematic Diagram

Fig. 8.

R.F. CIRCUIT

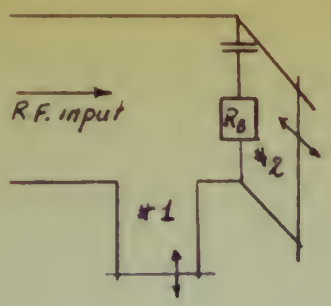

Fig. 9 (a)

A.F. CIRCUIT

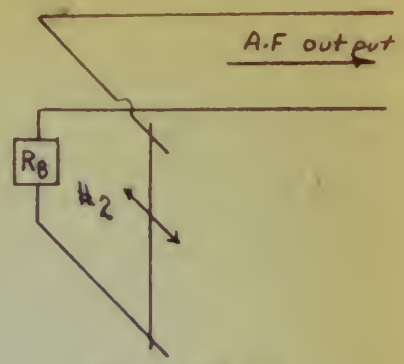

Fig. 9 (b)

WAVEGUIDE TO COAXIAL TO PRD

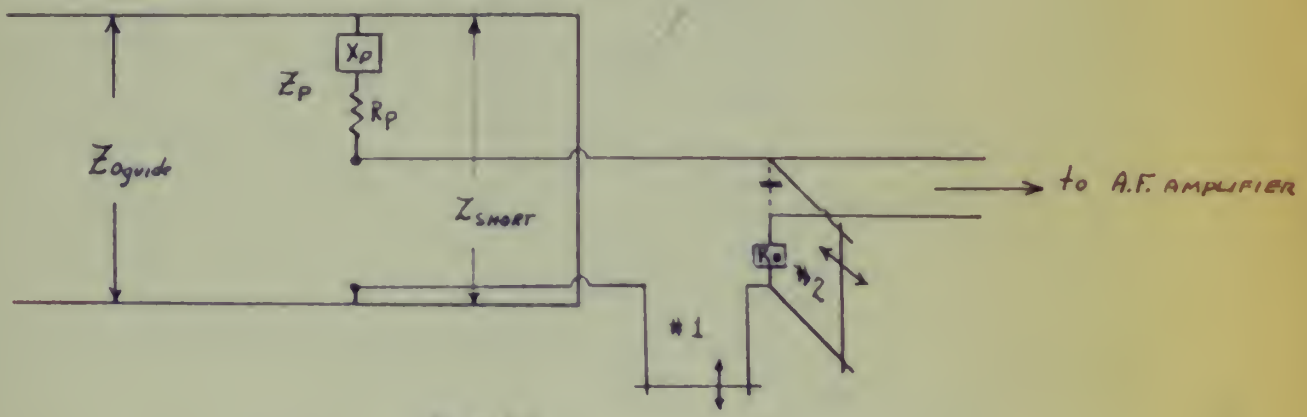

FIG. 10

ANTENNA TO CABLE TO PRD

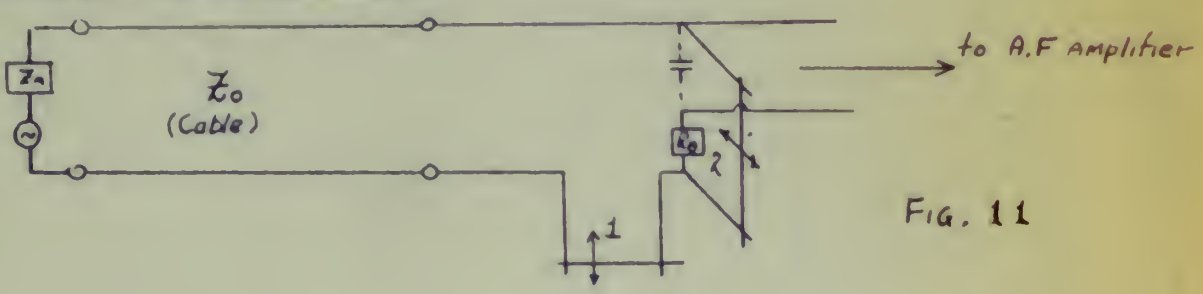

FIG. 11

ANTENNA TO PRD (WITH PRD IMBEDDED IN model aircraft)

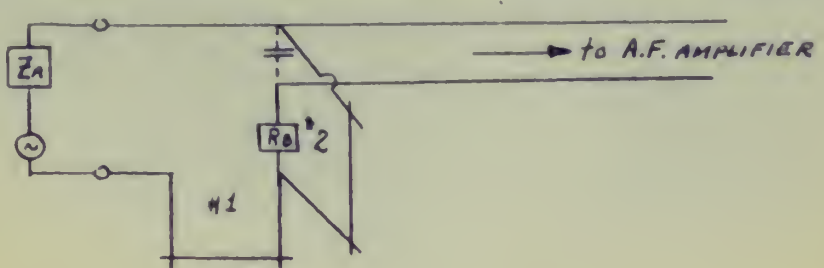

FIG. 12

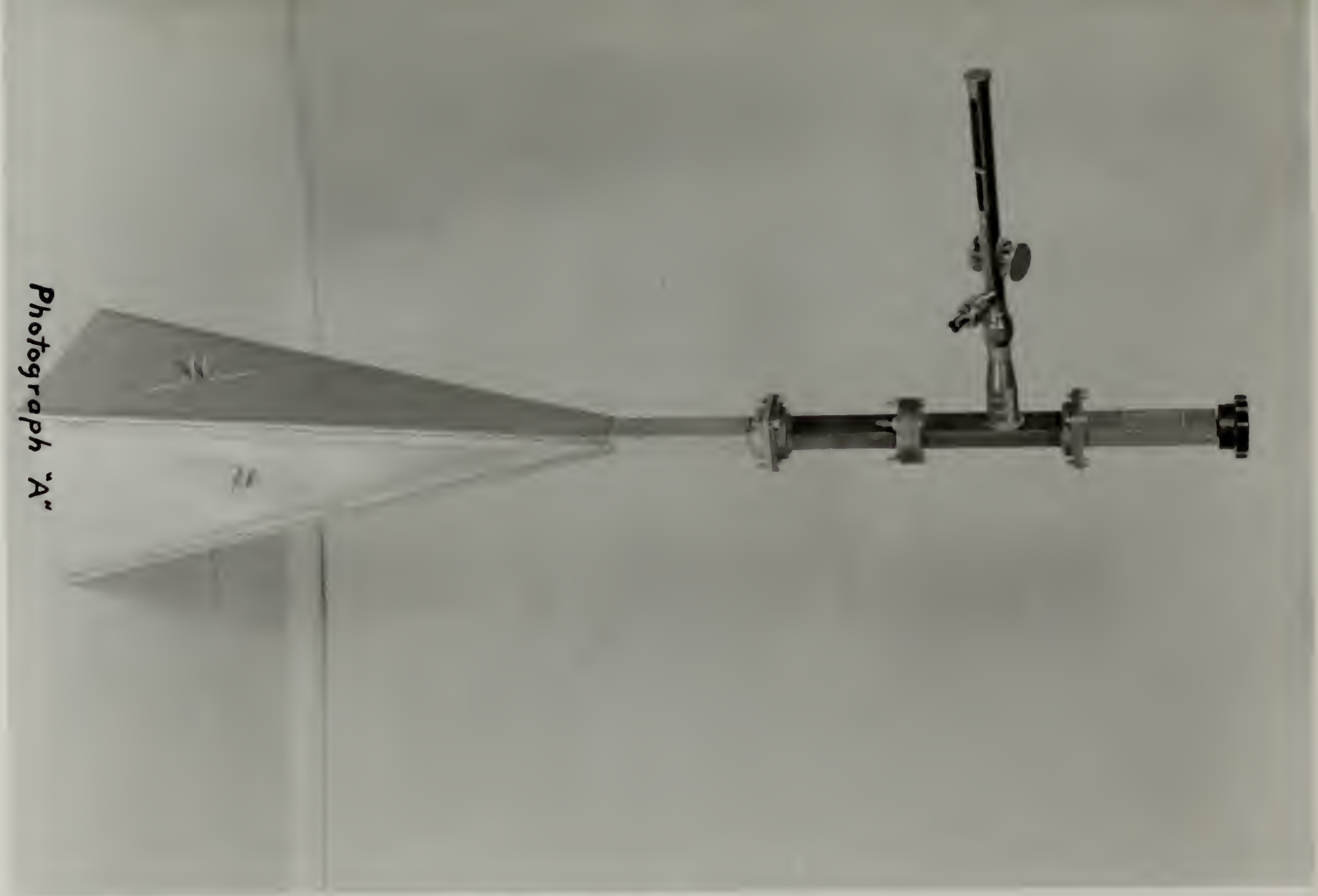

Photograph "A"

ES 96885 DOUGLAS
XF3D-1 155.1 4-2-53
COMPARISON RECEIVING ASSY. ANTENNA EFFICENCY MEASUREMENTS

Photograph "B"

ES 96884 DOUGLAS
XF3D-1 155.1 4-2-53
MODEL, ANTENNA EFFICIENCY MEASUREMENTS

~~RESTRICTED~~
~~SECURITY INFORMATION~~

Photograph "C"

96883

XF3D-1 155.1 4-2-53

~~RESTRICTED~~
~~SECURITY INFORMATION~~

ANTENNA, DETECTOR ASSY. ANTENNA EFFICIENCY MEASUREMENTS

The derivative of R_{in_2} with respect to X_2 is $\frac{2 R_b^3 X_2}{(R_b^2 + X_2^2)^2}$

When $X_2 = 0$ the derivative $= 0$, therefore the value of R_{in_2} varies from zero to a value asymptotic to R_b, $0 \leq R_{in_2} \leq R_b$. However the value of X_2 limits the value of R_{in_2}. In most cases R_{in_2} should be near 50 ohms. The tuner willprovide a match as long as $R_b > R_{in_2}$, with limitations fixed by the range of X_2 and X_3.

3. Matching the receiver to the terminating impedance.

a. General considerations:

The expression for efficiency derived above, $\eta = \frac{W_1 \ A_{2m}}{W_2 \ A_{1m}}$, is composed of two measured values (W_1 and W_2), one derived value (A_{1m}), and one computed value (A_{2m}). A_{2m} and A_{1m} are determined from sources independent of the efficiency measuring experiment and therefore are not considered as a part of the matching problem. The effective aperture decreases for an increase in mismatch, or for an increase in loss resistance. From the definition of the effective aperture ($W = P_o A$) it can be seen that the power received in the terminating impedance is proportional to the effective aperture. The power density of the incident wave is the same for the model and comparison antennas, and does not enter the problem. Therefore any change in the effective apertures due to mismatch will effect the values W_1 and W_2. These will change the value of η, and instead of giving the true value of the efficiency they will give a value which will include the losses due to mismatch as well as the heating losses in the antenna structure. Therefore it is desirable to eliminate mismatch as much as possible.

Occasionally the physical size of the antenna and the terminating impedance are such that they can not be located conveniently. Such is the case here, where a small size cable, RG 58/U, is used to connect the antenna to the bolometer resistance. If the cable were lossless the matching problem would be simplified. The maximum power transfer would occur when the line impedance was matched to the generator impedance. For a maximum power transfer the impedance looking to the right from an arbitrary point must be the complex conjugate of the impedance looking to the left from the same point; the reactances equal and opposite and the resistances equal. For the lossless transmission line a conjugate match at one point will insure a conjugate match at all other points. Therefore for a maximum power transfer into the terminating impedance all that is necessary is that the impedance at the input terminals of the connecting line be equal to the complex conjugate of the antenna impedance, or that the terminating impedance be equal to the conjugate impedance of the connecting line at the termination. However, with losses existing in the line, it does not follow that a conjugate match at one point will insure a match at all other points. The general approach will consider the networks lossless, and then will account for the losses.

b. For the horn antenna.

The comparison horn receiver should convey the received power to the bolometer resistance. The actual receiver is shown in Photograph A. Losses can lower the received power in the bolometer. Sources of power loss are the ohmic losses of the waveguide walls, of the

waveguide to coaxial transition, and of the PRD tuner. If the losses are sufficiently small they may be neglected. The matching of the bolometer resistance to the coaxial line was accomplished by a double stub PRD tuner. Matching the coaxial line to the waveguide was accomplished by a variable short and a probe of a preset length. These four variables were considered sufficient to match the comparison antenna.

c. For the model antenna.

The receiving circuit of the model is shown in Figures 11 and 12. The aircraft model and the tuner connected to the antenna are shown in Photographs B and C. In Figure 11 cable losses would need to be calculated to correct for the received power at the input or output terminals of the antenna. However with the tuner placed at the input terminals of the antenna the line losses would not occur and the double stub tuners could provide the correct matching. This was done to the extent that the tuner was embedded in the aircraft model (see Photograph C and Figure 12). A very small section of the cable remained between the antenna cavities and the connection to the PRD tuner. At 9000 mcs. the imput terminals to such an antenna, two parallel cavities with a balun connection into a coaxial line, were not easily specified. Arbitrarily the input terminals were defined to be the junction of the antenna lead and the tuner. Regardless of the possible error of this approximation, the following assumptions were made:

(1) the PRD tuner was a reactive circuit with losses negligible.

(2) the losses in the small section of cable were considered as part of the antenna losses.

(3) the bolometer resistance was matched to the model when the detected signal was a maximum in the bolometer amplifier.

4. Correction for transmission losses.

Where the losses can not be considered negligible it becomes necessary to correct for them. When the input power is attenuated and voltage standing waves exist the following equation* may be used to find the input power providing the output power is known.

$$P_{IN} = P_{OUT} \frac{1 - |\Gamma|^2 \eta_m^2}{(1 - |\Gamma|^2)\eta_m}$$

where η_m = the ratio of the power received to the power transmitted when there are no standing waves.

Γ = the reflection coefficient.

P_{in} = the transmitted (input) power.

P_{out} = the received (output) power.

*Principles of Radar, (17) pp 8-47 to 8-49.

CHAPTER IV

EXPERIMENTS

1. Preliminary experiments.

All experiments other than those taken to determine the antenna efficiency are placed together as preliminary data. The power transfer and the degree of matching had to be checked prior to taking the final measurements. The preliminary experiments are divided into those pertaining to waveguides and those to coaxial lines. The data taken appears in the appendix. The results and conclusions are given here.

a. Waveguide experiments.

(1) It became necessary to obtain some idea of the relative power transfer in the waveguide and in the coaxial fitting of the PRD tuner. This brought forth the problem of probe transition within the waveguide, as well as the overall transfer of energy. Several experiments were made using different frequencies. The general setup was to transmit square-wave modulated signals through the waveguide to the detector. Photograph A shows the comparison horn with detector section. In these experiments the horn was disconnected and the detector section was excited through the waveguide directly. The relative power level and the VSWR were observed for the following variables: probe tip length, probe diameter, length of short in the waveguide, and the length of the shunt and series short circuit stubs of the PRD tuner (see Figures 7, 8, 10 and 13). The results of these experiments were:

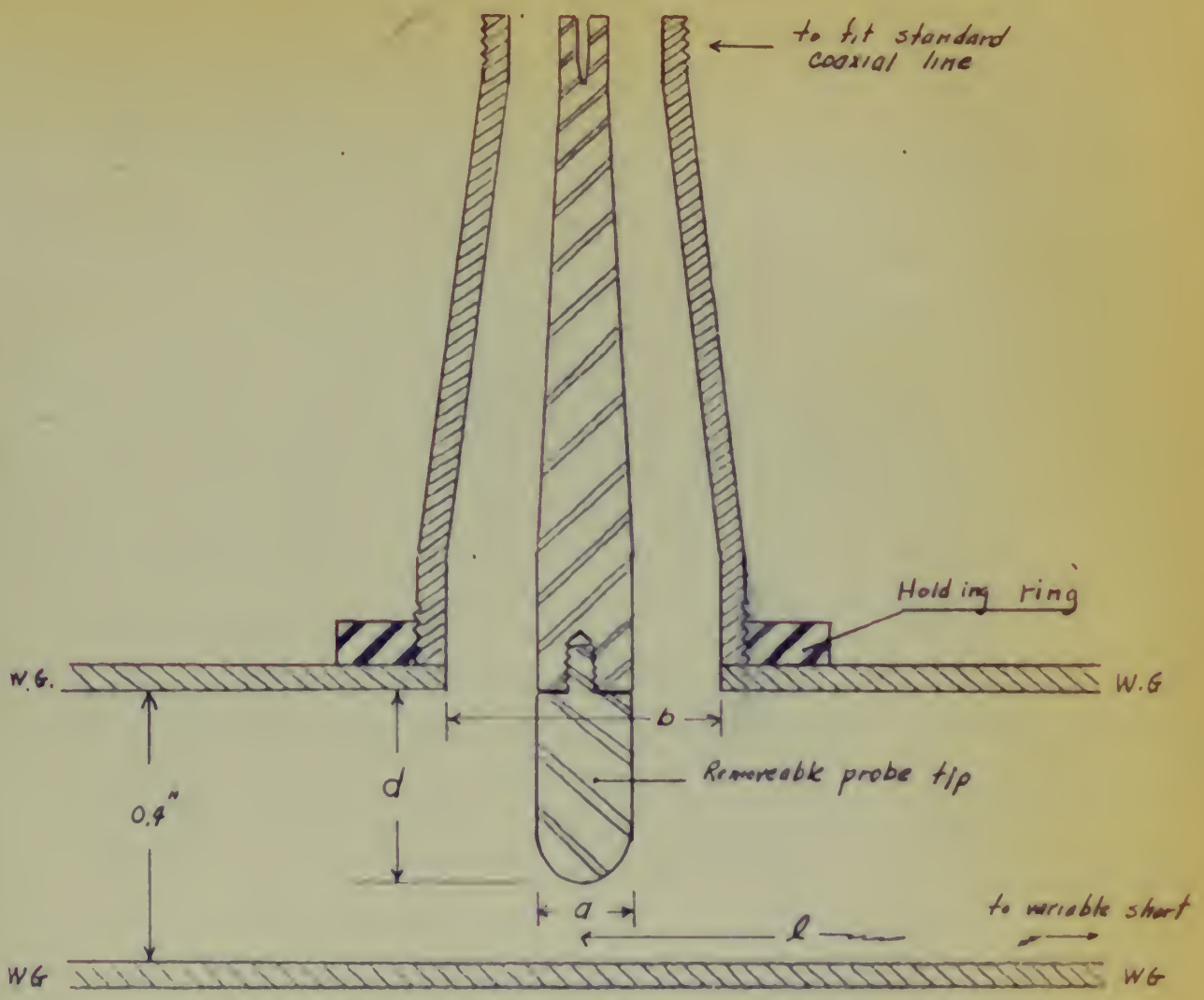

$a = 16/64$" $\quad b = 2.3\,a \quad Z_o$ section = 50 to 51 Ω

d - probe depth variable (approx. 72% of waveguide depth)

WAVEGUIDE TO COAXIAL LINE TRANSITION

FIG. 13.

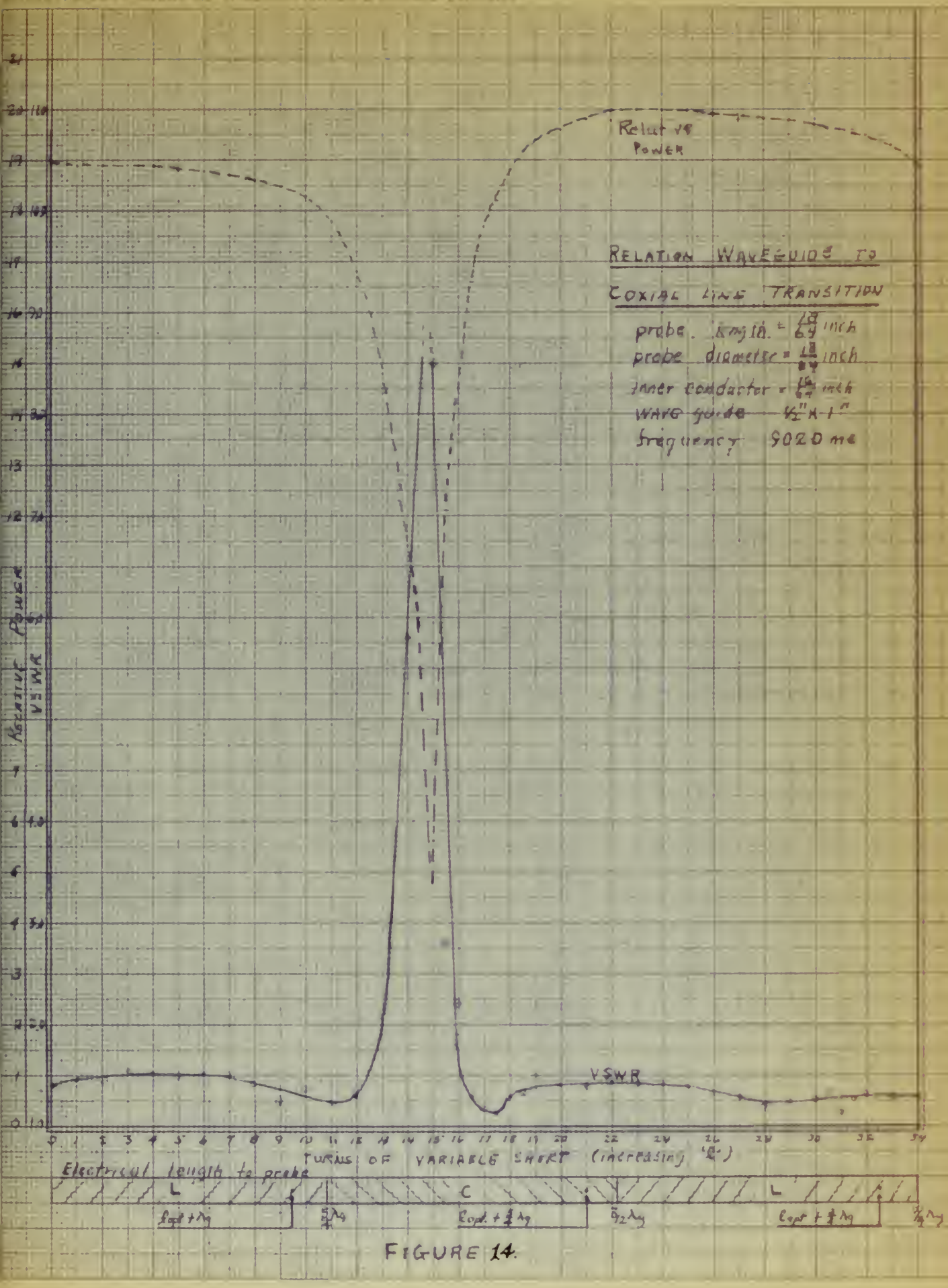
Relat vs Power
RELATION WAVEGUIDE TO COXIAL LINE TRANSITION
probe length = 19/64 inch
probe diameter = 1/8 inch
inner conductor = 5/64 inch
wave guide ½" x 1"
frequency 9020 mc
RELATIVE POWER
VSWR
VSWR
TURNS OF VARIABLE SHORT (increasing 'L')
Electrical length to probe
L
C
L
λg/4
λg/2
3λg/4

FIGURE 14.

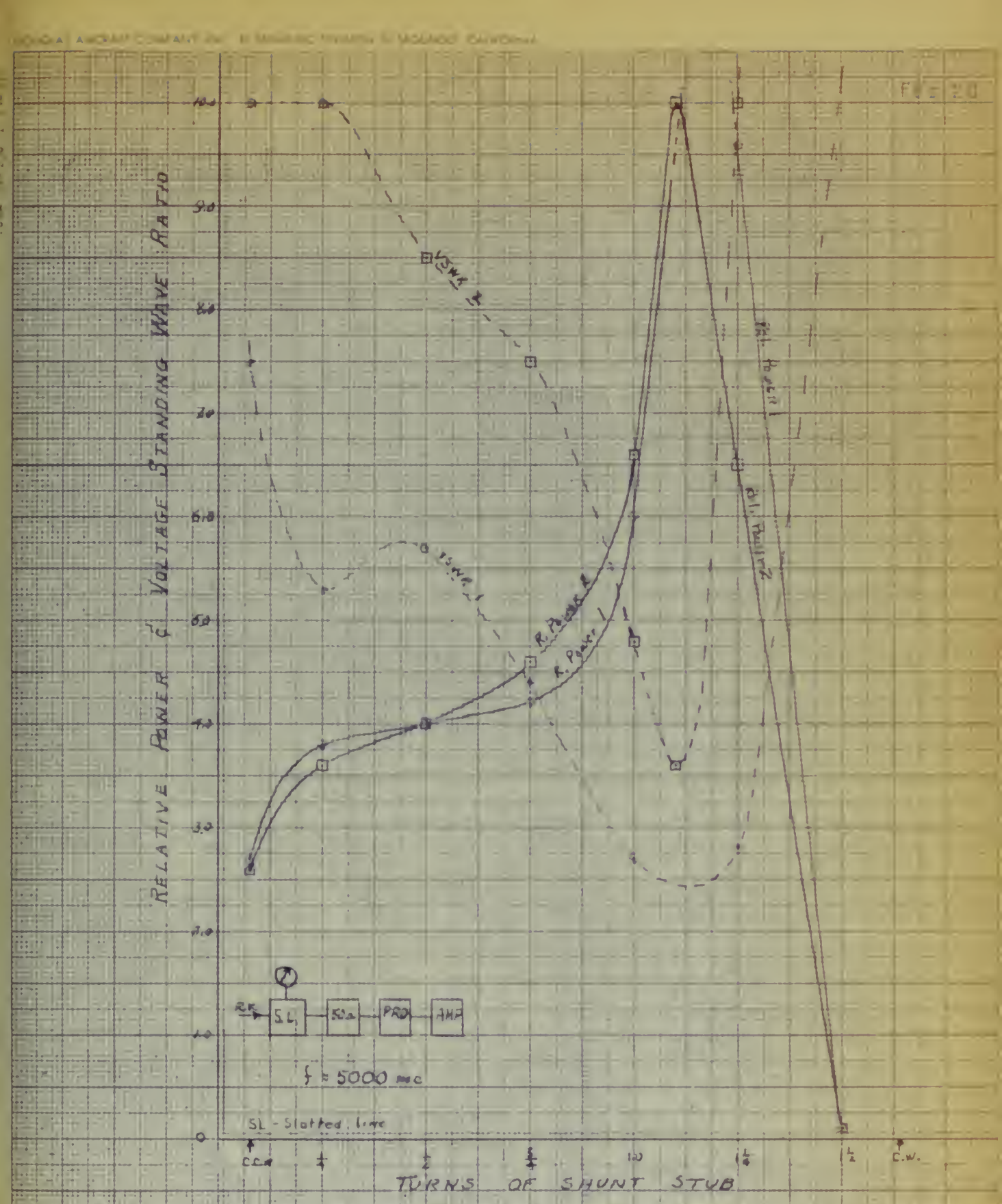

TUNING CHARACTERISTICS OF PRD TUNER Ser No 200 Mod 612A
(Tuned for two max positions (power) varied shunt stub, series stub fixed.

FIGURE 15

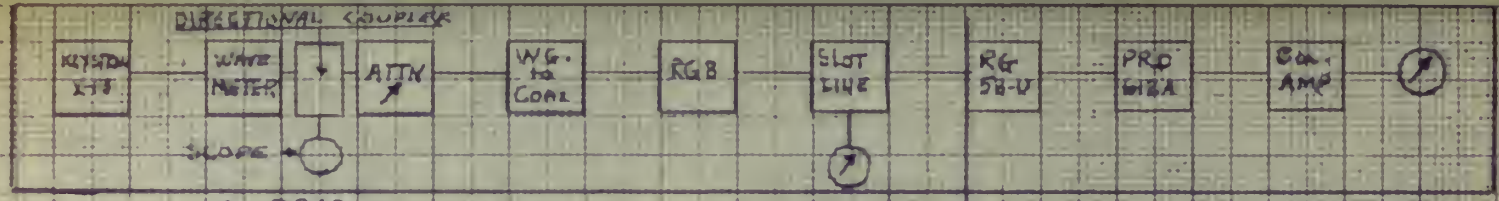

MAR 3

f = 9840mc

f = 8200mc

RELATIVE POWER

VOLTAGE STANDING WAVE RATIO

VSWR

Rel. Power

VSWR

RELATIVE POWER

SHUNT STUB TURNS CLOCKWISE →

SHUNT STUB TURNS CLOCKWISE →

FIG. 16.

FIG. 17.

TUNING CHARACTERISTICS OF P.R.D. BOLOMETER & TUNER MODEL 612A SERIAL NO 200

Tuned for maximum power then held series stub fixed and varied shunt stub.

31

(a) The probe tip diameter should be the same size as the center conductor of the probe transition. The probe length should be about one sixth of the wave length in the guide, or it should project into the waveguide about 73 per cent of the waveguide depth. Although these results were obtained experimentally, they can be obtained from the literature.*

(b) The probe length, the short length, and the series and shunt stub length of the PRD tuner were sufficient variables and provided appropriate matching. Figure 14 shows the VSWR and the relative power to the detector versus the short length (in turns and in wave lengths).

(2) The impedance measuring experiments were inconclusive. The experiments were performed within the Fresnel region and inside a closed area. Reflections and coupling were too great to give satisfactory results.

b. Coaxial line experiments.

(1) The r.f. energy was fed directly to a slotted line and then into various terminations. When the PRD tuner was connected to the cable the VSWR varied from 3 to 1 to 1.3 to 1. Near the frequency of expected operation, 9000 mcs., the VSWR was about 1.3 or 1.5 to 1, when tuned for maximum power indication on the audio amplifier. Figures 15, 16 and 17 show the relationship of the VSWR and the relative power

*Principles of Radar (17) Ch 10 Art 13, WW Mumford (14), G. L. Ragan (15) Sections 6.3-6.4 and J. C. Slater (22).

as the frequency was changed.

(2) Experiments were made simulating model range conditions while inside an enclosed area. Probability for error was very high due to reflecting objects, strong coupling between antennas, and the antenna separation being within the near (Fresnel) zone. There was no correlation of the data taken. An additional experiment was made on the model range. The model aircraft, with a slotted line in the receiving circuit, was illuminated in accordance with model range requirements. The low r. f. power level and the relatively large amount of power absorbed by the slotted line made it advisable to locate the tuning section as closely as possible to the antenna terminals. Estimated VSWR under this condition should be no more than that observed above, about 1.2 to 1.5 to 1. Transmission losses due to this value of VSWR were negligible. The matching conditions were considered satisfactory when the detected power indication was a maximum.

2. Efficiency experiments.

a. Patterns of the model antenna to obtain the directivity.

Prior to the actual efficiency experiments a set of conical patterns was taken of the model antenna. These patterns are included as Figures 10 through 35. Figures 36 through 38 show the coordinate system, the transmitter and receiver orientation, and the conical patterns varied over the sphere of radiation. Procedure for taking model range data is included in the appendix. The only variation from the normal procedure was a change in the recording scale due to the low

DOUGLAS AIRCRAFT COMPANY INC

DATE 3-25-53 PLANT PAGE

PREPARED BY MODEL

TITLE REPORT

MODEL SCALE 1/20 MODEL FREQ. 9030 MC FULL SCALE FREQ. 420-460 MC

ANTENNA TYPE APN-1 XF30 ANTENNA LOCATION FWD NACELLE

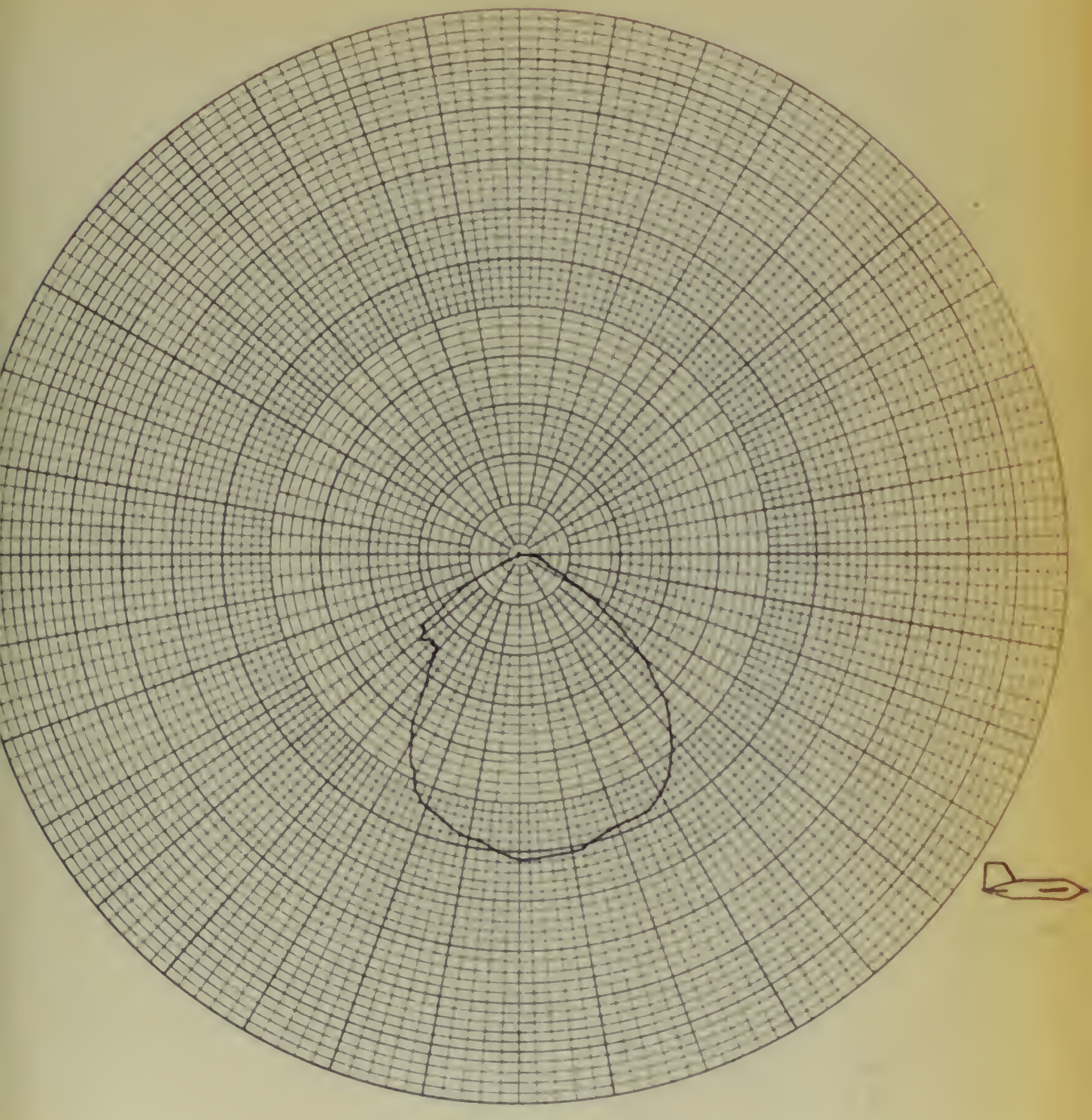

FIGURE 18

MODEL SURFACE ELEVATION PLANE

COORDINATE SYSTEM AZIMUTH PLANE

CURVE PLOTTED IN: VOLTAGE (✓) POWER ( ) DB ( ) POLARIZATION E_ϕ

DOUGLAS AIRCRAFT COMPANY, INC

DATE 3-25-53 PLANT PAGE

PREPARED BY MODEL

TITLE REPORT

MODEL SCALE 1/20 MODEL FREQ. 9030 MC FULL SCALE FREQ. 420-960 MC

ANTENNA TYPE APN 1 ANTENNA LOCATION FWD LEFT NACELLE

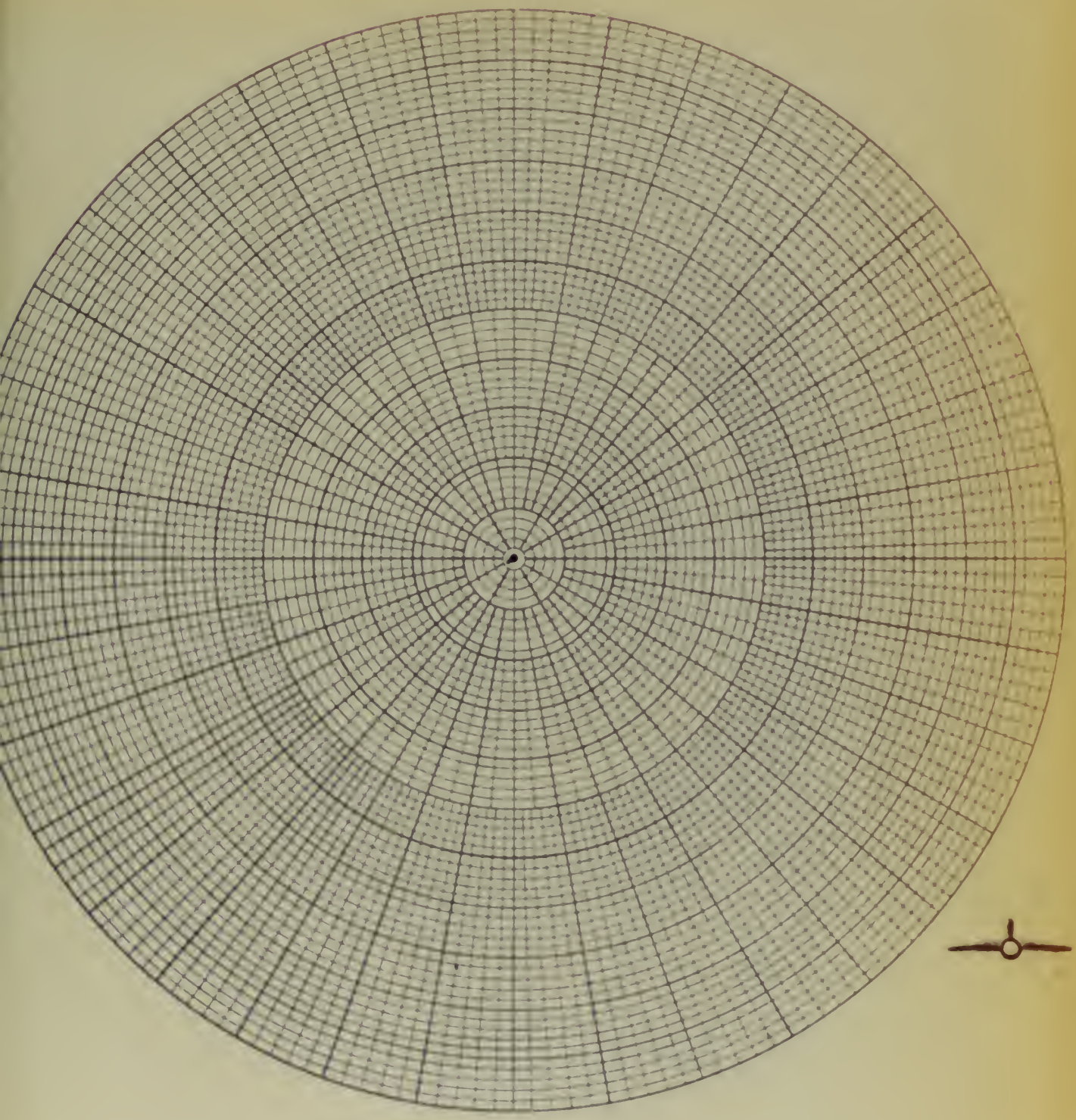

FIGURE 19

MODEL SURFACE ELEVATION PLANE

COORDINATE SYSTEM AZIMUTH PLANE

CURVE PLOTTED IN: VOLTAGE (X) POWER ( ) DB ( ) POLARIZATION Eφ

DOUGLAS AIRCRAFT COMPANY, INC

DATE 3-25-53 PLANT PAGE

PREPARED BY MODEL

TITLE REPORT

MODEL SCALE 1/20 MODEL FREQ. 9030 MC FULL SCALE FREQ. 420-460 MC

ANTENNA TYPE ADN-1 XF30 ANTENNA LOCATION FWD NACELLE

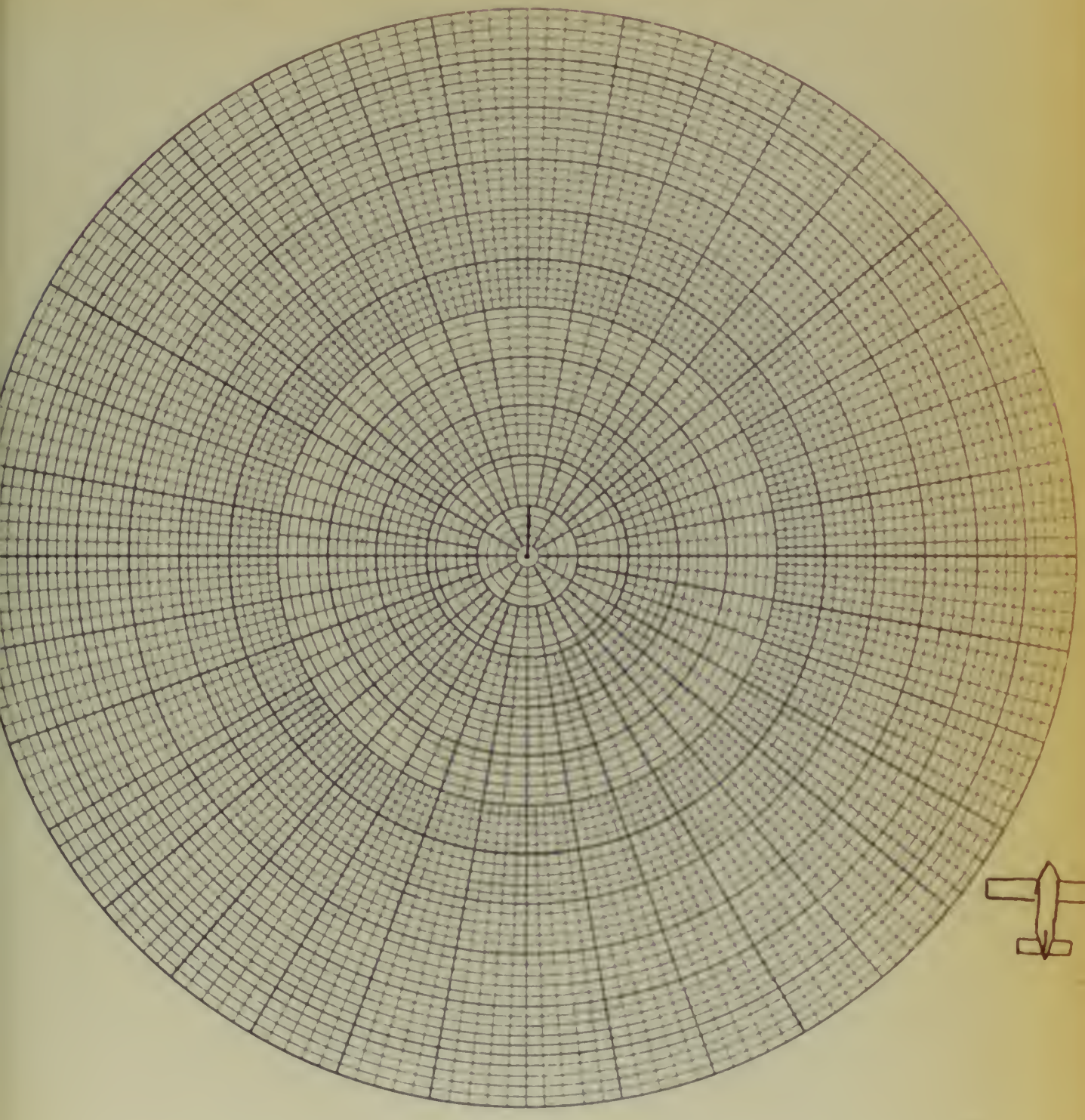

FIGURE 20.

MODEL SURFACE ELEVATION PLANE 0°

COORDINATE SYSTEM AZIMUTH PLANE

CURVE PLOTTED IN: VOLTAGE (✓) POWER ( ) DB ( ) POLARIZATION Eφ

DOUGLAS AIRCRAFT COMPANY, INC

DATE 3-25-53 PLANT PAGE

PREPARED BY MODEL

TITLE REPORT

MODEL SCALE 1/20 MODEL FREQ. 9030 MC FULL SCALE FREQ. 420-460 MC

ANTENNA TYPE APN-1 XF3D ANTENNA LOCATION FWD NACELLE

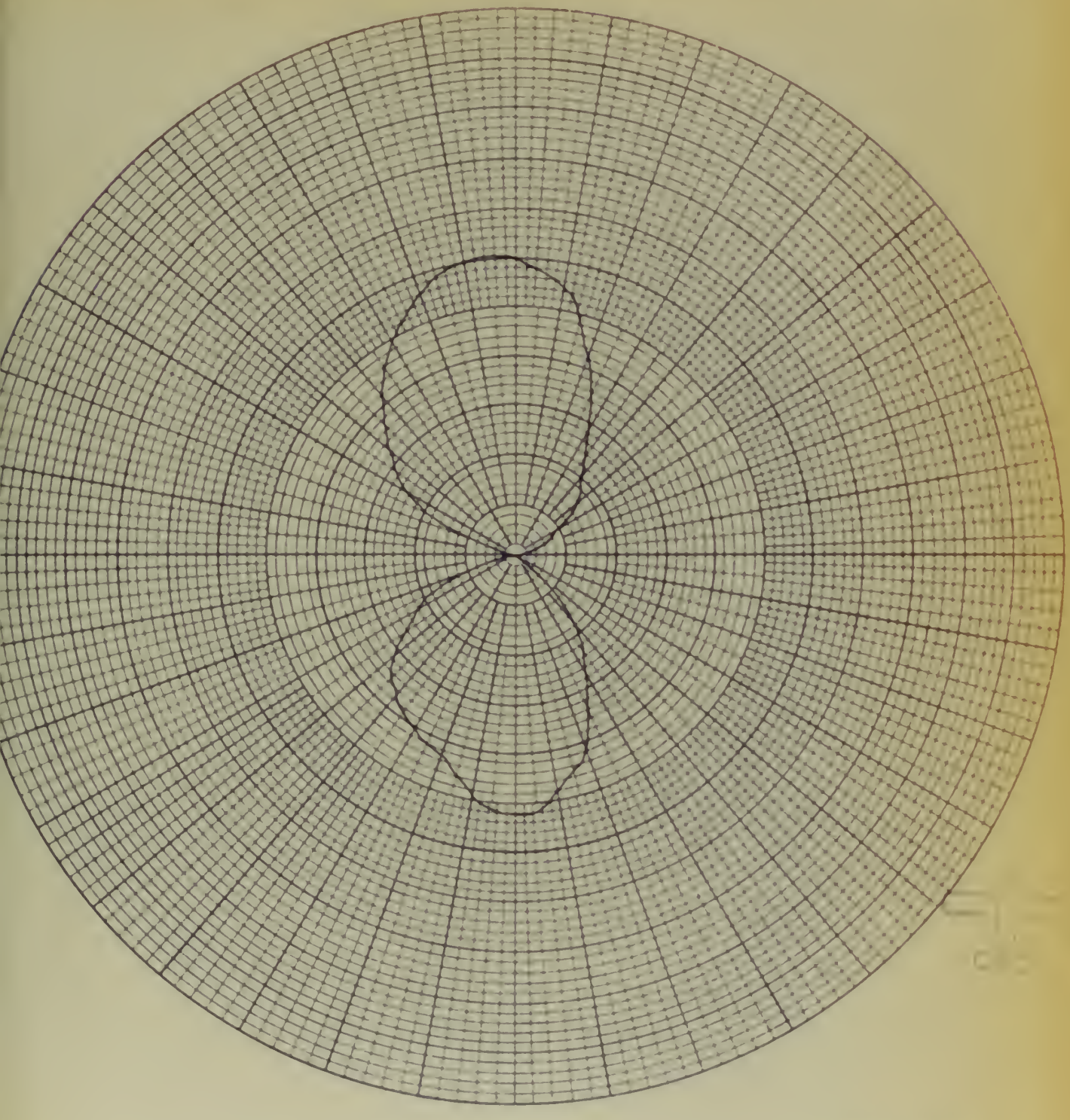

FIGURE 21. Int 57

MODEL SURFACE

COORDINATE SYSTEM

CURVE PLOTTED IN: VOLTAGE (✓) POWER ( ) DB ( )

ELEVATION PLANE −65°

AZIMUTH PLANE

POLARIZATION Eφ

DOUGLAS AIRCRAFT COMPANY, INC

DATE 3/25/53 PLANT PAGE

PREPARED BY MODEL

TITLE REPORT

MODEL SCALE 1/20 MODEL FREQ. 9030 MC. FULL SCALE FREQ. 470-460 MC

ANTENNA TYPE APN-1 XF30 ANTENNA LOCATION FWD NACELLE

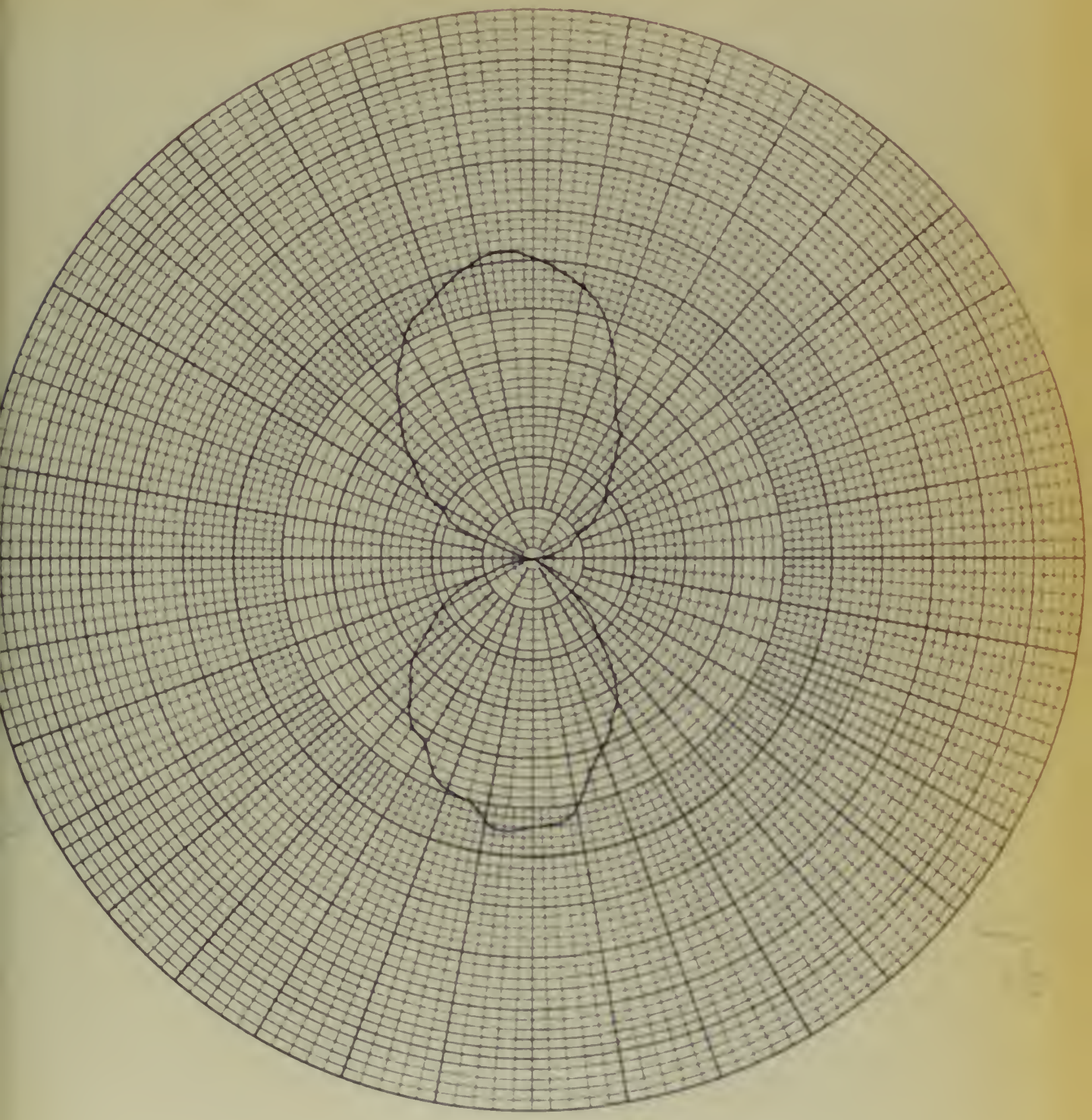

FIGURE 22.

INT 60

MODEL SURFACE

COORDINATE SYSTEM

CURVE PLOTTED IN: VOLTAGE (✓) POWER ( ) DB ( )

ELEVATION PLANE −70°

AZIMUTH PLANE

POLARIZATION Eφ

DOUGLAS AIRCRAFT COMPANY, INC

DATE 3-25-53 PLANT

PREPARED BY

TITLE

MODEL SCALE 1/20 MODEL FREQ. 9030 MC FULL SCALE FREQ. 420-460 MC

ANTENNA TYPE APN-1 / XF3D-1 ANTENNA LOCATION FWD NACELLE

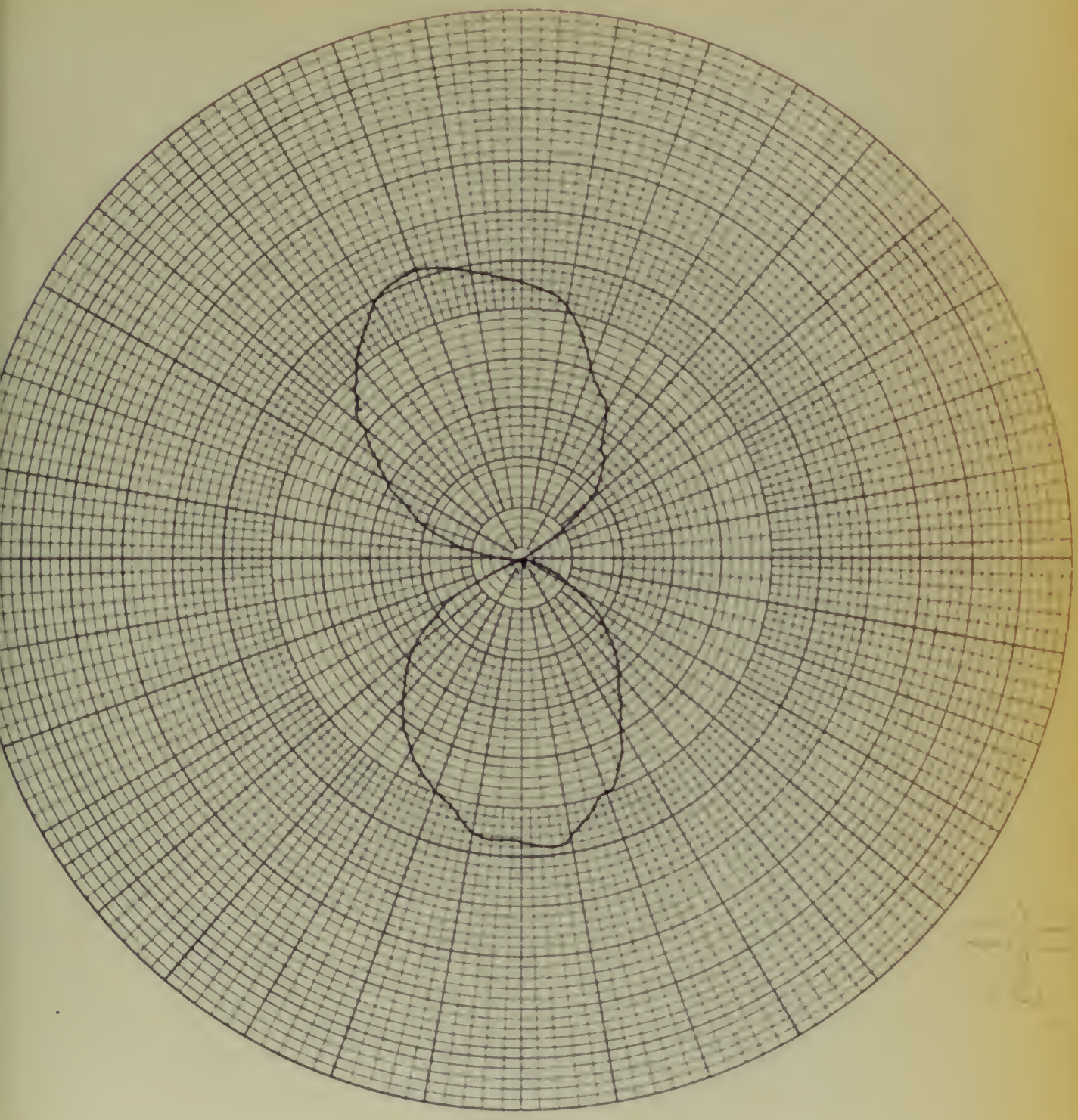

FIGURE 23. INT. 73

MODEL SURFACE

COORDINATE SYSTEM

CURVE PLOTTED IN: VOLTAGE (✓) POWER ( ) DB ( )

ELEVATION PLANE -75°

AZIMUTH PLANE

POLARIZATION Eφ

DOUGLAS AIRCRAFT COMPANY, INC.

DATE 3/25/53 PLANT PART

PREPARED BY MODEL

TITLE REPORT

MODEL SCALE 1/20 MODEL FREQ. 9030 Mc. FULL SCALE FREQ. 420-460 Mc

ANTENNA TYPE APN-1 ANTENNA LOCATION Fwd Nacelle

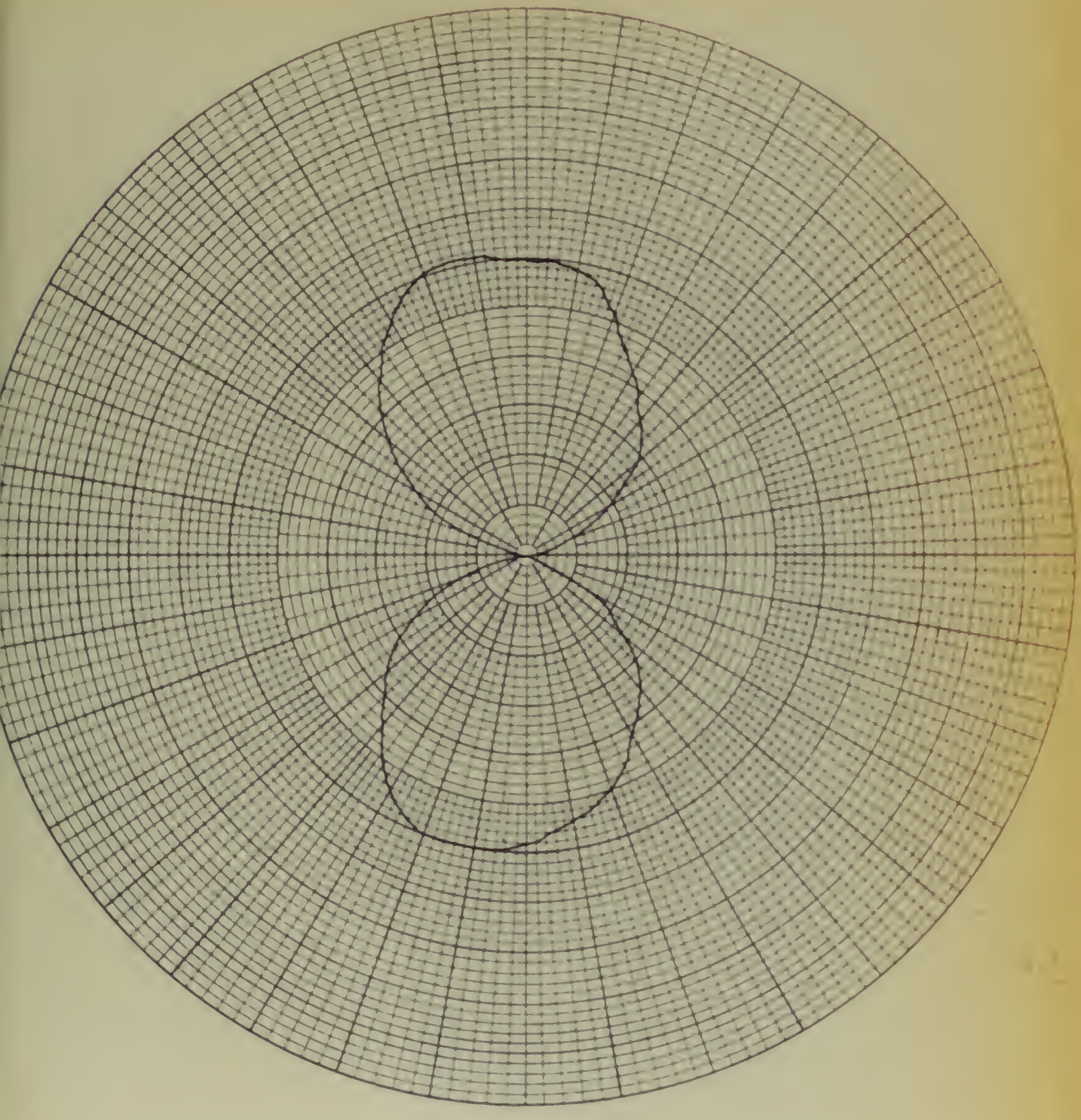

FIGURE 24

Int. 77

MODEL SURFACE

COORDINATE SYSTEM

CURVE PLOTTED IN: VOLTAGE (✓) POWER ( ) DB ( )

ELEVATION PLANE −80°

AZIMUTH PLANE

POLARIZATION Eφ

DOUGLAS AIRCRAFT COMPANY, INC

DATE 3-25-53 PLANT PAGE

PREPARED BY MODEL

TITLE REPORT

MODEL SCALE 1/20 MODEL FREQ. 9030 MC FULL SCALE FREQ. 420-460 MC

ANTENNA TYPE APN-1 ANTENNA LOCATION FWD LEFT NACELLE

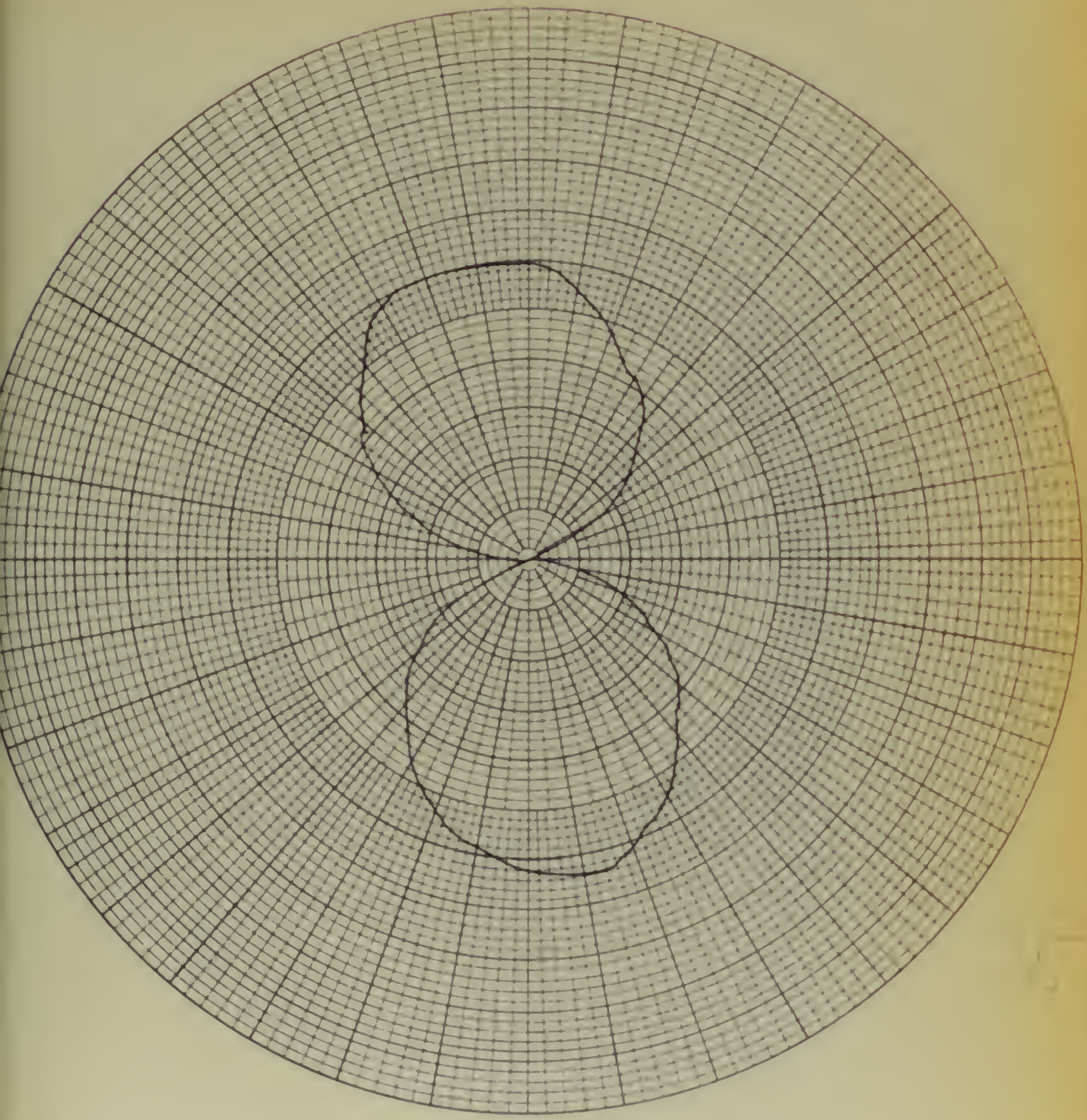

FIGURE 25. INT 87

MODEL SURFACE

COORDINATE SYSTEM

CURVE PLOTTED IN: VOLTAGE (✓) POWER ( ) DB ( )

ELEVATION PLANE -85°

AZIMUTH PLANE

POLARIZATION Eφ

DOUGLAS AIRCRAFT COMPANY, INC

DATE 3-25-53 PLANT PAGE

PREPARED BY MODEL

TITLE REPORT

MODEL SCALE 1/20 MODEL FREQ. 9030 MC FULL SCALE FREQ. 420-460 MC

ANTENNA TYPE APN-1 ANTENNA LOCATION Left nacelle, feed

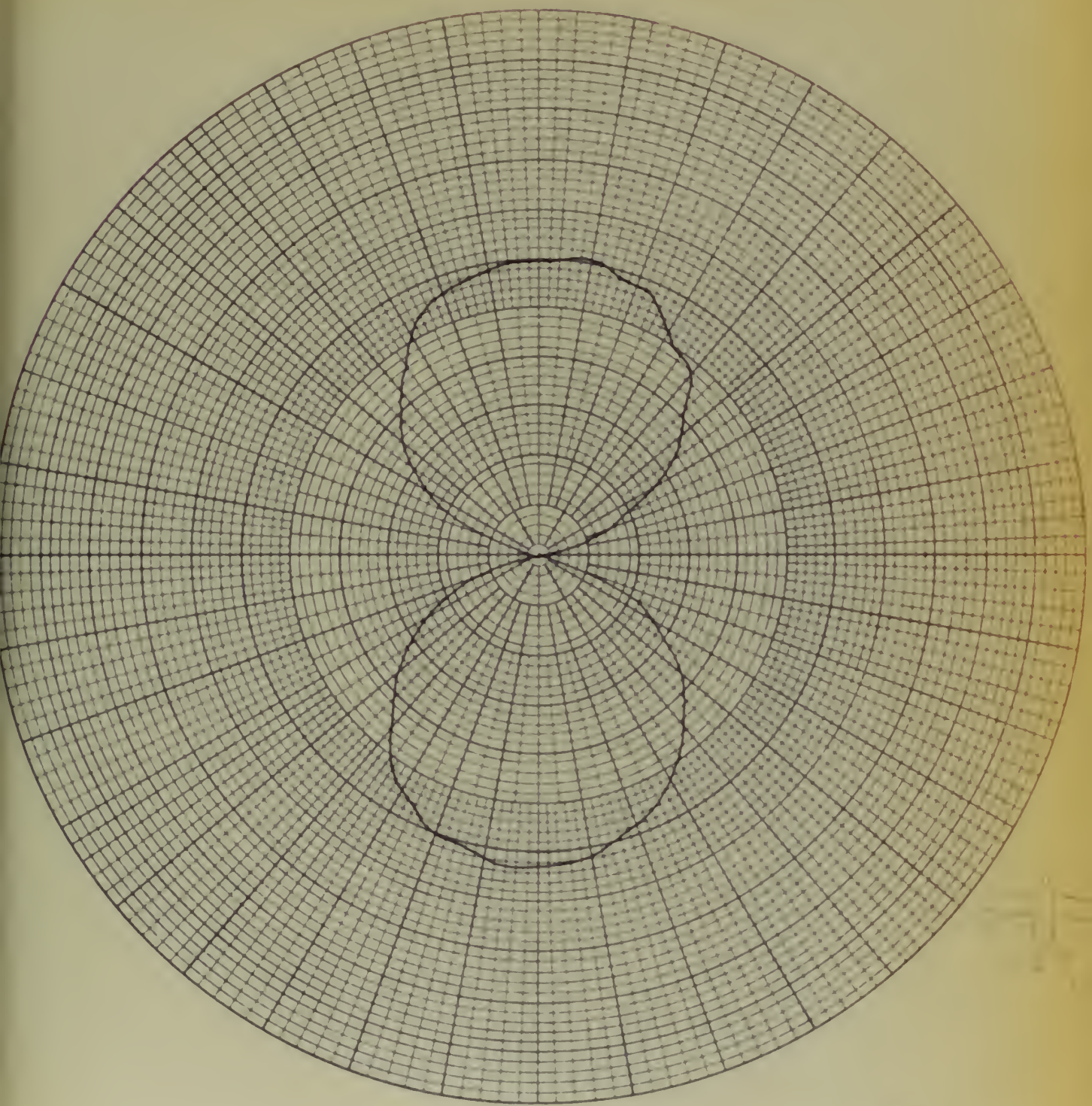

INT. 86

FIGURE 26.

MODEL SURFACE

COORDINATE SYSTEM

CURVE PLOTTED IN: VOLTAGE (X) POWER ( ) DB ( )

ELEVATION PLANE -90

AZIMUTH PLANE

POLARIZATION Eφ

DOUGLAS AIRCRAFT COMPANY, INC.

DATE 3-25-53 PLANT PAGE

PREPARED BY MODEL

TITLE REPORT

MODEL SCALE 1/20 MODEL FREQ. 9030 MC FULL SCALE FREQ. 420-460 MC

ANTENNA TYPE APN-1 XF3D ANTENNA LOCATION Tail Nacelle

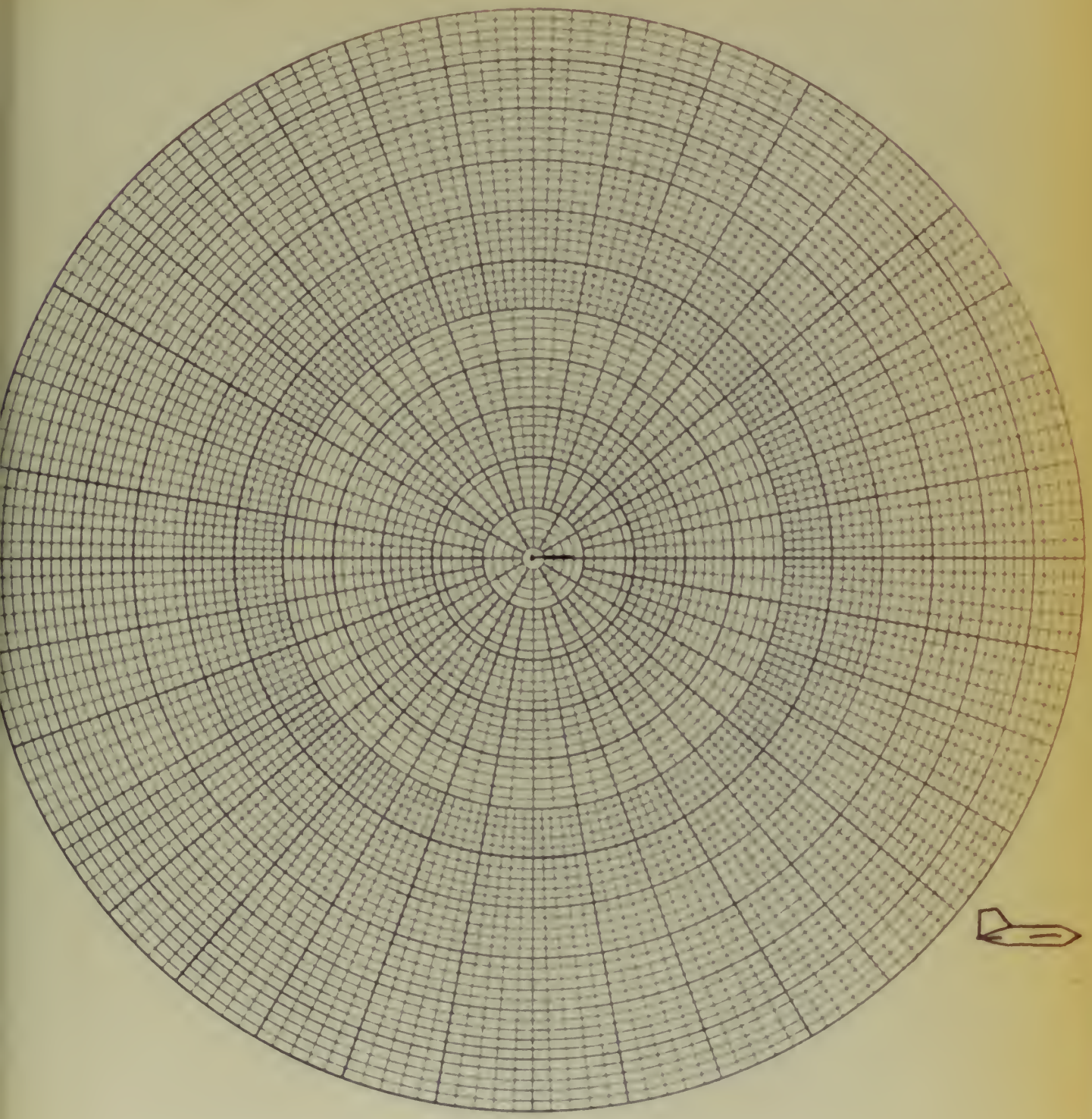

FIGURE 27.

MODEL SURFACE

COORDINATE SYSTEM

CURVE PLOTTED IN: VOLTAGE (✓) POWER ( ) DB ( )

ELEVATION PLANE

AZIMUTH PLANE

POLARIZATION E_θ

DOUGLAS AIRCRAFT COMPANY, INC

DATE 3-25-53 PLANT

PREPARED BY

TITLE

MODEL SCALE 1/20 MODEL FREQ. 9030 MC FULL SCALE FREQ. 420-460 MC

ANTENNA TYPE APN-1 XF3D ANTENNA LOCATION FWD UNDERSIDE

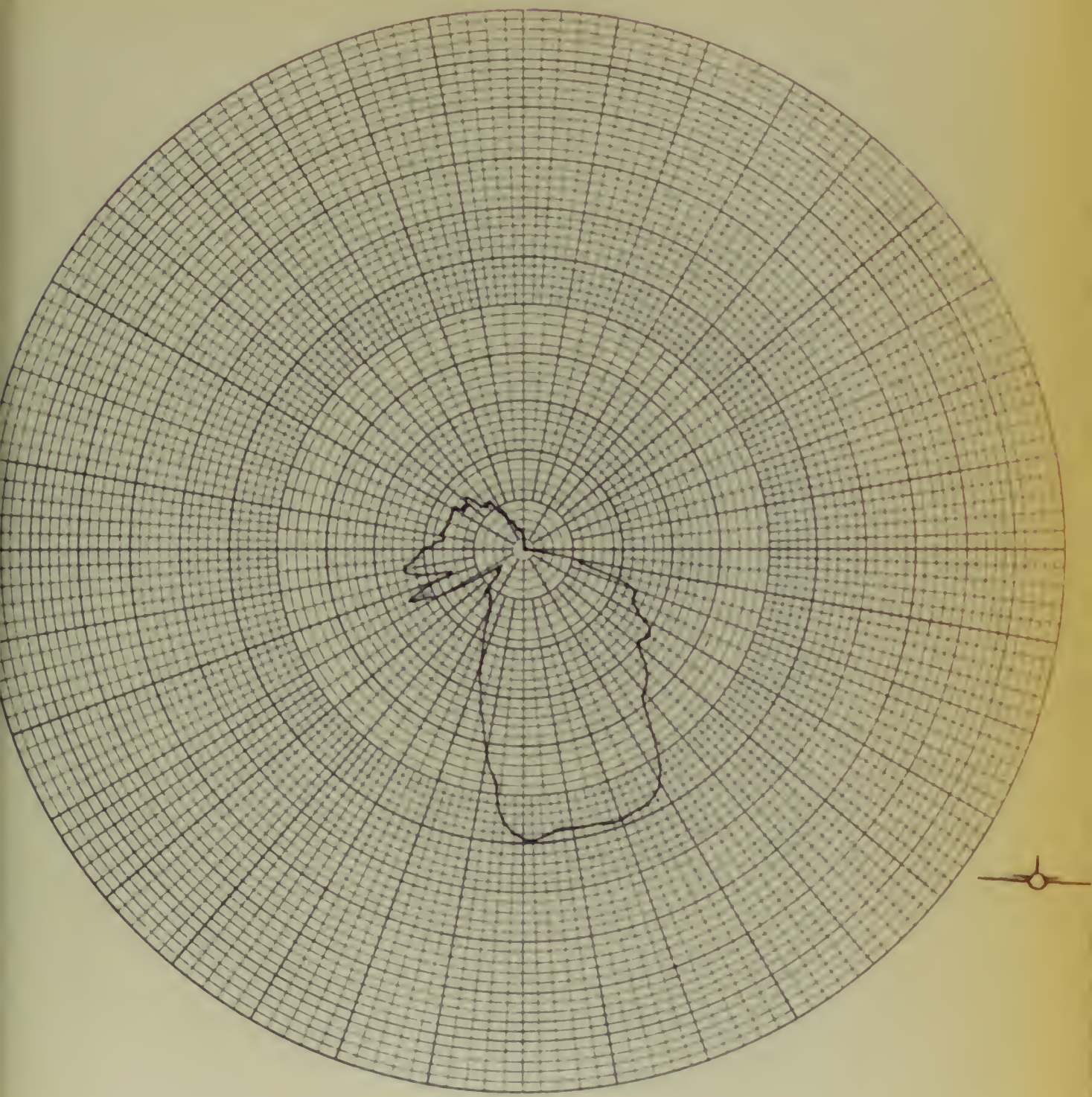

FIGURE 28.

MODEL SURFACE

COORDINATE SYSTEM

CURVE PLOTTED IN: VOLTAGE (✓) POWER ( ) DB ( )

ELEVATION PLANE

AZIMUTH PLANE

POLARIZATION E_θ

DOUGLAS AIRCRAFT COMPANY, INC.

DATE 3-25-53 PLANT PAGE

PREPARED BY MODEL

TITLE REPORT

MODEL SCALE 1/20 MODEL FREQ. 9030 MC FULL SCALE FREQ. 430-460 MC

ANTENNA TYPE HPN-1 XF3D ANTENNA LOCATION Fwd Nacelle

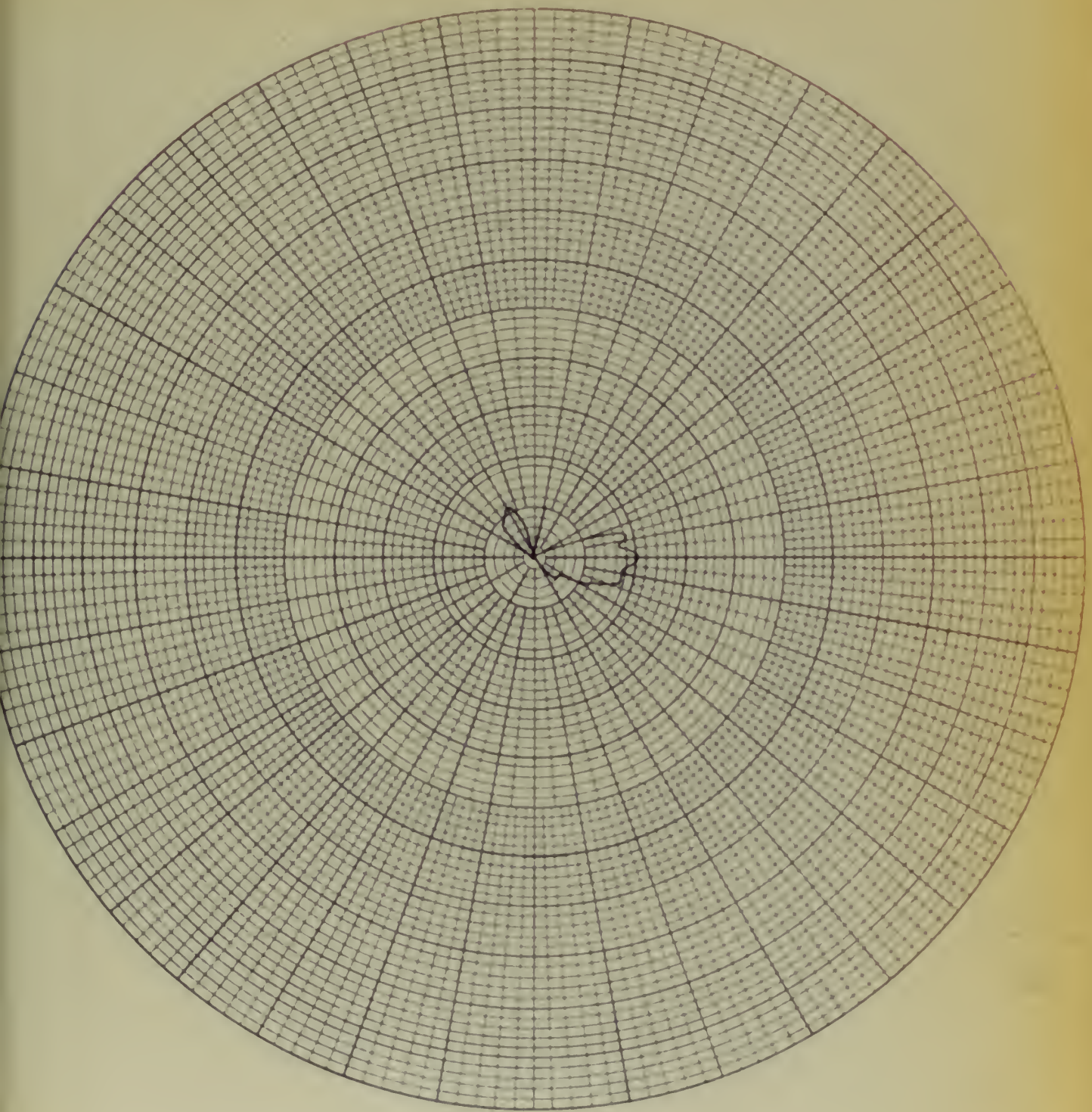

FIGURE 29.

MODEL SURFACE

COORDINATE SYSTEM

CURVE PLOTTED IN: VOLTAGE (✓) POWER ( ) DB ( )

ELEVATION PLANE 0°

AZIMUTH PLANE

POLARIZATION Eθ

DOUGLAS AIRCRAFT COMPANY, INC.

DATE 3-25-53 PLANT PAGE

PREPARED BY MODEL

TITLE REPORT

MODEL SCALE 1/20 MODEL FREQ. 9030 MC FULL SCALE FREQ. 426-460 MC

ANTENNA TYPE APN-1 XF-30 ANTENNA LOCATION Fwd Nacelle

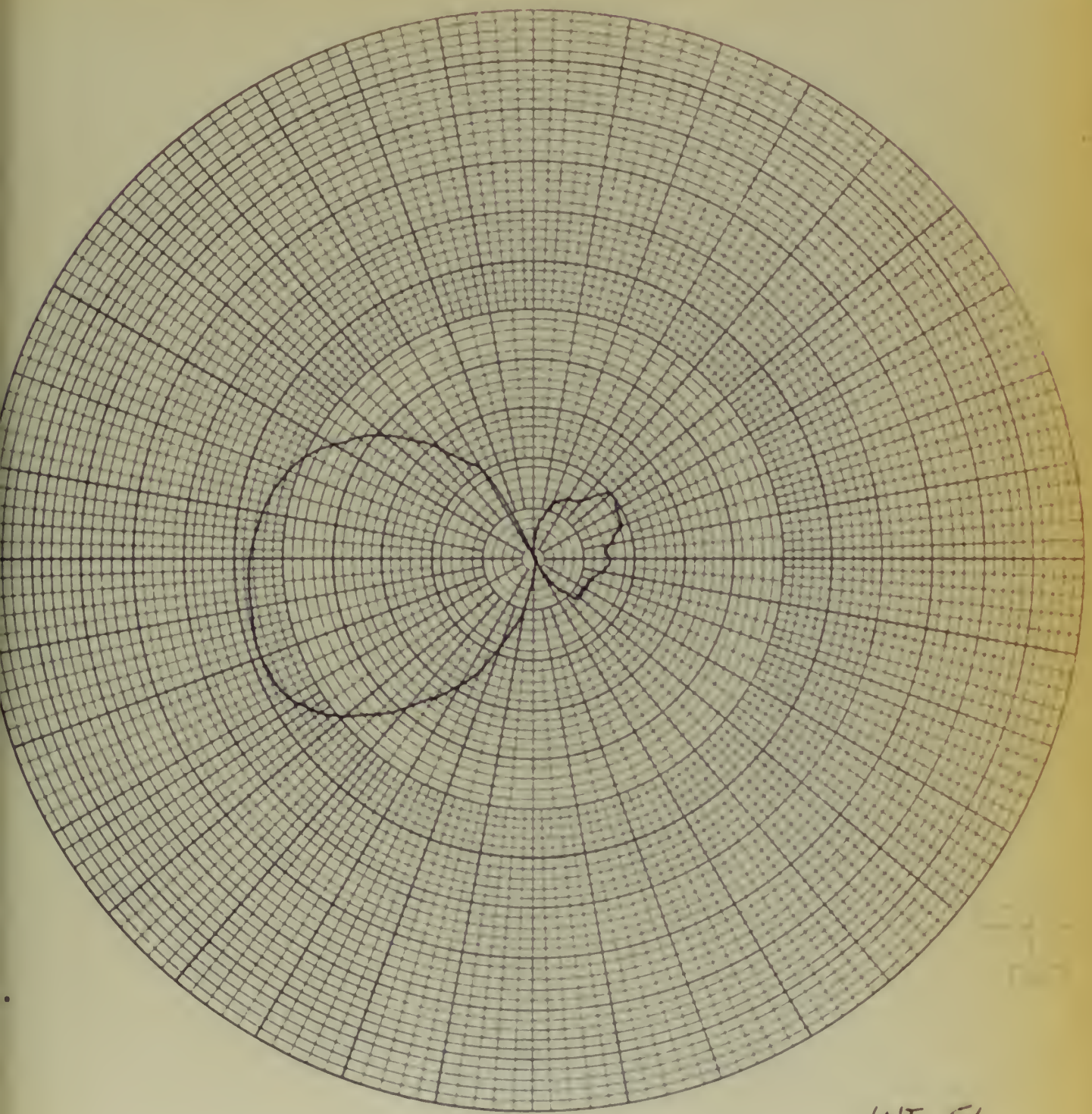

INT 51

FIGURE 30.

MODEL SURFACE

COORDINATE SYSTEM

CURVE PLOTTED IN: VOLTAGE (X) POWER ( ) DB ( )

ELEVATION PLANE -65°

AZIMUTH PLANE

POLARIZATION Eθ

DOUGLAS AIRCRAFT COMPANY, INC.

DATE 3-25-53 PLANT PAGE

PREPARED BY MODEL

TITLE REPORT

MODEL SCALE 1/20 MODEL FREQ. 9030 MC FULL SCALE FREQ. 420-460 MC

ANTENNA TYPE APN-1 XF3D ANTENNA LOCATION FWD Nacelle

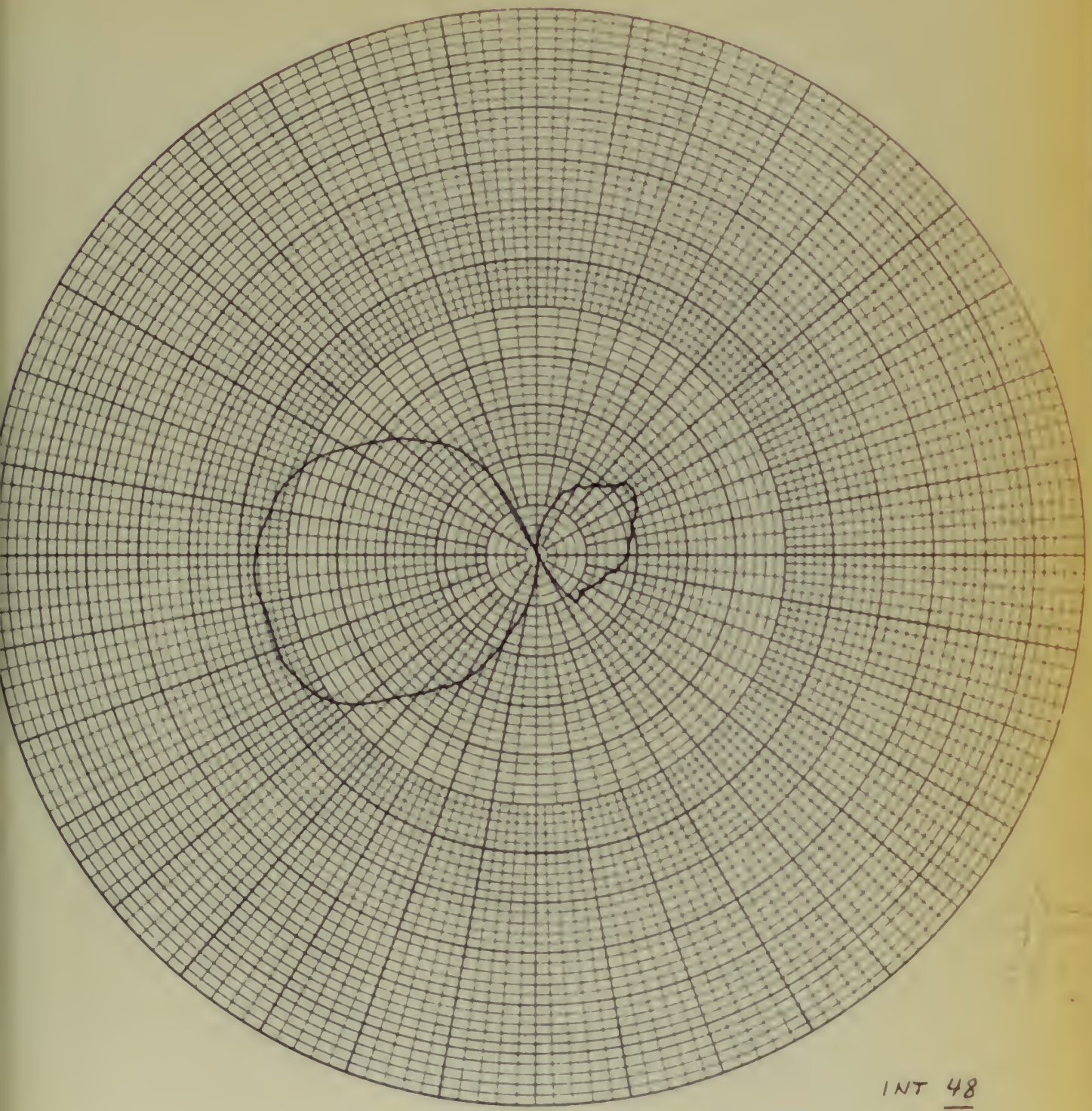

INT 48

FIGURE 31.

MODEL SURFACE ELEVATION PLANE -70°

COORDINATE SYSTEM AZIMUTH PLANE

CURVE PLOTTED IN: VOLTAGE (✓) POWER ( ) DB ( ) POLARIZATION Eθ

DOUGLAS AIRCRAFT COMPANY, INC

DATE 3-25-53 PLANT PAGE

PREPARED BY MODEL

TITLE REPORT

MODEL SCALE 1/20 MODEL FREQ. 9030 MC FULL SCALE FREQ. 430-460 MC

ANTENNA TYPE APN-1 XF3D ANTENNA LOCATION FWD NACELLE

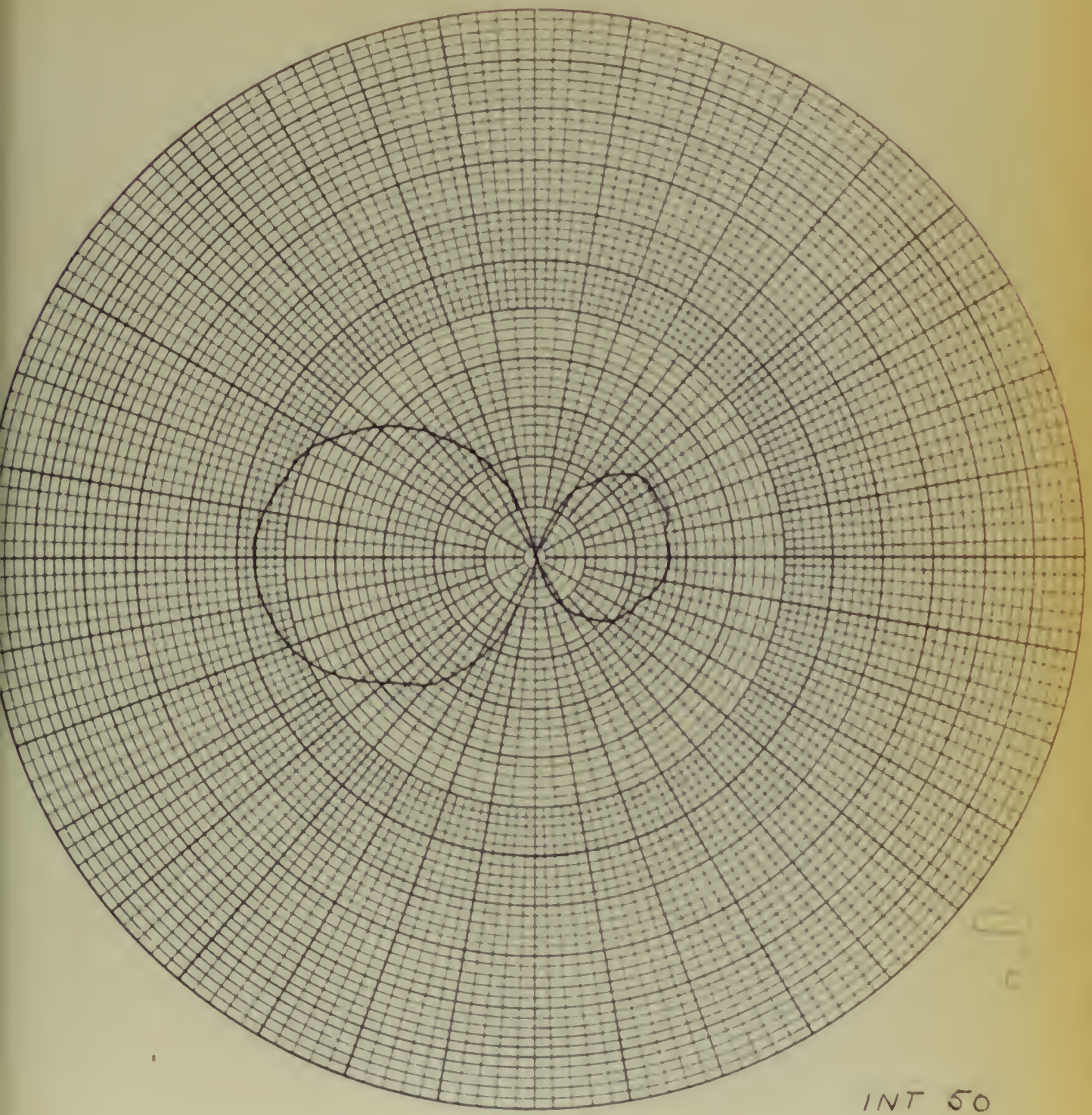

FIGURE 32.

MODEL SURFACE

COORDINATE SYSTEM

CURVE PLOTTED IN: VOLTAGE (✓) POWER ( ) DB ( )

ELEVATION PLANE -75°

AZIMUTH PLANE

POLARIZATION Eθ

DOUGLAS AIRCRAFT COMPANY, INC

DATE 8-25-53 PLANT PAGE

PREPARED BY MODEL

TITLE REPORT

MODEL SCALE 1/20 MODEL FREQ. 9030 MC FULL SCALE FREQ. 420-460 MC

ANTENNA TYPE APN-1 XF3D ANTENNA LOCATION Fwd. Nacelle

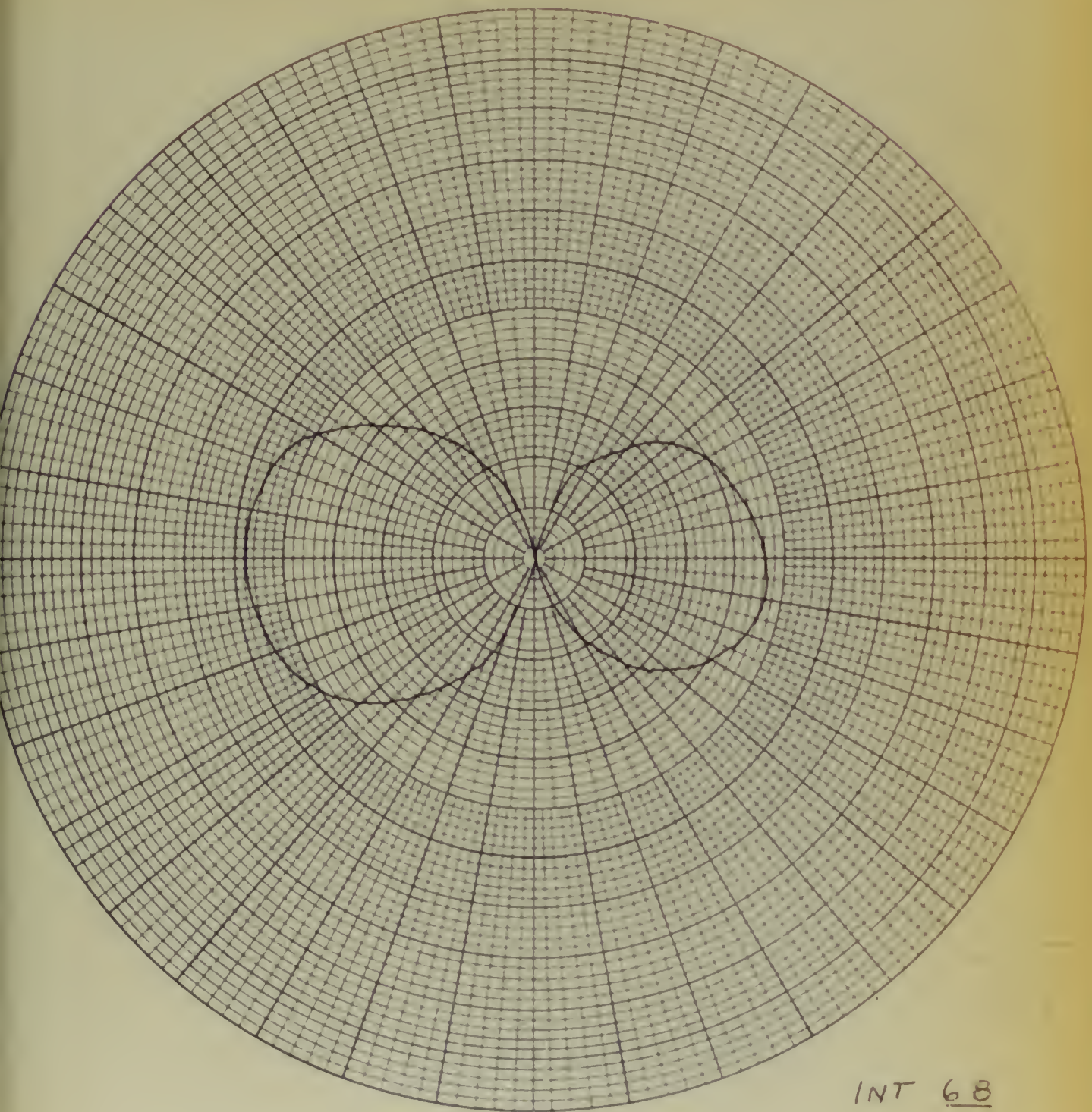

FIGURE 33

MODEL SURFACE ELEVATION PLANE -85°

COORDINATE SYSTEM AZIMUTH PLANE

CURVE PLOTTED IN: VOLTAGE (✓) POWER ( ) DB ( ) POLARIZATION E_θ

DOUGLAS AIRCRAFT COMPANY, INC.

DATE 3-25-53 PLANT PAGE

PREPARED BY TABLE

TITLE REPORT

MODEL SCALE 1/20 MODEL FREQ. 9030 MC FULL SCALE FREQ. 420-460 MC

ANTENNA TYPE APN-1 XF30 ANTENNA LOCATION FWD NACELLE

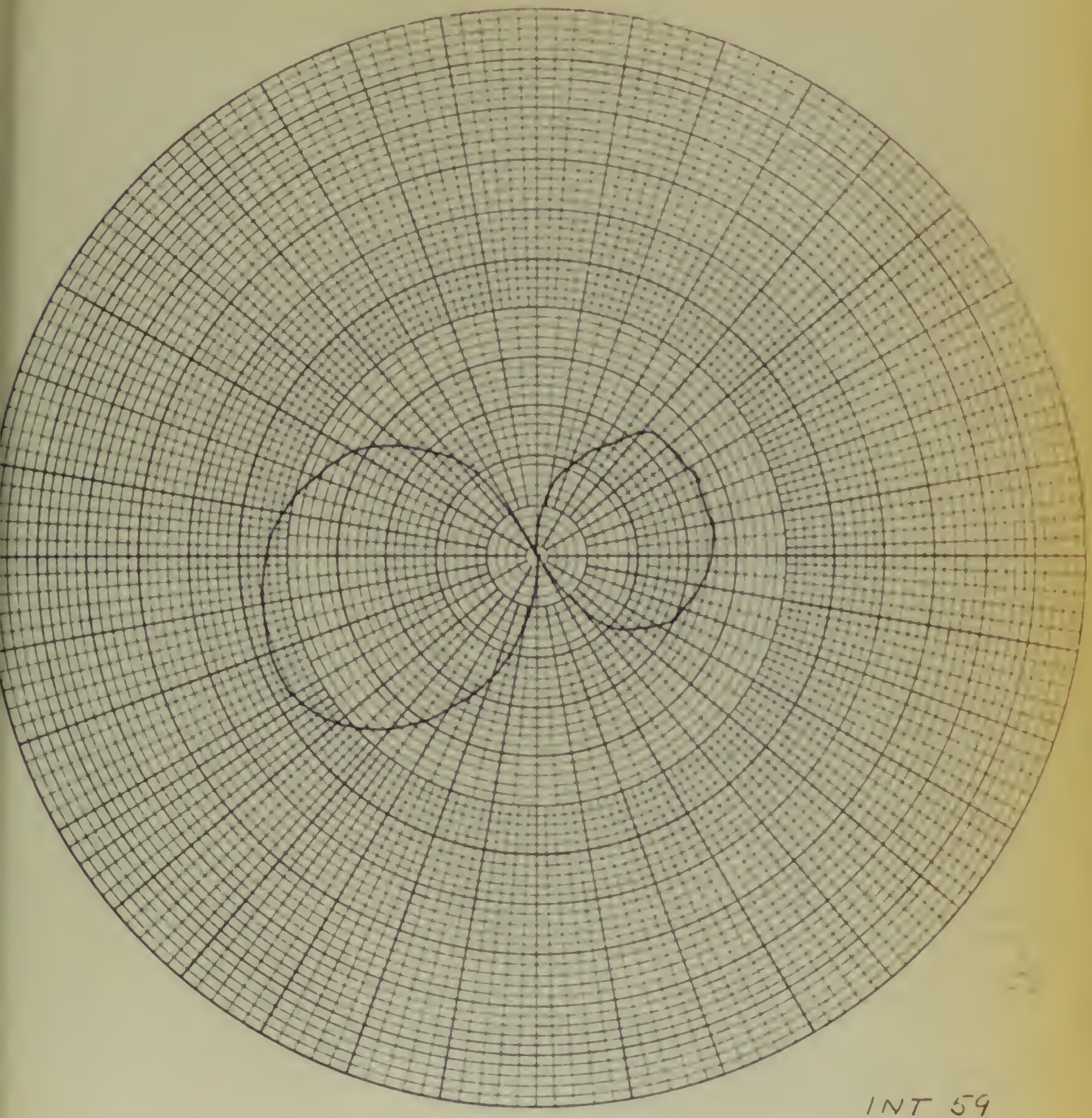

INT 59

FIGURE 34.

MODEL SURFACE

COORDINATE SYSTEM

CURVE PLOTTED IN: VOLTAGE (✓) POWER ( ) DB ( )

ELEVATION PLANE -80°

AZIMUTH PLANE

POLARIZATION E_θ

DOUGLAS AIRCRAFT COMPANY, INC

DATE 3-25-53 PLANT PAGE

PREPARED BY MODEL

TITLE REPORT

MODEL SCALE 1/20 MODEL FREQ. 9030 MC FULL SCALE FREQ. 420-460 MC

ANTENNA TYPE APN-1 XF3D ANTENNA LOCATION FWD NACELLE

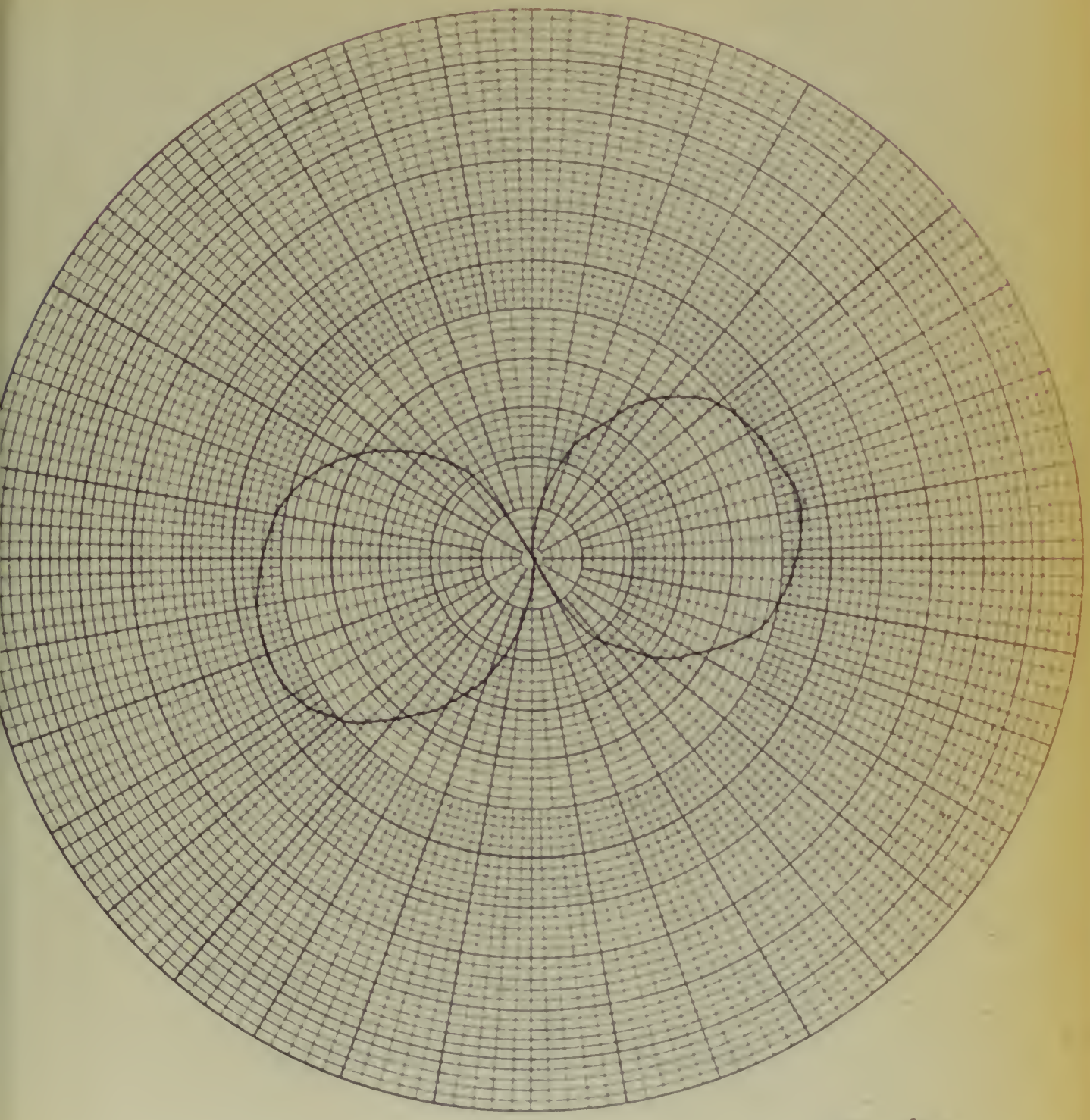

INT 80

FIGURE 35.

MODEL SURFACE

COORDINATE SYSTEM

CURVE PLOTTED IN: VOLTAGE (✓) POWER ( ) DB ( )

ELEVATION PLANE −90°

AZIMUTH PLANE

POLARIZATION Eθ

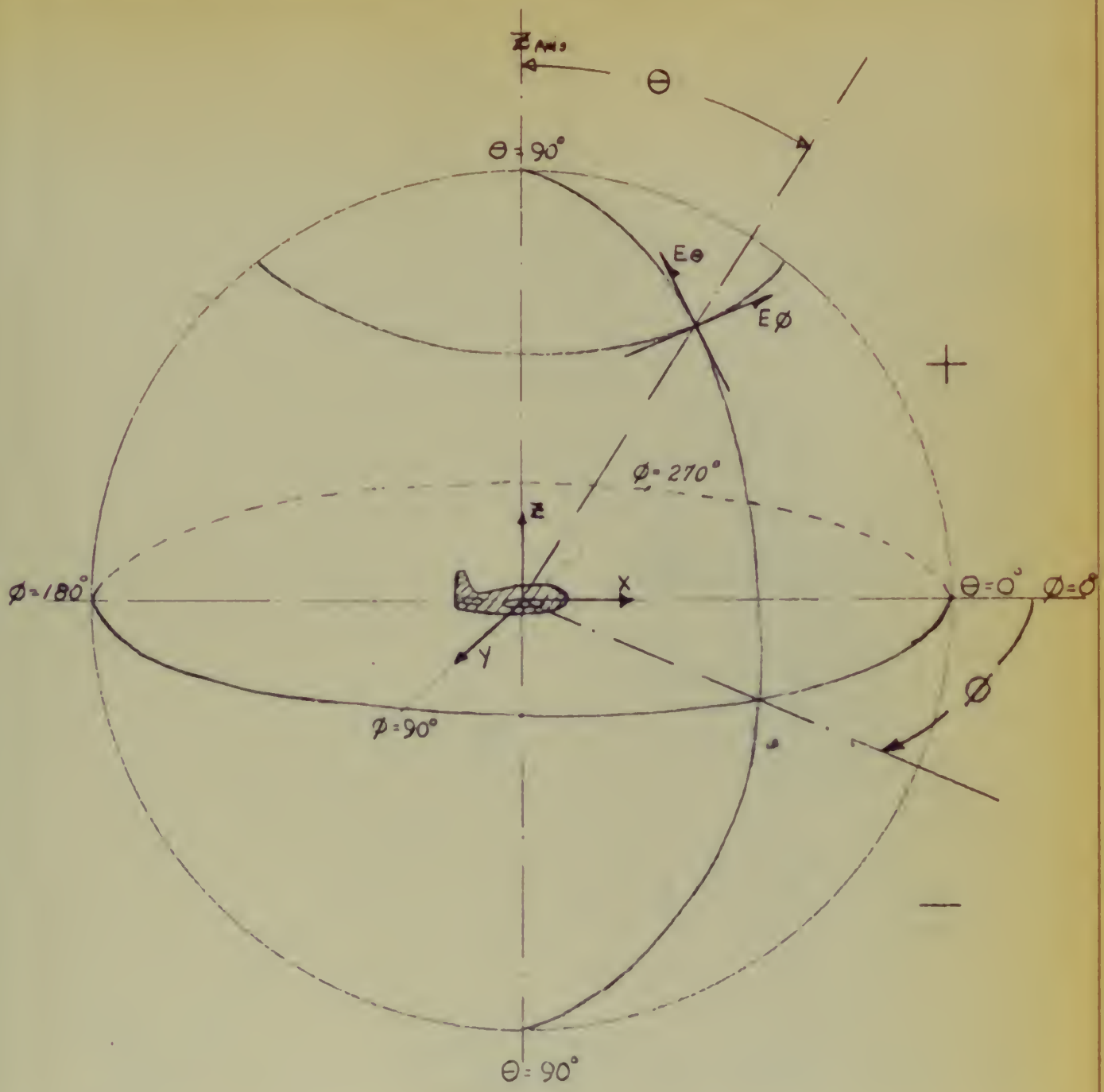

SPACE COORDINATE SYSTEM

ANTENNA MODEL RANGE

FIG. 36.

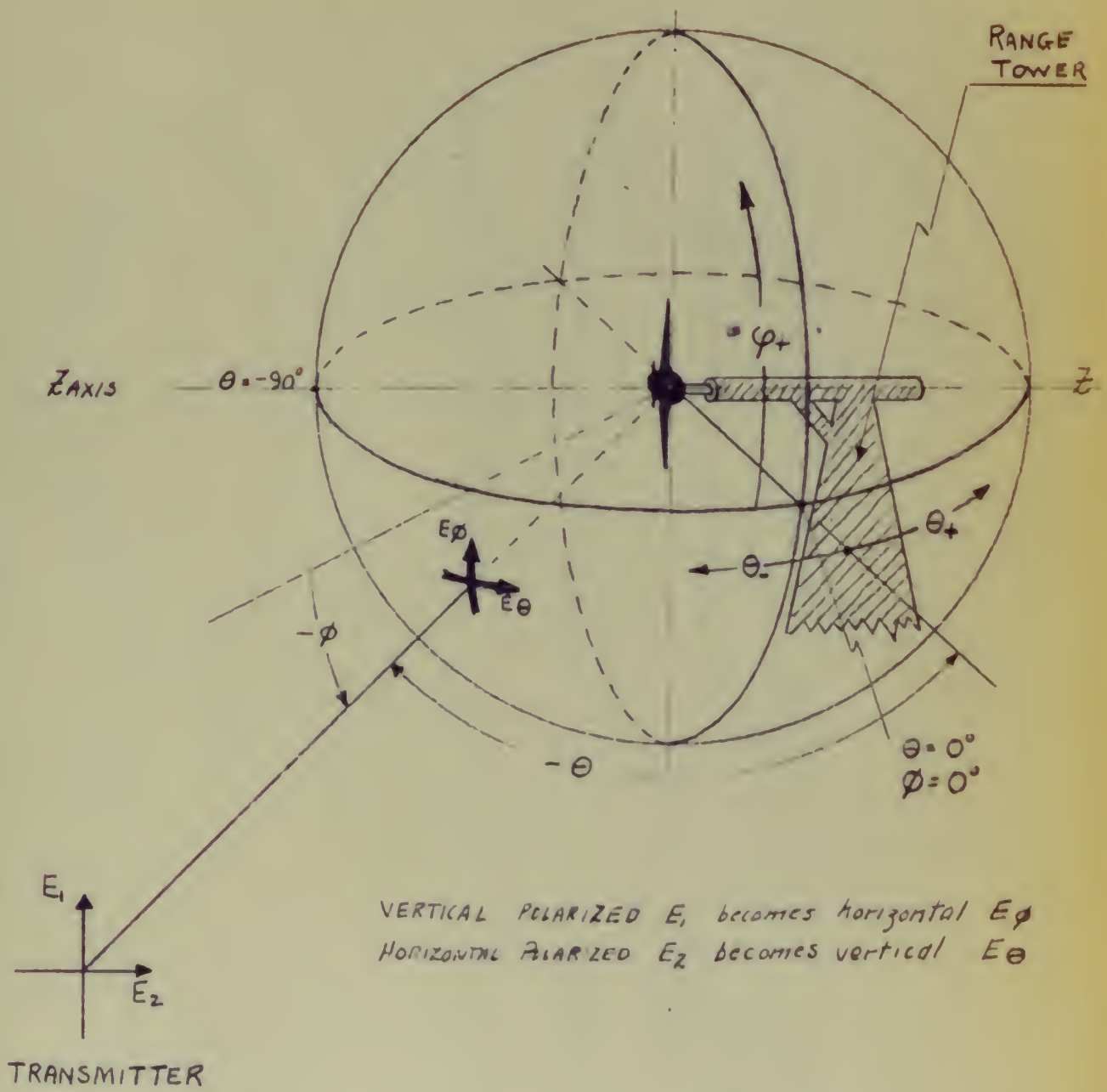

RELATION OF TRANSMITTER AND MODEL

FIG. 37.

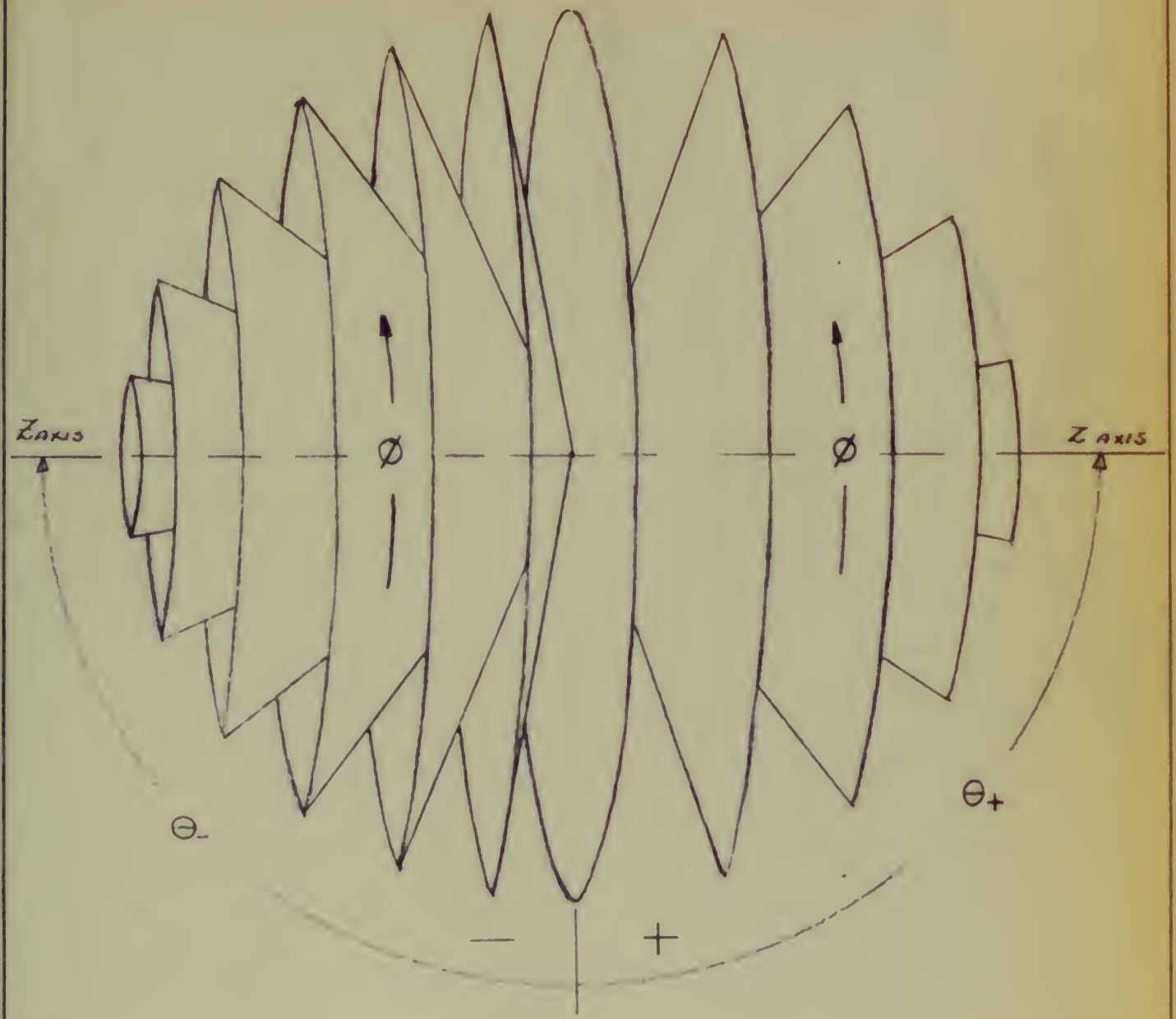

CONICAL CUTS to OBTAIN PAVERAGE

EACH CONE REPRESENTS A FIXED LATITUDE θ
RIGHT SIDE FIXED TO RANGE TOWER

FIG. 38.

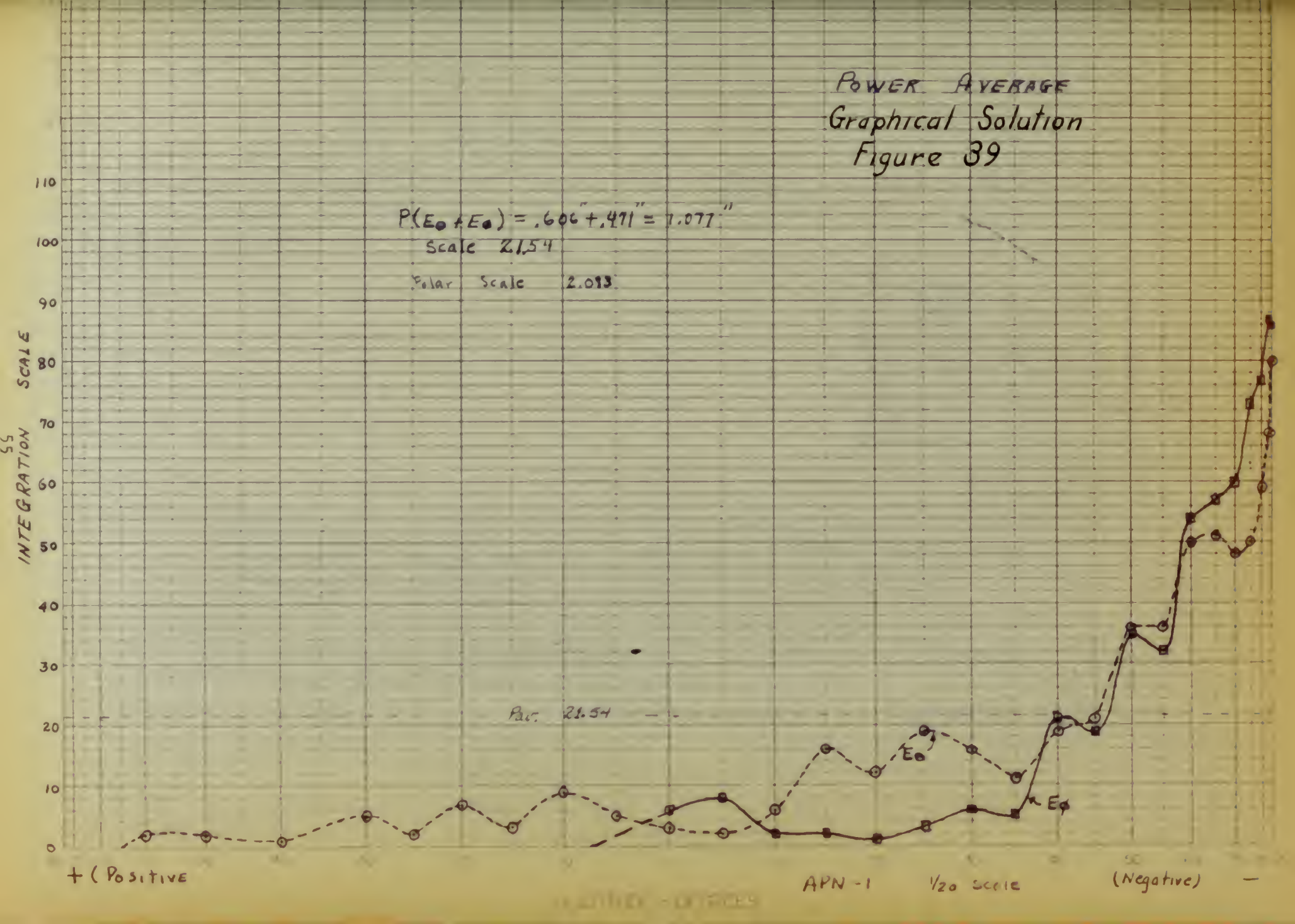
POWER AVERAGE
Graphical Solution
Figure 39
P(E₀ + E₀) = .606" + .471" = 1.077"
Scale 21.54
Polar Scale 2.013
INTEGRATION SCALE
110
100
90
80
70
60
50
40
30
20
10
0
Pol. 21.54
E₀
E₀
+ (Positive
APN-1
1/20 scale
(Negative)
—

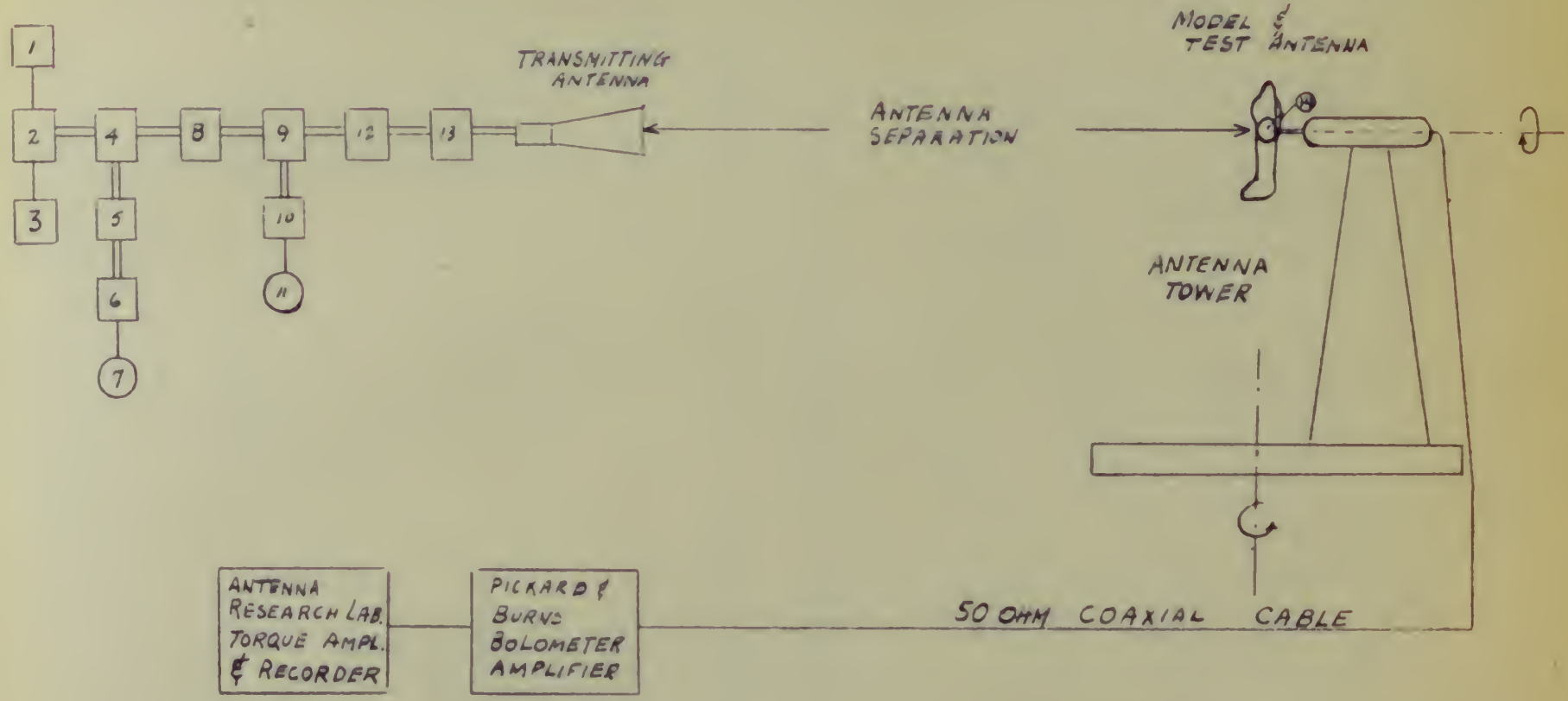

1.-Power Supply - HP 715A
2-Klystron - VARIAN X-13
3-Modulator - HP 715A
4-Directional Coupler (20db)
5-Wave Meter - Cavity
7-Scope - DuMont
6. Untuned Detector

8-Variable attenuator
9-Directional Coupler (20db)
10-Tuned Detector (PRD 612A-Ser 198)
11-HP 415A indicator
12-Waveguide section (to change polarization)
13-Flexible waveguide
14-Tuned Detector (PRD 612A Ser 200)

ANTENNA RANGE SCHEMATIC DIAGRAM

FIGURE 40.

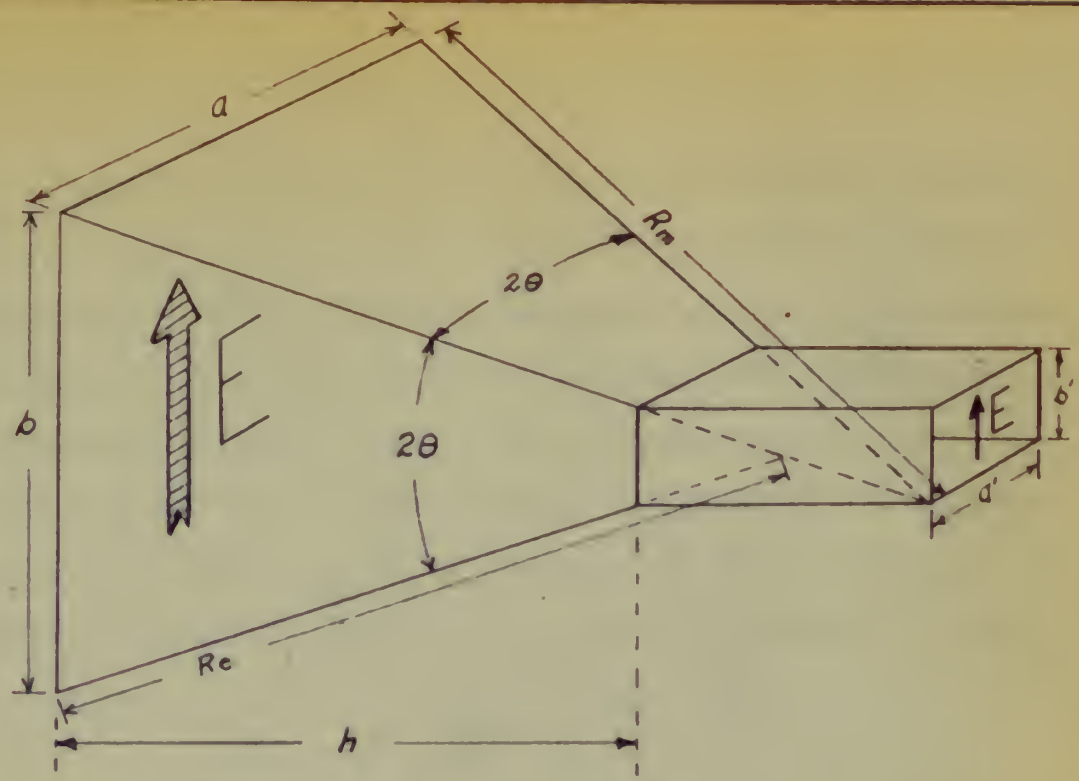

ELECTROMAGNETIC HORN

USED AS RECEIVER & COMPARISON ANTENNA

DIMENSIONS (inner)

a' = .9 inch = 2.286 cm	h = 15.75 inch
b' = .4 inch = 1.016 cm	θ = 8 3/4° (flare angle)
a = 5.8 inch = 14.72 cm	Re = 17.41 inch = 44.2 cm
b = 5.3 inch = 13.45 cm	Rm = 19.05 inch = 48.4 cm

FIG. 41.

power output of the klystron. Due to the radiation pattern of the model antenna it was not necessary to cover the entire spherical surface. The conical cuts were taken over the lower hemisphere from -65 to -90 degrees in 5 degree steps. Integrated values were taken over the spherical surface where the radiation pattern existed. The integrated values, proportional to power, are included in Table 1. These integrated values were plotted versus the cosine of the latitude, and then reduced to an equivalent sphere, (see Figure 39). From these plots the directivity and the maximum effective area were obtained.

b. Model range conformity.

The model range and matching requirements were observed as closely as possible. All of the model range requirements were properly satisfied, with the exception that it was necessary to be in the illuminating field when the measurements were taken. This was due to the fact that each receiving setup had to be tuned for a maximum power indication. In all cases the receiving setups were tuned for a maximum power with an operator located behind the antenna. This was an effort to disturb the field as little as possible. The effect of a person being in the field during this adjustment was observed for the model antenna, but was not noticeable for the comparison antenna. This condition was unavoidable and foreseen. The model antenna used was chosen for its' high directivity in an effort to reduce these undesirable mutual coupling effects.

c. Equipment used.

The equipment used for the transmitter, model antenna, and comparison antenna are shown on a schematic diagram in Figure 40. The model antenna was located underneath the model aircraft at the forward part of the left engine nacelle, as shown in Photograph B. There were four different measurements taken with the first one being incomplete. The three completed measurements differ somewhat. The difference between measurements two and three was that a slotted line was inserted in the receiving circuit of the comparison antenna. Measurements two and four differ in polarization, aircraft model orientation, distance between transmitter and receiver, and output power of transmitter.

The power density was maintained constant by maintaining the power at the throat of the transmitting horn constant. This was accomplished by using a directional coupler (20 db attenuation) located near the throat of the transmitting horn, a tuned detector (HRD 612-A, No. 198), and an audio amplifier. These are shown, in block form, in Figure 40.

The gain of the comparison antenna (Figure 41 and Photograph A) was obtained by using Schelkunoff's (19) curves and equations. The two values are nearly equal.

d. Data and calculations.

(1) Calculations of model range distances.

The dimensions of the transmitting and receiving apertures are:

Transmitting horn = 7.5" x 8.2" = 19.06 x 20.82 cm^2

Receiving horn = 5.3" x 5.6" = 13.47 x 14.7 cm^2

Receiving model = 65 x 75 cm^2

The lobe structure of the model was such that the major portion of the radiation was in the lower hemisphere. Range experience indicated that certain portions of the aircraft structure could be omitted since they would not contribute anything to the radiation pattern. This was a valid assumption in this case due to the shape of the radiating pattern and the location of the model antenna on the model aircraft. Sixty per cent of the wing span and the fuselage length were considered to be the physical aperture. Therefore the receiving aperture was 40 x 45 cm^2.

The frequency of the experiment was limited between 9000 mcs. and 9200 mcs. The receiving horn had a lower limit of 9000 mcs. and the FRD tuner an upper limit of 10,000 mcs. The APN-1, 1/20th scaled antenna, had a frequency range of 8400 to 9200 mcs. The full scaled antenna had a frequency range from 420 to 460 mcs. The scheduled frequency was 9000 mcs. and the actual frequency used was 9030 mcs. At 9000 mcs

$$\lambda = \frac{10}{3}\text{cm} \quad d_r = 45 \text{ cm} \quad d_t = 20.8 \text{ cm} \quad d_{r_h} = 14.7 \text{ cm}$$

For uniform field $R = \frac{2d_r^2}{}$, $R_{model} = 40$ ft and $R_{horn} = 4.2$ ft.

For constant phase $R = \frac{2d_t d_r}{}$, $R_{model} = 18.5$ ft and $R_{horn} = 6$ ft.

For minimum height $h = d_r^2/dt$, $h_{model} = 3.2$ ft and $h_{horn} = 4.1$ inches.

The minimum height was 3.2 feet and the minimum range was 40 feet. The actual separation between the transmitter and the receivers was 40 feet

or more, and the height of the receiver was about 12 feet above the ground plane. These values were satisfactory for the frequency equal to 9030 mcs.

(2) Computations for the directivity and the effective aperture of the model antenna.

INTEGRATED VALUES OF MODEL PATTERNS

Elevation angle Latitude θ	Value Eθ	Value Eø	Elevation angle Latitude θ	Value Eθ	Value Eø
+60°	2	--	-25°	19	3
+50°	2	--	-30°	16	6
+40°	1	--	-35°	11	5
+30°	5	--	-40°	19	21
+25°	2	--	-45°	21	19
+20°	7	--	-50°	36	35
+15°	3	--	-55°	36	32
+10°	9	--	-60°	50	54
+ 5°	5	--	-65°	51	57
0°	3	6	-70°	48	60
- 5°	2	8	-75°	50	73
-10°	6	2	-80°	59	77
-15°	16	2	-85°	68	87
-20°	12	1	-90°	80	86

These values were recorded by the ball and disc integrator on the automatic recorder. The values of Eθ and Eø were proportional to the power received.

TABLE I

Frequency of operation = 9030 mcs. λ = 3.32 cm

Power averaging. Planimeter No. 45522, K&E was used to obtain area under the curves of Figure 39.

Planimeter Reading	Value under Eθ curve	Value under Eø curve
1.	5.99	4.73
2.	6.24	4.70
3.	6.11	4.71
4.	5.91	
average	6.06	4.71

Total value 10.77 square inches

Length of base of area covered 10 inches

$P_{average} = P_{E\theta} + P_{E\phi} = 1.077$ inches

$P_{average}$ = 21.54 (on same scale as integrated values)

E_s = 2.072

E_s Was set to the same scale as the polar plots so that no further scale factors were needed.

For experiments 2 and 3

E = 5.5 (selected point on lobe)

E_s = 2.072

Directivity = 7.04 = P/P av

Effective Area = 6.16 = $D\lambda^2/4\pi$

For experiments 1 and 4

E = 6.0

E_s = 2.072

Directivity = 8.4

Effective Area = 7.36

Eθ and Eϕ are properly labeled as shown on Figures 35 and 37 for the receiving conditions. Due to the method of taking the polar patterns there was a 90 degree change in orientation. A vertical polarized wave at the transmitter appeared as a horizontal polarized wave at the model aircraft.

(3) Computations for the horn antenna.

The horn antenna used was a result of compromise between the available waveguide components, the available power source, and the desired optimum horn. The data below is for a frequency of 9030 mcs. Figure 41 shows the relationship of the horn parameters, which are:

a	= 13.46 cm	Re/λ	= 13.32 cm
b	= 14.73 cm	Rmλ	= 160.888 cm
a/λ	= 4.437 cm	$\sqrt{Rm\lambda}$	= 12.676 cm
b/λ	= 4.055 cm	$\sqrt{Rm\lambda}/a$	= .86055 cm
Rm	= 48.4 cm	$a/\sqrt{\lambda Rm}$	= 1.162 cm
Re	= 44.2 cm	$\sqrt{2\ Re\lambda}$	= 17.131 cm
Rm/λ	= 14.75 cm	$b/\sqrt{\lambda 2Re}$	= .7857 cm

By using Schelkunoff's (19) curves the gain and the effective aperture were found to be:

$g_m \frac{\lambda}{b} = 43.9 \qquad g = \frac{\pi}{32}\left(g_m \frac{\lambda}{b}\right)\left(g_e \frac{\lambda}{a}\right) = \frac{1}{10.2}(43.9)(37.2) = 160$

$g_e \frac{\lambda}{a} = 37.2 \qquad A_{em} = \frac{\lambda^2 g}{4\pi} = 140.5\ cm^2$

Due to the fact that these curves were printed in a text and difficult to read with any degree of accuracy the effective aperture was calculat-

ed from the following equations. They were broken apart to agree with the values found separately from the printed curves. Schelkunoff defined parts of the equations as related to Fresnel Integrals. The publication used for the following calculations was "Tables of Functions", Jahnke and Emde, (11). Because the definition of the Fresnel integral was different than that given by Schelkunoff the "Error Integral" on page 34 was used instead of the "Fresnel Integral" tabulation on page 35.

Equations:

$$g_m = \frac{4\pi R_m}{a}\left\{\left[C(u)-C(v)\right]^2+\left[S(u)-S(v)\right]^2\right\}$$

$$g_e = \frac{64 R_e}{\pi b}\left[C^2(w)+S^2(w)\right] \qquad w = \frac{b}{\sqrt{2\lambda R_e}} = .7857$$

$$u = \frac{1}{\sqrt{2}}\left(\frac{\sqrt{\lambda R_m}}{a}+\frac{a}{\sqrt{\lambda R_m}}\right) = 1.43 \qquad v = \frac{1}{\sqrt{2}}\left(\frac{\sqrt{\lambda R_m}}{a}-\frac{a}{\sqrt{\lambda R_m}}\right) = -.213$$

$C(u)$	$= .5138$	$S(u)$	$= .7067$
$C(v)$	$= -.2128$	$S(v)$	$= -.0055$
$C(w)$	$= .7138$	$S(w)$	$= .2383$
$C(u)-C(u)$	$= .7266$	$[C(u)-C(v)]^2$	$= .5279$
$S(u)-S(v)$	$= .7142$	$[S(u)-S(v)]^2$	$= .5101$
$C^2(w)$	$= .5095$	$C^2(w)+S^2(w)$	$= .5666$
$S^2(w)$	$= .0571$		

$$g_m \frac{\lambda}{b} = \frac{(12.566)(48.4)}{14.73}\{1.038\} = 42.75$$

$$g_e \frac{\lambda}{a} = \frac{(64)(44.2)}{(3.14)(13.46)}\{.5666\} = 37.92$$

$$g = \frac{\pi}{32}\left(g_m \frac{\lambda}{b}\right)\left(g_e \frac{\lambda}{a}\right) = \frac{1}{10.2}(42.75)(37.92) = 159$$

$$A_{zm} = \lambda^2 g/4\pi = 139.7\ cm^2$$

This value of A_{2_m} was used in preference to the value obtained from the curves.

(4) Measurements of the model antenna and the comparison antenna mounted on the model range.

POWER MEASUREMENTS

	1	2	3	4
Date	Mar 25	Mar 26	Mar 26	April 1
Polarization at the transmitter	Vertical	Horizontal	Horizontal	Vertical
Noise level	.0025 v	.0025 v	.0025 v	.0035 v
W1θ	.0036 v	.054 v	.054 v	in noise
W1Ø	.055 v	in noise	in noise	.038 v
W2θ	lost det.	" "	" "	1.3 v
W2Ø	" "	2.180 v	1.80 v	in noise

TABLE XI

The voltage values were proportional to the power in the bolometer detector. The voltage readings were those of the bolometer amplifer which was calibrated and linear.

The third run had a slotted line inserted in the receiving circuit of the comparison antenna. The VSWR, when this measurement was taken, was 1.06 to 1. This verified loose coupling between the transmitter and the receiver and good matching for the comparison antenna. The receiving equipment was tuned in the same manner for all runs. The distance between transmitter and receiver was 45 feet for runs 1, 2 and 3 and 40 feet for run 4.

SUMMARY OF DATA

Experiment No.	1	2	3	4
Date taken	March 25	March 26	March 26	April 1
Polarization at transmitter	Vertical	Horizontal	Horizontal	Vertical
Noise level	.0025 v	.0025 v	.0025 v	.0035 v
$W_{1\theta}$	.0036 v	.054 v	.054 v	in noise
$W_{1\phi}$	.055 v	in noise	in noise	.038 v
$W_{2\theta}$	lost det.	" "	" "	1.30 v
$W_{2\phi}$	" "	2.180 v	1.80 v	in noise
A_{2m} (calculated)	139.7 cm^2	139.7 cm^2	139.7 cm^2	139.7 cm^2
A_{2m} (curves)	140.5 cm^2	140.5 cm^2	140.5 cm^2	140.5 cm^2
E_a	2.073	2.073	2.073	2.073
E (max on lobe)	6.0	5.5	5.5	6.0
Directivity	6.4	7.04	7.04	6.4
A_{1m} (aperture)	7.36 cm^2	6.16 cm^2	6.16 cm^2	7.36 cm^2
Efficiency with A_{2m} calculated	insufficient data	56.1%	68.0%*	55.4%
Efficiency with curves	insufficient data	56.5%	68.4%*	55.8%
A_{2m} (corrected)**	133.2 cm^2	133.2	113.2	133.2
Efficiency with A_{2m} from corrected calculations	-	53.6%	65.0%	53.0%
Misc.	slotted line with No. 3 with VSWR of 1.06:1			

TABLE III

*The slotted line probe took a considerable portion of the energy in the waveguide thereby lowering value W_2 and increasing the efficiency figure.

**Correction for edge effects, W. C. Jakes (10).

CHAPTER V

EVALUATIONS AND RECOMMENDATIONS

1. Evaluations.

One of the objectives of this paper was to search the literature for the methods of finding the antenna efficiency by using scaled models. Then a specific evaluation by a selected method was to be made. These objectives have been completed.

Four methods of obtaining antenna efficiency have been outlined, however three are rejected for various reasons. Some of the reasons for rejection are: (1) the lack of control of the reflections when the model is used as a transmitter, (2) there are no existing absolute field intensity measuring instruments at microwave frequencies and (3) that an absorbent, non-reflecting material is unavailable. The fourth method, the comparison method, appeared to have more chance of successful completion. The outstanding advantages of the comparison method are: (1) absolute power measurements are unnecessary and (2) the model may function as a receiver thereby permitting use of the model range. (The model range can be used for receiving and transmitting, however reflections are controlled more easily when the model is used as a receiver). There is the possibility that the integration process used to obtain the average power radiated (reduction to an istropic source) may contain information for other solutions. If these solutions existed the necessity for accurate matching would be eliminated and the model range technique improved. This thought was considered, but nothing profitable was for-

seen and therefore abandoned as a method of solution.

The validity of the presented method depends upon five equations, $G_o = \alpha D$ $\alpha = \eta \gamma$ $D = \frac{4\pi A_{em}}{\lambda^2}$ $A_e = \alpha A_{em}$ $W = P_o A_e$ and the assumption that the comparison antenna (an electromagnetic horn) has an efficiency of 100 per cent. From these equations an expression is derived for the efficiency in terms of quantities that can be measured on the model range or computed from known data, $\eta = \frac{W_1 A_{2m}}{W_2 A_{1m}}$. This has circumvented the necessity for an absolute measurement of either power or field intensity at the operating frequency. The latter equation expresses the efficiency of the model antenna when there are no losses in the available power due to matching conditions of either receiving circuit.

The model range requirements were observed as closely as possible. However there were two departures that were unavoidable. The gain of the comparison antenna was more than 10 db greater than the gain of the model antenna. There was the possibility of unwanted reflections since it was necessary that someone be in the illuminating field to tune the receiving antennas. There were no noticeable effects when the comparison horn measurements were taken, but there were slight flucuations of the bolometer amplifier voltage when the model antenna was being tuned. For all measurements a position was found, in line with the range tower, where small movements caused no variation of the bolometer amplifier

voltage. This position was considered the point of minimum reflection.

The question of accuracy is not too easily answered. The efficiency of the comparison horn is very likely to be less than 100 per cent due to ohmic losses. The factors that can cause changes in the observed power indications are: a mismatch not permitting all the received power to reach the bolometer detector, ohmic losses between the antenna and the detector, and transmission losses due to standing waves. The physical dimensions were kept as short as possible. The PRD tuner was located close to the "input terminals" of the model antenna. Transmission losses were considered negligible. In run 3 a VSWR of 1.06 was measured. This value of the VSWR is a good indication that the comparison antenna was matched. However the degree of matching for the model is doubtful, but there is no reason to believe that it was any more unfavorable than that of the preliminary experiments where the VSWR was in the neighborhood of 1.2 to 1.5. It will be concluded that the model antenna was matched when the bolometer amplifier voltage was a maximum. (It may be mentioned that if this assumption is in error the efficiency, as given by the derived expression, will vary greatly).

There is an additional correction for the comparison antenna for edge effects in accordance with the experimental data of W. C. Jakes (10). The antenna used was not an optimum horn, however very close, therefore a maximum of .2 db will be taken from the computed gain. This reduces the computed gain to 152, the computed aperture to 133.2, and the efficiencies to 53.6 per cent for measurement 2, to 65.0 per cent for

measurement 3, and to 53.0 per cent for measurement 4.

Based on the data taken, the efficiency varied between 53 per cent and 56 per cent. In the expression $\eta = \frac{W_1 A_{2m}}{W_2 A_{1m}}$, W_1 appears to be the quantity most open to question. W_2 appears more reliable due to the low VSWR of run 3 and the data of the preliminary experiments. A_{2m} has been taken from curves, checked by computations, and then corrected for edge effects. A_{1m} is independent of ohmic and mismatch losses. The efficiency of the comparison horn, if less than the assumed value of 100 per cent, will lower the value of the antenna efficiency of the model. Conceding that there may have been mismatch and ohmic losses between the model antenna and the detector, the value of W_1 can only increase when any correction is made. Therefore, assuming the horn efficiency equal to 100 per cent, the low value of η has been obtained. Any matching refinements or any calculation of transmission losses will increase the efficiency. Negligible transmission losses and a high horn efficiency seem to be reasonable assumptions. Therefore the value of 54 per cent for the antenna efficiency of the model appears very reliable. However there is the need of another method to check these values experimentally.

2. Recommendations.

The physical arrangement for receiving with the comparison antenna is considered satisfactory. The arrangement with the model antenna is somewhat doubtful, in that better knowledge of the degree of matching should be available. If further tests were to be made it is recommended that a highly efficient matching network be devised, at lease some

arrangement where more information would be available when the measurements were made. The model used was of one polarization and it is not known, from the data taken, if there were any radiation in the other plane of polarization below the noise level of the bolometer amplifier. Since the bolometer amplifier had a sensitivity of .1 microvolt there is little that can be gained in the receiving section, however the r. f. power radiated by the transmitter could be increased. In addition to raising the power level of the measurements above the noise level, an increase in r.f. power would permit a greater distance between the transmitting and receiving antennas, and permit maintaining the effective power density of the incident wave constant by using the feedback network in the bolometer amplifier. This provision is included in the bolometer amplifier when the transmitting power is of sufficient strength. (The only source of power at this frequency capable of square-wave modulation was the $\frac{1}{4}$ watt Varian X-12 klystron. A 5 watt klystron was available, but it could not be modulated).

In the event that this method should be investigated further and found satisfactory for use, it is recommended that these measurements be made at the same time that the radiation patterns are recorded. Some other check on the efficiency figures obtained should be made. One method could be a direct absolute measurement and another method could be an investigation of the performance records of flight tests.

BIBLIOGRAPHY

1. P. S. Carter, *RCA report CM-45-9, August 28, 1944.
2. C. C. Cutler, A. P. King, and W. E. Kock, Microwave Antenna Measurements, IRE Proc., 35, December 1947, pp. 1462-1471.
3. Development Report, Douglas Airoraft, Santa Monica Div, Douglas No. 1092.**
4. Development Report, Douglas Aircraft, Santa Monica Div, Douglas No. 1093.**
5. Measurements of Antenna Patterns, Douglas No. EG-MR-1.**
6. Computation of Absolute Field Strength and Effective Communication Range, Douglas No. EG-MR-7.**
7. W. L. Everitt, Communication Engineering, McGraw-Hill, New York, 1937.
8. Harald T. Friis, a note on a simple Transmission Formula, IRE Proc., 34, May 1946, pp. 254-256.
9. Edwin Istvanffy, Antenna Impedance Measurements, Reflection Method, IRE Proc., 37, June 1949, pp. 604-608.
10. W. C. Jakes, Gain of Electromagnetic Horns, IRE Proc. 39, February 1951, pp. 160-162.
11. Jahnke and Emde, Table of Functions, Dover Publications, New York, 1945
12. D. D. King, Two Standard Field Intensity Meters for VHF, IRE Proc., 38, September 1950, pp. 1048-1051.
13. John D. Kraus, Antennas, McGraw-Hill, New York, 1950.

*Exact title is not known. The subject material concerns field strength, directivity and radiation patterns.

**Douglas Reports, recent issue, exact date unknown.

14. W. W. Mumford, The Optimum Piston Position for Wide Band to Coaxial to Wave Guide Transition, IRE Proc., 41, February 1953, pp. 256-261.

15. G. L. Ragan, Microwave Transmission Circuits, McGraw-Hill, New York, 1948.

16. H. J. Reich (Editor), Very High-Frequency Techniques, Vol. I and II, McGraw-Hill, New York, 1947.

17. J. F. Reintjes (Editor), Principles of Radar, McGraw-Hill, 1946.

18. M. W. Scheldorf, Antenna Gain by Graphical Means, Electronics 25, No. 3, March 1952, pp. 144-147.

19. S. A. Schelkunoff and H. T. Friis, Antennas Theory and Practice, John Wiley and Sons, New York, 1952.

20. C. G. Seright, Open Field Test Facilities for Measurements of Incidental Receiver Radiation, RCA Review, XII, March 1951, pp. 45-52.

21. Samuel Silver, Microwave Antenna Theory and Design, Chapter 15, McGraw-Hill, New York, 1949.

22. George Sinclair, E. C. Jordan, and Eric W. Vaughn, Measurement of Aircraft Antenna Patterns Using Models, IRE Proc., 35, December 1947, pp. 1452-1462.

23. J. C. Slater, Microwave Transmission, Chapters 1 and 7, McGraw-Hill, New York, 1942.

24. R. S. Wehner, Absolute Signal Strength and Minimum Range of Aircraft Antennas, unpublished report of R. S. Wehner of Airborne Instruments Lab., Mineola, N. Y., December 26, 1946.

25. Project TED No. PTR EL 577 ET315-047, 16 June 1952, Electronics Test DIV USNATC PAX RIV MD, Correlation of model and flight measurements.

APPENDIX A

THE MODEL RANGE

The theory of the model range is contained in articles by various authors.* It has been established by a series of comprehensive tests conducted over a two to three year span by the Naval Test Center at Patuxent River, Maryland that there is good correlation of model and flight measurements.**

One path propagation is simulated without ground reflections or sky return. Due to the ease of construction and data taking, the information is obtained from the model when it is in a receiving condition. The model, mounted in a moveable tower is illuminated by a fixed transmitter, see Figure 40. A set of conical receiving patterns is obtained over the complete sphere. The coordinate system, illustration of conical patterns, and the physical arrangement are shown in Figures 36, 37, 38 and 40. The model may be mounted as desired, at the nose or tail of the fuselage, or at the top center position as shown. Frequently the nose position is used for coverage of one half of the sphere and the tail position for coverage of the other half. This prevents the tower from being between the transmitter and the receiver. (The experiments conducted did not include this refinement.) As shown in Figure 36, for a given polarization of the

*The theory of the model range and many of the techniques are given by J. D. Kraus (13), S. Silver (21), C. C. Cutler (2), R. S. Wehner (24), P. S. Carter (1) and G. Sinclair (22).

**Project TED No PTR EL 577 ET315-047 16 June 1952 ELECTRONICS TEST DIV USNATC PAX RIV MD.

incident wave at the model, the latitude θ is varied in increments of 5 or 10 degrees. The longitude ϕ is varied from 0 to 360 degrees for each latitude increment. The number of variations in latitude depends upon the degree of accuracy desired and the characteristics of the radiation patterns. Two sets of conical patterns are obtained, one for E_θ and one for E_ϕ polarizations.

In the antenna laboratory at the Douglas Aircraft Company, Inc. the illuminating field was square-wave modulated. The detector was usually mounted as close to the model antenna as space would permit. Both tuned and untuned detectors were used. For the radiation patterns the matching conditions were not important providing sufficient signal was available and the system was loosely coupled. The detector signal was sent to a bolometer amplifier, a torque amplifier, a ball and disc integrator, and an automatic pattern recorder. The integrator received signal proportional to the received power, and the recorder received signal proportional either to power or voltage. An integrated sum proportional to the received power was recorded along with each voltage pattern for each variation of latitude θ. Similar data was taken for the other polarization. The integrated sums were then plotted against the variable cosine θ, see Figure 39. The average area of this plot was obtained with a planimeter. The average power was the sum of the average power areas of the E_θ and E_ϕ polarizations. With the proper scale choice the average area was equated to the average power from which the spatial r.m.s. voltage of an equivalent istropic source was computed. This voltage was

proportional to the square root of the average power. Since this value contained only root mean square values and was derived from the average power after the integration process, it was used with the instantaneous voltages of the recorded patterns to obtain the directivity. $D = \frac{P}{P_{Av}} = \left(\frac{E}{E_s}\right)^2$ The relationship between this spatial r.m.s. voltage and the average power was $E_s = \sqrt{P_{Av}/5}$.

The bolometer amplifier had four ranges of amplification, each range constant and calibrated. The maximum amplification was 80 db and the sensitivity was 0.1 microvolt. The scale relation between the integrator and the recorder was $Y = 5X^2$, where X was the recorder scale in voltage and Y was the sum of the integrated values on a counter. If the recorder traced a pattern of a constant circle of 10 units through 360 degrees, the integrator counter would read 500. Only the directivity and the relative radiation patterns were obtained from the model range. The average power, considered as an isotropic source, was plotted as a circle on the radiation patterns. The field strength at one mile from an isotropic radiator radiating one watt of power is 3.4033 millivolt per meter.* With the output powers of the isotropic source and the model equal a scale existed for predicting the field strength at any point in the radiation pattern.

Figure 40 shows the components of the measurement experiments and their relative relationship. The receiving horn is shown in Photograph A. The audio lead to the bolometer amplifier is disconnected. The distance from the throat of the receiving horn to the center of the probe

* P. S. Carter (1).

transition, Figure 13 was 12.655 inches. The distance from probe transition to the variable short was between 4.875 and 8.653 cm, depending upon the short position. The model antenna was a 1/20th scale APN-1 radio altimeter antenna with a full scale frequency of 420 to 460 mcs. and a model frequency of 8400 to 9200 mcs. The location of the model antenna was on the underneath side and forward in the starboard engine nacelle as shown in Photograph B. Photograph C shows the PRD tuner in the aircraft model. The cable seen at left center connects to the antenna and to the tuner. Due to practical considerations this length could not be shortened. The PRD tuner and bolometer mount, (model 612-A), included in Photographs A and C, was made by the Polytechnic Research and Development Company, Inc. One tuner, serial number 200, was used for all measurements. The other tuner was used in the monitor circuit which insured that the incident power intensity was constant for the experiments. RG 58/U cable was used for part of the model antenna, and for the audio circuit from the bolometer resistance to the amplifier. The bolometer amplifier was made by Pickard and Burns. The torque amplifier and the automatic recorder, including the ball and disc integrator, were made by the Antenna Research Laboratory of Ohio State University.

APPENDIX B

WAVEGUIDE TO COAXIAL LINE TRANSITION

It was necessary to transfer the incoming energy to the bolometer detector with as few losses as possible. The PRD detector and tuner had a coaxial fitting and it was necessary to transform the energy from a rectangular waveguide to a coaxial line. Waveguide to coaxial line coupling can be made by proper choice of variables providing the impedance of the coaxial line is equal to or less than twice the characteristic impedance of the waveguide. There are several waveguide couplers that could have been used.*

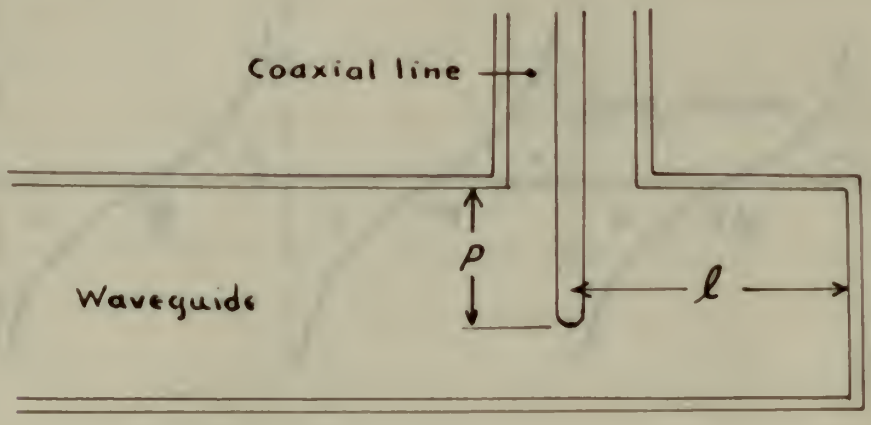

Figure 42.

Waveguide to Coaxial Line Coupler

Figure 42 shows the type of coupler used, a single probe projecting into the waveguide, and a variable short. The variables are the probe length "p" and the distance to the waveguide short "l". Figure 13 shows the

*Waveguide to coaxial coupling is covered in detail in other publications as Slater (23) pp. 296-300, Ragan (15) Ch. 6, MIT, Principles of Radar (17) Ch. 10 Art. 13, and Mumford (14) article in IRE.

detail structure of the coaxial transition. Photograph A shows the actual receiving arrangement, not including the bolometer amplifier.

For matching, "p" and "l" should be variable. One experiment showed that the variable short had the required change in electrical length for correct matching. The other experiment selected the optimum probe tip length which remained fixed throughout the remainder of its use. The distance of the variable short from the probe had an optimum* value of about .22 λ_g at an operating frequency of about 9000 mcs. Practical considerations made it necessary to use greater values of "l".

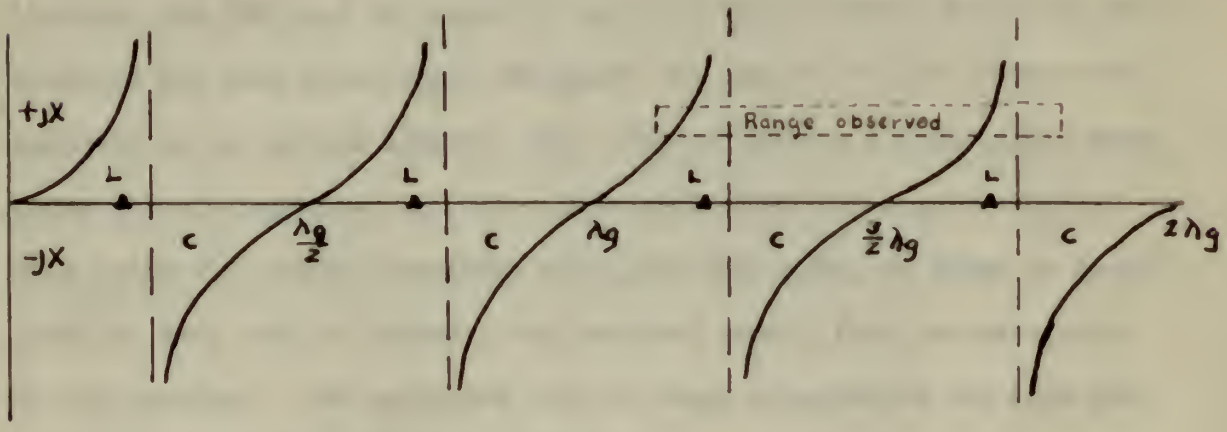

Figure 43.

Reactance vs. Electrical Length of Waveguide Short

▲ = Optimum Position of Waveguide Short.

It can be seen from Figure 43 that various positions of the variable short ($\ell = \ell_{opt} + \frac{n\lambda_g}{2}$) will repeat the match value for the optimum

*W. W. Mumford (14).

position. Figure 14 shows the results of one of these measurements. The true location of the electrical length of the waveguide and the optimum positions are difficult to show. The true shorting position within the waveguide of the waveguide short was not known accurately, therefore exact location of the scale was not possible. With a correction for the position of the scale it can be seen that good matching occurred where the length was between 3/2 λ_g and 7/4 λ_g, near $\ell = \ell_{opt} + \frac{3}{2}\lambda_g$. The probe tip of the center conductor, for the curves of Figure 14, was not the optimum diameter. A set of probe tips was made of the same size as the inner conductor. Their lengths varied from 16/64 inches to 22/64 inches. The VSWR and the relative power in the bolometer amplifier were observed for each probe tip. The probe tip length of 19/64 inches was selected as an optimum length. When used in the $\frac{1}{2}$ x 1 inch (o.d.) waveguide the tip projected into the guide about 73% of the guide depth.* This probe tip length, variable short, and PRD tuner, as shown in Photograph A, were used to transfer the received energy from the waveguide to the detector. The equipment used in these experiments was arranged as shown in the following block diagram.

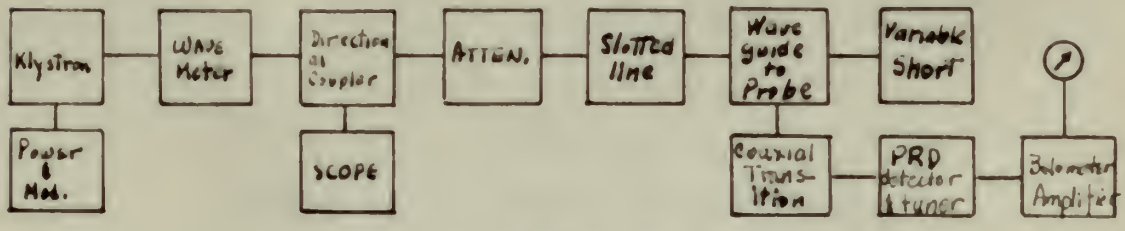

Figure 44.

Diagram of Transition Experiments

*The probe tip length agreed with that given by the following authors. These experiments showed about 73% projection into the waveguide. Ragan (15) and Mumford (14) show the same percentage. MIT (17) gives $\lambda_g/6$, which in this case is about 80% projection into the guide.

Informational data:

Variable short length, 0 to 3.578 cm.

Probe tip to minimum short length, 4.875 cm.

Wave length in waveguide, 4.85 cm.; in air, 3.328 cm.

Frequency, 9020 mcs.

Optimum length, 1.067 cm.

Probe tip data:

Order	1	2	3	4	5	6	7
Size	16	17	18	19	20	21	22
VSWR	1.23	1.24	1.22	1.12	1.17	1.24	1.31
Rel. Power	6.4	6.4	6.4	6.4	6.3	6.3	6.0

(Size 19 means 19/64 inches diameter.)

turns of short	0	10	20	30	per turn
length in cm.	4.92	5.973	7.026	8.079	.1053

APPENDIX C

PRELIMINARY EXPERIMENTS

The preliminary experiments were made to obtain data on the matching and power transfer of available components in the antenna laboratory. Some parts were made to supplement existing equipment. The experiments were divided between those pertaining to coaxial lines and those confined to waveguides.

1. Coaxial line experiments:

The coaxial line experiments were made to find the PRD tuner characteristics and the matching conditions when the model antenna was used.

a. PRD Characteristics.

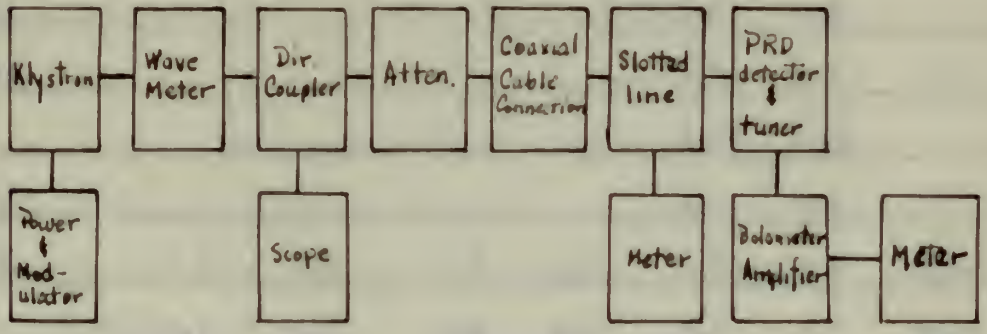

FIGURE 45.

Diagram of PRD Characteristics Experiment

The PRD tuner was connected directly to the slotted line. The purpose of these experiments was to see how the VSWR in the slotted line and the relative power received in the bolometer amplifier would change

for small changes in the length of the tuning stubs. This was the detection system for the model and comparison antennas. The length of the series and shunt stubs were moved until the bolometer amplifier reading was a maximum. The readings of the VSWR and relative power were recorded with the shunt stub length being varied and the series stub length being fixed. The following data was taken.

PRD Characteristics, Coaxial

Shunt length in turns	f 5000 mcs.(1) VSWR	Rel.Power	f 5000 (2) VSWR	Rel.Power	f 8640 mcs. VSWR	Rel.Power	f 8200 mcs. VSWR	Rel.Power
0	7.5	2.7	10.0	2.6	1.5	.3		
4/16	5.3	3.8	10.0	3.6	1.38	.3	4.2	.56
5/16							1.3	10.00
6/16					2.2	1.6	3.7	5.0
8/16	5.7	4.0	8.5	4.0	4.0	4.0	4.0	1.35
9/16					2.2	8.4		
10/16					1.5	8.8	5.5	.7
					1.55	10.0		
11/16					2.1	5.4		
12/16	4.4	4.2	7.5	4.6	2.15	4.3	6.0	.42
1	2.7	6.0	4.8	6.6	2.8	.9	high	low
1¼ loss than			3.6	10.0			"	"
1½	2.8	9.6	10.0	6.5	1.75	.4	"	"
1⅝	10.0	.2	10.0	.2			"	"

TABLE IV

The data for the frequency of 5000 mcs. is shown plotted in Figure 15. These curves show that there was a maximum power indication and a

lowering of the VSWR at the same physical position of the shorted stub. The data for 8840 mcs. and 8200 mcs. is plotted in Figures 16 and 17. There was fair evidence that the power transfer and the low VSWR were occurring at the same time, and that the matching desired was being accomplished.

b. Impedance measurements, coaxial.

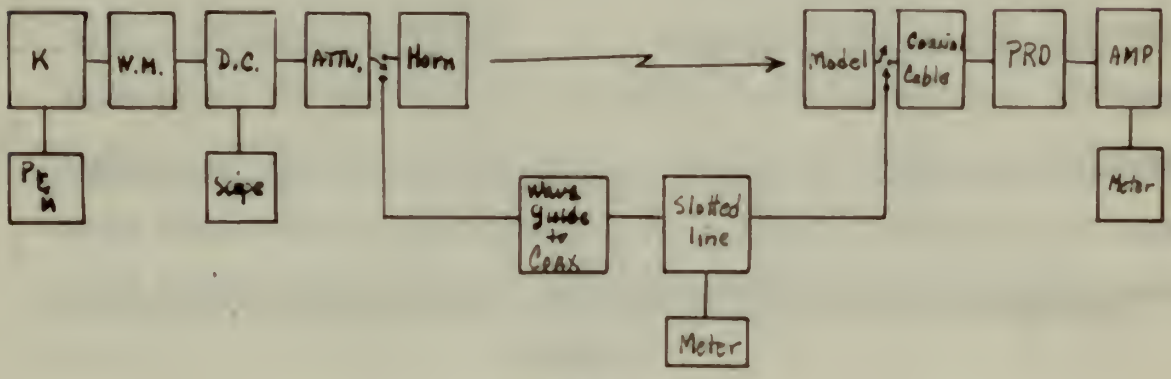

Figure 46.

Diagram for Impedance Measurements

An attempt was made to determine the impedance at the model antenna terminals. The reason for the measurements was: what was the impedance value presented to the antenna terminals when the maximum power indication was observed in the bolometer amplifier? The model antenna was partly constructed of RG 58/U cable. Small sections of the cable were cut to the same length as the cable feeding the antenna. This permitted substituting a short and an open circuit for the antenna without removing it from the model. The impedance was measured at the antenna terminals

looking into the antenna and then into the detecting network. There were many detrimental factors in these measurements such as different velocities of propagation, large reflections, different current distributions, and non-conformity with model range practices. The data taken, although of doubtful value, was:

Impedance Measurements, Coaxial

No	Min Short	Min Load	Diff	λ_g	Diff $\frac{\lambda_g}{}$	Dir. toward	$\bar{z}$	Z	Z Recomputed	VSWR	Looking Toward
1	7.23	7.41	.18	3.4	.053	G	.33-j.31	16.5-j15.5	16.25-j15.75	3.4	Antenna
	8.14	8.01	.13	3.4	.0382	L	--	32.5+j 6.0	32.5+j 7.5	1.6	Detector
2	10.34	10.05	.29	3.4	.0853	G	.46-j.5	23.0-j25.0	23.0-j23.0	2.8	Antenna
	11.03	9.37	1.66	3.4	.4881	G	.80-j.03	40.1+j 1.5	40.0+j 1.5	1.26	Detector
3	10.27	12.22	1.95	3.4	.574	L	1.23-j.77	61.5-j38.5	28.0+j18.5	2.12	Antenna
	11.07	9.65	1.37	3.4	.4032	G	.85-j1.0	42.5-j50.0	25.0+j29.5	2.84	Detector

TABLE V

c. Model antenna and slotted line on the range tower.

The model aircraft, including the model antenna (see Photograph B), was mounted on the model range. A slotted line was inserted between the model antenna and the detector. The purpose of this particular experiment was to observe the VSWR between the antenna and the detector, and the effect of the slotted line, when the model was being illuminated on the model range. A range separation equal to or greater than the model range requirements was desired. Sufficient signal for tuning the detector was received when the range separation between the transmitter and the receiver was over 50 feet. However, for sufficient

r.f. power to permit a determination of the VSWR with the slotted line, the range separation had to be decreased to 20 feet. The value of the VSWR at this distance was about 3.5 to 1. According to the model range requirements this distance was too small, so this type of mounting was unsatisfactory. An increase of r.f. power would have allowed an increase in the range separation. However a klystron, capable of being square-wave modulated and with a greater power output, was not available at the time of the experiment. Therefore the detection system, the PRD tuner, was embedded within the aircraft model (see Photograph C). This permitted compliance with model range requirements and improved the matching conditions.

2. Waveguide experiments.

Experiments of the same nature as those made for the coaxial line were made with the waveguide components.

a. Tuning characteristics.

Figure 45 and Photograph A, less the electromagnetic horn, show the connection of the waveguide components. Five sets of data were taken, each for a different probe tip diameter. The set given below is for a diameter of 13/64 inches. The actual probe tip used in the efficiency measurements was 16/64 inches in diameter, however no data was taken for this size. Figure 14 shows these values plotted. This experiment is discussed elsewhere in this paper and will not be repeated.

PRD Characteristics, Waveguide
Frequency 9020 mcs.

Waveguide Short length, in turns	VSWR	Rel. Power	Waveguide Short length, in turns	VSWR	Rel. Power
0	1.4	19.0	16½	1.32	19.2
1	1.48	18.9	19	1.5	19.4
2	1.46	18.9	20	1.4	19.6
3	1.55	18.9	21	1.4	19.8
4	1.53	18.9	22	1.44	20.0
5	1.50	18.8	23	1.42	20.0
6	1.52	18.8	24	1.42	20.0
7	1.50	18.7	25	1.38	20.0
8	1.42	18.6	26	1.32	19.9
9	1.24	18.5	27	1.28	19.8
10	1.36	18.3	28	1.20	19.8
11	1.23	17.8	29	1.25	19.8
12	1.30	16.8	30	1.26	19.7
13	2.1	14.8	30½	1.34	19.6
14	5.8	11.4	31	1.13	19.6
15	8.5	5.6	31½	1.26	19.6
15½	2.8	12.1	32	1.32	19.5
16	2.2	14.6	33	1.28	19.3
16½	1.29	16.6	34	1.28	18.9
17	1.17	17.7	Near 31	1.01	19.8*
17½	1.12	18.2	Near 31	1.13	19.8**
18	1.28	18.8			

TABLE VI

*When tuned for Minimum VSWR

**When tuned for Maximum Power

b. Impedance measurements, waveguide.

A set of tests were made with the comparison circuit similar to those made with the model antenna. The slotted line was varied in position. Sometimes it was in the receiving circuit and other times it was in the transmitting circuit. Values for the impedance were found at a point near the throat of the horn. Z_h is the horn impedance and Z_d is the detector impedance.

Impedance Measurements, Waveguide

No	Min Short	Min Load	Diff	λ_g	Dir. toward	Diff $\overline{\lambda_g}$	VSWR	z	Z	Looking
1	10.26	9.72	.54	5.18	G	.1061	1.32	.9+j.25	45+j12.5	Z_d
	10.26	10.48	.22	5.18	L	.0425	1.064	.95-j025	47.5-j1.25	Z_h
2	10.29	9.5	.79	5.18	G	.1525	1.48	1.06+j.38	53+j19	Z_d
	10.29	10.47	.18	5.18	L	.0375	1.055	.95-j.025	47.5-j1.25	Z_h
3	9.13	8.66	.47	4.6	G	.102	1.14	.955+j.12	47.75+j6.0	Z_h
	9.13	8.65	.48	4.6	G	.1042	1.26	.92+j.2	46+j10	Z_d
4	9.14	8.81	.33	4.6	G	.072	1.145	.915+j0.09	45.75+j4.5	Z_h
	9.14	9.09	.05	4.6	G	.01085	1.22	.89+j.025	44.5+j1.25	Z_d
5	9.13	8.79	.34	4.7	G	.068	1.15	.9+j.09	45+j4.5	Z_h
	9.13	8.63	.50	4.7	G	.1063	2.4	.66+j.55	33+j27.5	Z_d
6	9.12	8.68	.44	4.6	G	.0956	1.16	.94+j.12	47+j6	Z_h
	9.12	9.96	.84	4.6	L	.1826	1.55	1.25-j.41	62.5-j20.5	Z_d

TABLE VII

Measurements 1 and 2 were made at frequency of 8820 mcs. and 3 through 6 were at 9255 mcs.

The sixth experiment was taken with extreme care. Simultaneous readings of the VSWR were taken in the transmitter and the receiver circuits. The VSWR for the transmitter was 1.01 to 1 and that for the receiver was 1.05 to 1. This showed that the system of transmitter and receiver, although the Fresnel zone conditions prevailed, was matched. Actual model range conditions should improve the matching conditions.